STATE OF ALASKA

DEPARTMENT OF NATURAL RESOURCES

DIVISION OF GEOLOGICAL AND GEOPHYSICAL SURVEYS

Steve Cowper, *Governor*

Lennie Gorsuch, *Commissioner*

Robert B. Forbes, *Director and State Geologist*

December 1988

By
R.J. Motyka, L.D. Queen, C.J. Janik,
D.S. Sheppard, R.J. Poreda, and
S.A. Liss

STATE OF ALASKA
Department of Natural Resources
DIVISION OF GEOLOGICAL & GEOPHYSICAL SURVEYS

According to Alaska Statute 41, the Alaska Division of Geological and Geophysical Surveys is charged with conducting 'geological and geophysical surveys to determine the potential of Alaskan land for production of metals, minerals, fuels, and geothermal resources; the locations and supplies of ground water and construction materials; the potential geologic hazards to buildings, roads, bridges, and other installations and structures; and shall conduct such other surveys and investigations as will advance knowledge of the geology of Alaska.'

In addition, the Division of Geological and Geophysical Surveys shall collect, record, evaluate, and distribute data on the quantity, quality, and location of underground, surface, and coastal water of the state; publish or have published data on the water of the state and require that the results and findings of surveys of water quality, quantity, and location be filed; require that water-well contractors file basic water and aquifer data, including but not limited to well location, estimated elevation, well-driller's logs, pumping tests, flow measurements, and water-quality determinations; accept and spend funds for the purposes of this section, AS 41.08.017 and 41.08.035, and enter into agreements with individuals, public or private agencies, communities, private industry, and state and federal agencies; collect, record, evaluate, archive, and distribute data on seismic events and engineering geology of the state; and identify and inform public officials and industry about potential seismic hazards that might affect development in the state.

Administrative functions are performed under the direction of the Director, who maintains his office in Fairbanks. The locations of DGGS offices are listed below:

.794 University Avenue
(Suite 200)
Fairbanks, Alaska 99709
(907)474-7147

.400 Willoughby Avenue
(3rd floor)
Juneau, Alaska 99801
(907)465-2533

.3700 Airport Way
Fairbanks, Alaska 99709
(907)451-2760

.18225 Fish Hatchery Road
P.O. Box 772116
Eagle River, Alaska 99577
(907)696-0070

This report is for sale by DGGS for $6. DGGS publications may be inspected at the following locations. Mail orders should be addressed to the Fairbanks office.

.3700 Airport Way
Fairbanks, Alaska 99709

.400 Willoughby Avenue
(3rd floor)
Juneau, Alaska 99801

.U.S. Geological Survey
Public Information Office
701 C Street
Anchorage, Alaska 99513

.Information Specialist
U.S. Geological Survey
4230 University Drive, Room 101
Anchorage, Alaska 99508

CONTENTS

FIGURES

iv

TABLES

v

FLUID GEOCHEMISTRY AND FLUID-MINERAL EQUILIBRIA IN TEST WELLS AND THERMAL GRADIENT HOLES AT THE MAKUSHIN GEOTHERMAL AREA, UNALASKA ISLAND, ALASKA

by

R.J. Motyka,[1] L.D. Queen,[2] C.J. Janik,[3] D.S. Sheppard,[4] R.J.Poreda,[5] and S.A. Liss[2]

INTRODUCTION

The Makushin geothermal area is located on northern Unalaska Island in the east-central Aleutian Chain (fig. 1). The explored portion of the geothermal field lies on the east and southeast flanks of Makushin volcano, about 20 km west of the villages of Unalaska and Dutch Harbor. Surface manifestations of the hydrothermal system include numerous fumaroles, bicarbonate-sulfate thermal springs, and zones of intense alteration at the heads of Makushin and Glacier valleys (fig. 2). Additional fumaroles occur on the north and south flanks of the volcano, and areas of warm ground are found near Sugarloaf and at the head of Nateekin Valley. Results of reconnaissance investigations indicated these thermal areas are underlain by a boiling hot-water reservoir capped by a shallow vapor-dominated zone (Motyka and others, 1981; Motyka and others, 1983).

A state-funded exploration drilling program was initiated in 1982 by Republic Geothermal, Inc. (RGI) of Santa Fe Springs, California, under contract to the Alaska Power Authority (APA) (RGI, 1983). In late August 1983, a test well located near the head of Makushin Valley (ST-1, fig. 2) intersected a large fracture at a depth of 593 m from which hot waters were successfully produced at the wellhead. The well was flowed over a five-day period, shut down until early July 1984, then reopened and allowed to flow for a period of 45 days. The flowing bottom-hole temperature (BHT) in both cases measured 193°C. Although fluid enthalpy was relatively low, results of the reservoir engineering tests indicated that productivity of the fracture was sufficient for at least two production wells which could each drive 5 MW generators (RGI, 1985).

Through the cooperation of RGI and APA, the authors were able to obtain samples of ST-1 fluids at the wellhead during the initial testing of the well in 1983 and again in August of 1984 after the well had flowed for approximately 40 days. Rock cores extracted from a thermal gradient hole

---

[1] Division of Geological and Geophysical Surveys, 400 Willoughby, 3rd fl., Juneau, Alaska 99801.

[2] Division of Geological and Geophysical Surveys, 3700 Airport Way, Fairbanks, Alaska 99709.

[3] U.S. Geological Survey, Igneous Geothermal Processes Section, 345 Middlefield Rd., MS-910, Menlo Park, California 94025.

[4] Department of Science & Industrial Research, Wellington, New Zealand.

[5] Isotope Laboratory A-20, Scripps Institute of Oceanography, La Jolla, California 92037.

NORTHERN UNALASKA ISLAND

Wide Bay Cone

Table Top Mt.

Pt. Kadin ☆ Vents

Sugarloaf Cone

Dutch Harbor

Makushin Volcano

ST-1

Unalaska

Makushin Geothermal Area

Pakushin Cone
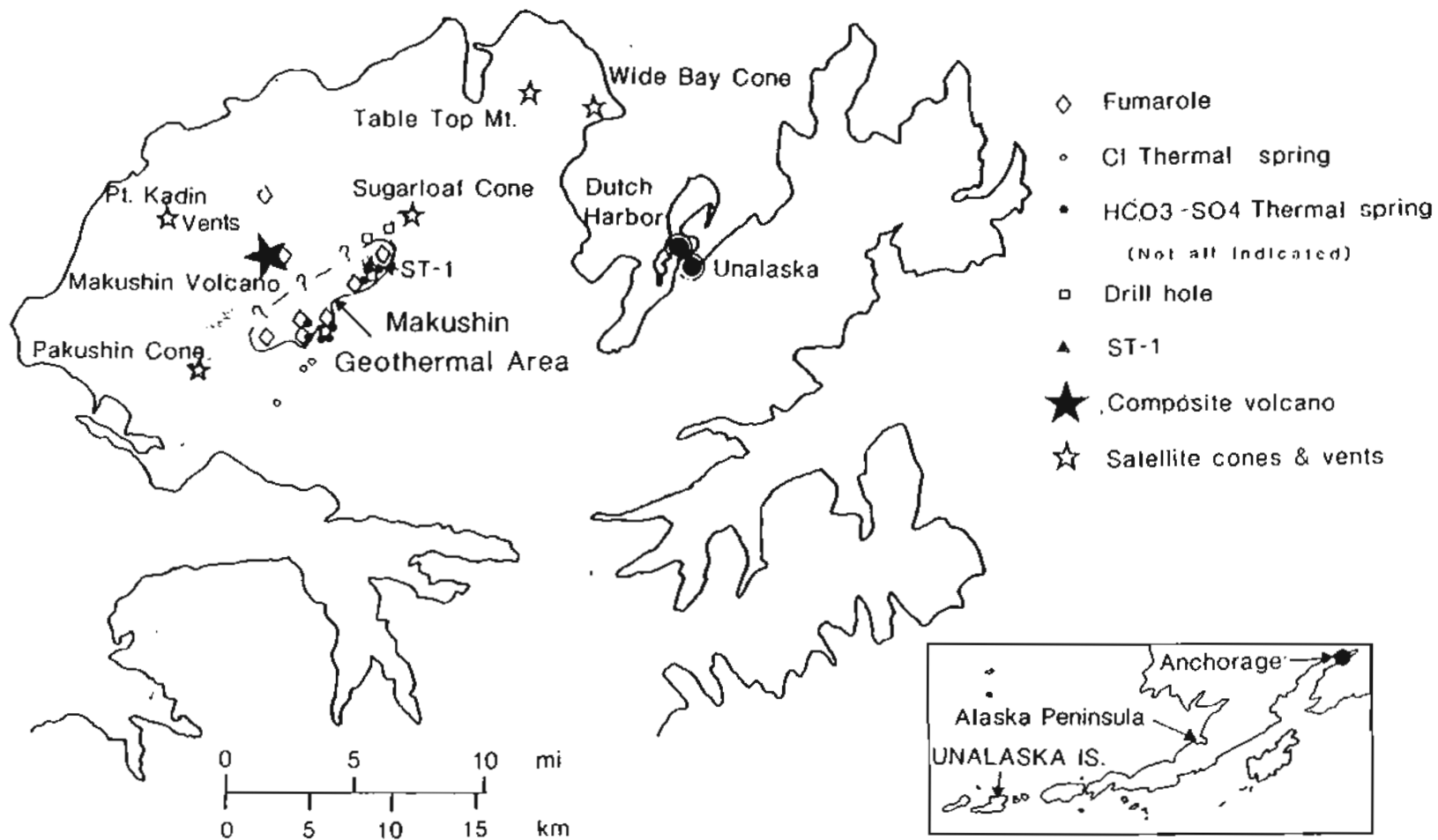
Legend:
- ◇ Fumarole
- ○ Cl Thermal spring
- ● HCO3-SO4 Thermal spring (Not all Indicated)
- □ Drill hole
- ▲ ST-1
- ★ Composite volcano
- ☆ Satellite cones & vents

Scale:
0 — 5 — 10 mi
0 — 5 — 10 — 15 km

Location Map

Anchorage

Alaska Peninsula

UNALASKA IS.
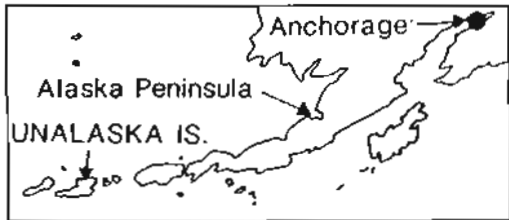
Figure 1. Location map for Makushin geothermal area.

- 2 -

Legend (left side):

- Tu — Unalaska Formation
- Tu — Contact metamorphosed Unalaska Formation
- Qa — Alluvium
- Qc — Colluvium
- Qp — Pyroclastic debris
- Ql — Glacial till
- Gabbronorite

- Homogeneous volcanics
- Inhomogeneous volcanics

Map labels:
SUGARLOAF CONE
MAKUSHIN VALLEY
NATEEKIN VALLEY
GLACIER VALLEY
ST. I.
A-1

Symbol key (lower right):

Fumarole	▲	Fault	U/D
Warm ground	■	Contact	.....
HCO_3-SO_4 Thermal springs		Thermal gradient well	○
Cl-Thermal springs		Test Well	◆

Miles
Kilometers

Figure 2. Geologic map of the Makushin geothermal area.

(TGH) drilled near Sugarloaf in 1984 (A-1, fig. 2) were shipped to Fair-banks, examined for mineral alteration, and compared to well logs for ST-1 and TGH E-1, D-1, and I-1 which were previously examined by Queen (1984). This report presents the findings of our geothermal fluid, mineral altera-tion, and fluid-mineral investigations of well ST-1 and the thermal gradient holes. Appendix A of this report also contains updated geochemical data on fumaroles, thermal springs, and cold waters in the Makushin geothermal area which were first discussed in Motyka and others (1983).

Objectives of our investigations were:

(1) to determine reservoir fluid geochemistry;
(2) to provide a pre-development geochemical data base;
(3) to study fluid-mineral equilibria;
(4) to determine deeper reservoir characteristics and origin of chemical constituents in the reservoir fluids;
(5) to perform geothermometry;
(6) to analyze mixing relations;
(7) to assess potential scaling and environmental problems;
(8) to compare isotopic and chemical composition of ST-1 fluids to neighboring fumaroles and springs; and
(9) to reconstruct the history of the hydrothermal system.

The Makushin geothermal system is the first in the Aleutian arc of active volcanism to have been successfully drilled and to produce fluids at temperatures above atmospheric boiling. As such, the Makushin program has provided us with a unique opportunity to study arc-related hydrothermal systems and the dynamic interactions between volcanism, glaciation, and hy-drothermal systems.

The findings of our study, combined with our previous observations, and with results of volcanic investigations by Nye and others (1985), measure-ments and tests made by RGI on the thermal gradient holes and test well (RGI, 1983; 1984; 1985), and the results of an electrical resistivity survey conducted in 1984 by Shore (1985), have led us to the following model for the Makushin geothermal system:

(1) The heat source driving the hydrothermal system is presumed to be a shallow-lying body of magma as suggested by the geologically young caldera at the summit of Makushin volcano. The magma chamber is thought to be related to post-Pleistocene outpouring of homogeneous lavas on the northeast flank of Makushin volcano and pyroclastic flows at the head of Makushin Valley.
(2) The main hydrothermal reservoir has a temperature of 250°C and is located over the heat source. Hot waters from the reservoir ascend through the core region of the volcano then cool as they spread laterally. Steam and gases evolve from the boiling of the outflowing plume of hot water as it nears the surface and feed the fumaroles and

bicarbonate-sulfate thermal springs which abound at mid-elevations on the south and east flanks of the volcano.

(3) The reservoir is recharged by meteoric waters that infiltrate the system along fractures located at mid- to lower elevations of the volcano. The chemical composition of reservoir waters is partially derived from release of volatile gases from the underlying magma system, but mainly from interaction with the reservoir rock. ST-1 waters are moderately rich in sodium and chloride and have relatively high concentrations of calcium. The latter is attributed to the interaction of hot waters with the gabbronoritic intrusive that appears to act as the host rock for at least a portion of the reservoir waters.

(4) Fluids produced from ST-1 are out of equilibrium with the measured flowing BHT. Geothermometry indicates the waters were hotter and must have cooled before entering the borehole. Fluids at the bottom of ST-1 are below the pressure boiling point, ruling out adiabatic cooling. The remaining alternatives are that the waters cooled conductively, or by dilution with colder waters, or both.

(5) Results of electrical resistivity surveys, conducted by Premier Geophysics of Vancouver, British Columbia, indicate that the hydrothermal system at the head of Makushin Valley is bounded by faults and fractures north and east of ST-1 and that the hydrothermal system extends west and south of ST-1 and E-1. The electrical resistivity survey showed no evidence for any hydrothermal system east of fumarole field 1 nor for any linear hydrothermal system offset to the east from the main volcano. These findings indicate that any future production wells should be sited at or up-valley of ST-1.

(6) A wealth of evidence derived from mineral alteration and fluid inclusion studies indicates that the chlorine-rich hot-water system extended to the surface at the heads of Makushin and Glacier valleys in the recent past and that the near-surface system temperature reached 250°C. The change in hydrostatic pressure caused by the advance and retreat of Holocene glaciers is proposed as the cause of these changes in the near-surface regime of the hydrothermal system.

(7) Paleotemperatures determined from fluid inclusions trapped in hydrothermal quartz veins are substantially higher than present-day temperatures in ST-1 and E-1. The temperature change indicates that at least the upper portion of the geothermal system has cooled. Nevertheless, ample energy should remain for geothermal resource development in the foreseeable future.

GEOLOGIC SETTING

The Makushin area is one of over 70 major volcanic centers within the Aleutian arc of active volcanism. The Aleutian Chain lies immediately north of the Aleutian Trench, a convergent boundary between the North American and the Pacific lithospheric plates. The eruption of Aleutian magmas appears to

be closely related to the subduction of the Pacific plate beneath the North American plate.

Makushin Volcano (2,000 m) is a large composite, polygenetic volcanic center that dominates northwestern Unalaska Island. The broad dome-shaped summit is capped by an ~5-km-diam. ice-filled caldera with glaciers descending the larger valleys to elevations as low as 300 m. Four satellitic late-Pleistocene to Holocene volcanic cones also occur in the area and are aligned in a northeasterly trend, roughly subparallel to the strike of this portion of the Aleutian arc.

Geology of the Makushin study area, generalized from Nye and others (1984), is shown in figure 2. The oldest unit exposed in the study area is the Unalaska Formation which consists of Miocene to early Pliocene volcaniclastic rocks, dikes, sills, lava flows, and minor sedimentary rocks. The upper part of the formation consists primarily of pyroclastic rocks, whereas lava flows dominate the lower section. The formation has been metamorphosed to grades as high as the pyroxene hornfels facies near contacts with an un-zoned gabbronoritic stock that is extensively exposed at the heads of Makushin and Glacier Valleys. The intrusive is medium-grained, equigranular to porphyritic, and consists primarily of plagioclase (50-75 modal percent, $An_{50}-An_{70}$) with subequal amounts of clinopyroxene and orthopyroxene (Nye and others,1984). The gabbronorite is thought to be roughly correlative with other intrusives exposed on the island and which have been dated at 10-13 Ma.

Fumaroles and hot springs at the heads of Makushin and Glacier Valleys emanate almost exclusively from the gabbronorite and hornsfelsic border zone. The gabbronorite was encountered in all five holes drilled at the Makushin geothermal area and appears to be acting as the primary reservoir rock at least in the explored portions of the field. Interfingering of the Unalaska Formation with the gabbronorite is common, suggesting that only the roof of the stock has been exposed.

The volcanic rocks which comprise Makushin Volcano and the satellitic vents are discussed in detail by Nye and others (1985). Makushin Volcano is a polygenetic composite stratovolcano that is primarily composed of basalt and andesite flows, lahars, and pyroclastic flows. Available K-Ar ages on the Makushin lavas are less than 1 Ma, indicating that the Makushin volcanics in the study area are exclusively Quaternary.

The satellitic cones are post-Wisconsinan monogenic vents consisting primarily of chemically homogeneous basaltic to andesitic flows and pyroclastic flows and cinders. A thick series of chemically homogeneous valley-filling, post Wisconsinan andesite flows also issued from the east flank of Makushin Volcano, enveloping Sugarloaf and filling Driftwood Valley. This large outpouring of post-Wisconsinan lavas and pyroclastic rocks suggests a Holocene magmatic pulse of exceptional volume. However, trace element

geochemical studies (Nye and others, 1985) indicate that the satellitic cones had source regions and plumbing systems separate from the ones supplying Makushin Volcano. The huge amount of lavas represented in the east flank Holocene Makushin eruption suggests that a large volume of residual magma may have lodged in the subcrustal region of the volcano and may be acting as the heat source for the existing hydrothermal system.

DRILLING HISTORY ST-1

Test well ST-1 is located near the head of Makushin Valley (fig. 2). The wellhead sits upon the upper edge of an apron of pyroclastic debris that fills the bottom of upper Makushin Valley. Details of the procedures followed in the drilling of test well ST-1 (and TGH A-1) can be found in RGI's 1984 report to the Alaska Power Authority. The site chosen for ST-1 was based on (1) proximity to E-1, the hottest of the thermal gradient holes drilled in 1982; (2) proximity to fumarole fields 1 and 2 and to a fault which runs up-canyon from ST-1; and (3) convenient logistical staging area for drilling. The upper part of ST-1 (to a depth of about 215 m) was drilled to ~15 cm diam.; below 215 m to well bottom, diam. is ~7.6 cm. Below the top 10 m, composed of pyroclastics, ST-1 penetrates gabbronorite to a depth of 593 m (Queen, 1984).

Drillers encountered a pressurized steam-filled fracture at 210 m. Wellhead pressures after shut-in indicated steam temperatures of 140-150°C. Samples of gases and steam evolving from the fracture were obtained from a wellhead release valve. Subsequent drilling and downhole pressure measurements showed the pressurized hydrothermal system water table lies ~30 m below this fracture; thus, steam in the fracture probably evolved from boiling of the water table.

The steam fracture was sealed and drilling continued. No additional open fractures were encountered until 585 m below surface. The well was shut and pressure allowed to build. Upon opening of the well hot waters spurted intermittently from the wellhead exhaust, but continuous flow was not sustainable. Field measurements of chloride concentrations in the flashed waters ranged from 5,000 to 7,000 ppm.

Drilling was continued to a depth of 593 m whereupon the drill string dropped an estimated 1 m, indicating a major open fracture had been intersected. The well was immediately shut, and the wellhead pressure was allowed to increase until it stabilized at approximately three bars. The well was then opened on August 27, 1983, and the resultant fluid flow up the borehole became self-sustaining. The well was briefly flowed, and exhaust-end water samples collected for chemical analyses, to determine if any adverse environmental effects would occur upon discharge of the well waters into a local stream. After approval for discharging the waters was obtained from the appropriate agencies, the well was reopened on August 29 for a five-day flow test which included downhole pressure and temperature

measurements by RGI staff scientists. During this period, the authors collected five separate suites of water and gas samples.

The well was then shut down and wellhead pressure monitored through the winter months. Static down-hole pressure and temperature measurements were made on July 5, 1984, and the well was reopened on July 7. The well was flowed almost continuously over a 45-day period until shutdown on August 10, 1984. Samples of well fluids were obtained by the authors on August 7 and again on August 9, 1984. Plans for 1984 originally called for a deepening of ST-1 after the flow test, but APA decided against deepening so as to maintain the well for demonstration purposes. Flowing bottom-hole temperatures measured 193°C both in 1983 and 1984 (RGI, 1985). The static downhole temperature measurements made by RGI on July 5, 1984 gave a maximum downhole temperature of ~198°C at a depth of ~460 m. Static bottom-hole temperature measured ~195°C.

FLUID GEOCHEMISTRY

Sampling Procedures

Samples of fluids produced from the test well were collected in both 1983 and 1984. Most were taken from the major production zone at 593-m depth between August 27 and September 3, 1983 and between August 1 and August 7, 1984. The test well was shut down from September 3, 1983 until July 4, 1984, then run continuously until shutdown on August 8, 1984.

Samples of gases and waters from ST-1 were collected with a Webre type mini-cyclone separator. (Design and use of the separator are described in Sheppard and Giggenbach, 1985; fig. 3 shows the separator in use at ST-1.) The separator was attached to the side of the exhaust manifold at a point about 5 m from wellhead and 2 m before the throttling orifice. Separator pressure was monitored with a high-pressure gauge just before the two-phase fluid entered the separator. Fluid collection pressures and temperatures, together with sampling dates and steam fractions, are given in table 1.

The separator was first adjusted for collection of the water fraction. Fluids emerging from the water exhaust port of the separator were routed through a condensing coil immersed in an ice bath, then collected and filtered through 0.45-μ filters. The sample suite normally consisted of 1 liter filtered untreated, 1 liter filtered acidified (HCl), 1 liter filtered and treated with formaldehyde for $\delta^{18}O$-SO_4 determinations, 100 ml of water at a dilution of 1:10 and 1:5 for silica determinations, 1 liter of untreated water for tritium determinations, and 30 ml of water for stable isotope determinations. In addition, raw untreated samples were collected for in-field determination of HCO_3, pH, H_2S, and NH_3. In two cases (samples 77 and 02), waters were filtered through 0.1-μ filters and treated in the field for aluminum analysis following methods described by Presser and Barnes (1974).
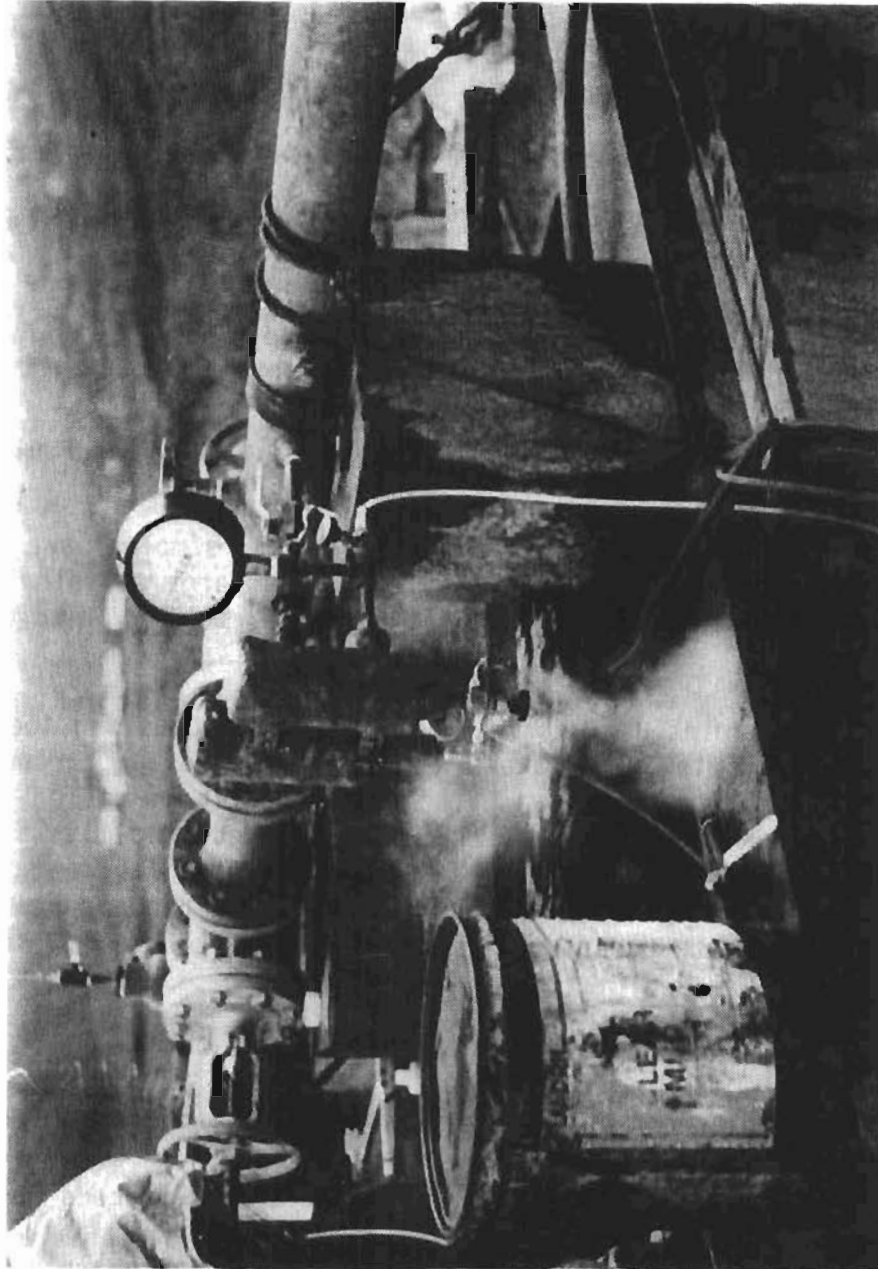
Figure 3. Webre mini-cycline separator in use at well ST-1, Makushin geothermal area.

Table 1. Fraction of steam separated from flashed well fluids.[1]

Sample # DGGS	USGS	Date	Time[2]	Collection pressure, bars[3]	Collection temperature, °C[4]	Steam fraction[5]
71	1	8-27-83	(+1.5 hr)	2.00	120	0.144
74	2A	9-1-83	17:30	3.17	135.5	0.116
75	3B	9-2-83	10:10	3.03	134	0.119
76	4B	9-2-83	16:20	4.48	147.5	0.093
77	5A	9-3-83	19:50	4.55	147.5	0.092
84-1	-	8-4-84	15:00	2.65	129.5	0.127
84-2	-	8-7-84	13:00	2.79	131	0.124

[1] Fluids collected using Webre type mini-cyclone separator.
[2] Parenthetical value for 71 is the time elapsed after initial discharge from fracture zone at 593 m depth. Well was then shut-off until 9-1-83. Well was reopened at 14:40, 9-1-83 and was run continuously until about 22:00, 9-3-83. Well was reopened again on 7-4-84 and run nearly continuously until 8-8-84.
[3] At the separator. These are absolute values calculated from gauge pressure plus atmospheric pressure which was assumed to be 0.96 bars.
[4] Determined from the collection pressure assuming liquid-vapor equilibrium (Keenan and others, 1969).
[5] Steam fraction calculated using a BHT=193°C and reservoir enthalpy value of 821 kJ/kg (Keenan and others, 1969).

As an additional check on water chemistry, water samples were collected from the end of the exhaust manifold, by placing a large polyethylene beaker beneath the pipe-end and allowing the flashed water to flow into the container.

Steam and gas samples were collected after first adjusting the separator for pure steam phase flow. The steam and gases were routed through the condensing coil then collected in evacuated flasks partially filled with sodium hydroxide. Additional samples were collected in evacuated flasks without NaOH for $^3He/^4He$ analyses. A 500-ml sample of the steam condensate was collected for chloride analyses as a check against water phase contamination; 30-ml samples of the condensate were also collected for stable isotope analyses.

Methods of Analyses

Water

HCO_3, pH, H_2S, and NH_3 were determined in the field by methods described in Presser and Barnes (1974). The remaining constituents were analyzed at the DGGS water laboratory in Fairbanks. Major and minor cation concentrations were determined using a Perkin Elmer atomic absorption spectrometer and following standard procedures. Sulfate and bromide concentrations were determined on a Dionex ion chromatograph. Fluoride was determined by specific ion electrode methods. Chlorides were analyzed by Mohr titration and boron by carminic acid spectroscopy. Silica concentrations were determined by the molybdinate blue method.

Stable isotopes ($^{18}O/^{16}O$ and D/H) were analyzed at Southern Methodist University, Dallas, Texas and at U.S. Geological Survey, Menlo Park, California. Tritium concentrations were determined at the Tritium Laboratory, University of Miami, Miami, Florida.

Gases

Residual gases, that is, gases not absorbed in the sodium hydroxide solution (He, H_2, Ar, O_2, N_2, and CH_4) were analyzed on a dual-column gas chromatograph with both argon and helium carrier gases at the U.S. Geological Survey, Menlo Park, California. Moles of residual gas were calculated from measured gas pressures and head space volumes. CO_2 and H_2S concentrations in the sodium hydroxide solutions were determined by titration and by ion chromatography respectively. Concentrations of these gases were also checked by gravimetric methods using $SrCl_2$ and $BaCl_2$ to precipitate $SrCO_3$ and $BaSO_4$. The $SrCO_3$ precipitate was then reacted with phosphoric acid to determine CO_2 yield. The evolved gas was saved and analyzed for $^{13}C/^{12}C$. Steam content of the gases was determined by weight difference before and after sampling. Ammonia was analyzed by specific ion electrode method.

Adjustments were made for head space gases dissolved in the solution by using Henry's Law. Moles of each constituent collected were then determined and the mole percentage of each constituent was calculated. If air was present in the sample, a correction was made for air by using the ratio of oxygen in the sample to oxygen in air. The gas concentrations in mole percent were then recalculated on an air-free basis.

Helium isotope ratios ($^3He/^4He$) were determined at the Scripps Institute of Oceanography, La Jolla, California. Carbon isotope ratios in CO_2 ($^{13}C/^{12}C$) were analyzed at the U.S. Geological Survey, Menlo Park, California.

Water Chemistry

Results of geochemical analyses of ST-1 waters obtained from the Webre mini-cyclone separator and from the end of the exhaust pipe are given in tables 2 and 3. Total discharge water chemistries, given in tables 4 and 5, were calculated using the separator water and steam fractions given in table 1, which are based on separator pressure and a discharge enthalpy of 821 kJ/kg (which corresponds to the measured flowing bottom-hole temperature of 193°C).

End-of-exhaust water analyses gave total discharge constituent concentrations 10 to 15 percent higher than separator values where exhaust water fraction was calculated on the assumption of atmospheric pressure-boiling point conditions. However, flashing at the exhaust end apparently occurs at pressures well below atmospheric (D. Michaels, personal commun., RGI, 1984).

Table 2. Chemical analyses of waters collected from Makushin Valley test well ST-1, 1983[1]
(Concentrations in mg/l unless otherwise specified).

	From Webre-separator[2]						Off end of exhaust			
	71	74	75	76	77	64	74	75	76	77
Cations										
Na	2120	2020	2010	1900	2010	2840	2400	2470	2420	2460
K	270	280	270	250	250	360	180	310	300	310
Ca	150	139	140	128	144	216	175	175	175	181
Mg	0.2	0.1	0.1	0.1	0.1	0.3	0.2	0.2	0.2	0.2
Li	11	11	11	10	10	14	13	13	13	13
Sr	2.4	2.3	2.8	2.5	2.6	3.1	3.2	3.3	3.3	3.1
Cs	1.4	1.4	1.4	1.4	1.4	1.6	nd	nd	nd	nd
NH_4	nd	nd	nd	nd	<1	nd	nd	nd	nd	nd
Total[3]	108.5	103.5	103.0	97.0	102.6	145.6	119.6	126.0	123.7	125.7
Anions										
HCO_3	<5	<5	<5	<5	<1.0	<5	nd	nd	nd	nd
SO_4	91	86	85	77	80	190	nd	nd	nd	nd
F	1.2	1.2	1.2	1.0	1.0	1.6	nd	nd	nd	nd
Cl	3670	3540	3500	3230	3370	4870	4160	4240	4200	4220
Br	14	13	12	12	13	19	nd	nd	nd	nd
Total[3]	105.7	101.8	100.6	93.0	96.9	141.8	117.3	119.7	118.5	119.1
Balance percent	2.6	1.7	2.4	4.2	5.7	2.7	1.9	5.2	4.3	5.4
SiO_2	343	335	340	306	323	450	393	395	402	395
H_2S	nd	2.7	1.5	nd	nd	nd	nd	nd	nd	nd
B	68	64	65	59	62	86	74	76	77	78
Al	nd	nd	nd	nd	0.02	nd	nd	nd	nd	nd
As	12	11	13	12	12	16	14	15	15	15
Fe	nd	nd	nd	nd	0.13	nd	nd	nd	nd	nd
TDS[4]	6760	6500	6450	5990	6280	9070	- -	- -	- -	- -
pH, field[5]	8.1	8.0	7.8	7.6	7.9	7.8	nd	nd	nd	nd
Date sampled	8/27/83	9/1/83	9/2/83	9/2/83	9/3/83	8/24/83	9/1/83	9/2/83	9/2/83	9/3/83

[1] Alaska Division of Geological and Geophysical Surveys, Fairbanks, M.A. Moorman and R.J. Motyka, analysts.
[2] Sampling conditions and steam fraction given in table 1.
[3] Cation and anion totals in milliequivalents/liter.
[4] Calculated.
[5] Sample 64 measured at T=50°C; all others measured after cooling to 15°C.

nd = not determined.

Table 3. Chemical analyses of waters collected from Makushin Valley test well ST-1, 1984.[1]
(Concentrations in mg/1 unless otherwise specified.)

	From Webre-separator[2]		Off end of exhaust	
	1W	2W	1E	2E
Cations				
Na	1910	1930	2290	2290
K	260	250	300	310
Ca	129	133	155	149
Mg	0.2	0.2	1.3	0.6
Li	10	10	12	11.5
Sr	2.7	2.7	3.2	3.2
Cs	1.4	1.3	1.6	1.5
NH_4	<1	<1	nd	nd
Total[3]	97.6	98.5	116.9	116.7
Anions				
HCO_3	26	12	nd	nd
SO_4	95	97	115	112
F	1.2	1.2	1.4	1.4
Cl	3480	3500	4180	4170
Br	12	12	14	14
Total[3]	100.9	101.3	120.5	120.2
Balance percent	-3.3	-2.8	-3.1	-3.0
SiO_2	- -	328	397	384
H_2S	<1	1	nd	nd
B	- -	67	78	79
Al	nd	0.004	nd	nd
As	12	11	15	14
Fe	0.26	0.20	0.32	0.24
TDS[4]	nd	6360	7560	7540
pH, field[5]	7.7	7.6	nd	nd
Date sampled	8/4/84	8/7/84	8/4/84	8/7/84

[1] Alaska Division of Geological and Geophysical Surveys, Fairbanks, R.J. Motyka and M.A. Moorman, analysts.
[2] Sampling conditions and steam fraction given in table 1.
[3] Cation and anion totals in milliequivalents/liter.
[4] Calculated.
[5] pH measured after waters cooled to 15°C.
nd = not determined.

Supporting evidence for the latter comes from a temperature measurement of the center of fluid flow from the exhaust made by P. Parmentier (RGI). The temperature measured was 60°C, which indicated that low-pressure effects that are not well understood cause increased flashing of the exhaust fluid. Use of the 60°C temperature in our calculations resulted in an exhaust-end water fraction of 0.75, and application of this water fraction to exhaust analyses gave total discharge chemistries which were in close harmony with those obtained from the separator method (table 6).

Additional support for basing total discharge chemistry on the separator water analyses comes from RGI's reported analyses of 1983 ST-1 water samples. Two of their samples were obtained under high pressures, using an entirely different technique than the mini-cyclone separator method (RGI

Table 4. Chemical analyses of 1983 waters from Makushin Valley test well ST-1, corrected to reservoir conditions without gas.
(Concentrations in mg/l unless otherwise specified.)

	71	74	75	76	77	Average	S.D.
Cations							
Na	1820	1780	1780	1730	1820	1786	37
K	230	250	240	230	230	236	9
Ca	128	123	124	116	131	124	6
Mg	0.2	0.1	0.1	0.1	0.1	0.12	0.04
Li	9	9	10	9	9	9.2	0.4
Sr	2.1	2.0	2.5	2.3	2.4	2.3	0.2
Cs	1.2	1.2	1.2	1.3	1.3	1.2	0.1
NH_4	nd	nd	nd	nd	1.0	1.0	- -
Anions							
HCO_3	<5	<5	<5	<5	<1.0	<5	- -
SO_4	78	76	75	70	73	74	3
F	1.0	1.1	1.1	1.1	0.9	1.0	0.1
Cl	3140	3130	3080	2930	3060	3068	84
Br	12	11	11	11	12	11.4	0.5
SiO_2	294	296	300	278	293	292	8
H_2S	nd	2.4	1.3	nd	nd	1.9	- -
B	58	57	57	54	56	56.4	1.5
Trace							
Al	nd	nd	nd	nd	0.02	0.02	- -
As	11	10	11	11	11	10.8	0.4
Fe	nd	nd	nd	nd	0.12	0.12	- -
TDS	5790	5750	5680	5430	5700	5670	141
Date sampled	8/27/83	9/1/83	9/2/83	9/2/83	9/3/83		

nd = not determined
S.D. = Standard deviation

Final Report, 1984, pg. XII). These samples yielded total discharge chemistries nearly identical to our separator samples.

The ST-1 waters are moderately saline and low in bicarbonate. Comparison of 1983 to 1984 chemistries show the waters to be nearly identical; the 1984 waters are slightly less saline and slightly richer in HCO_3. Although the ST-1 waters are moderately saline when compared to other geothermal systems in the world, they nevertheless contain more chloride than can be reasonably accounted for by leaching from the basic gabbronoritic wallrock. Apparently the reservoir waters either circulate through marine-laid deposits within the Unalaska Formation or the reservoir is being contaminated by seawater infiltration. The Cl/Br ratio of the Makushin Reservoir water is very similar to that of seawater (~280). A third possibility is that the chloride originates from the siliceous magmatic heat source.

The ST-1 waters are high in arsenic which could pose a potential water pollution problem for salmon spawning areas if exhaust waters are discharged

Table 5. Chemical analyses of 1984 waters collected from the Makushin
Valley test well ST-1, corrected to reservoir conditions without gas.
(Concentrations in mg/l unless otherwise specified.)

	1W	2W	Average
Cations			
Na	1670.	1690.	1680.
K	230.	220.	225.
Ca	112.	116.	114.
Mg	0.2	0.2	0.2
Li	9.	9.	9.
Sr	2.3	2.4	2.4
Cs	1.2	1.1	1.2
NH_4	<1.	<1.	<1.
Anions			
HCO_3	23.	11.	17.
SO_4	83.	85.	84.
F	1.0	1.1	1.1
Cl	3040.	3070.	3060.
Br	10.	10.	10.
SiO_2	nd	287.	287.
H_2S	nd	1.	1.
B	nd	59.	59.
Al	nd	0.004	0.004
As	10.	10.	10.
Fe	0.23	0.18	0.2
TDS		5570.	5570.
Date sampled	8/4/84	8/7/84	

nd = not determined.

directly into Makushin Valley streams. Compared to waters in other geo-
thermal systems, ST-1 waters are relatively rich in calcium, most likely
from alteration of plagioclase in the gabbronoritic host reservoir rock.
The plagioclase has a composition of An_{50}-An_{70}, which indicates that more
calcium than sodium should be dissolved by the waters. Much of the dis-
solved calcium, therefore, must be removed from reservoir waters through
precipitation of anhydrite, calcite, and formation of zeolites.

Gas Chemistry

Air corrected analyses of gases collected from test well ST-1 in mole
percentages are given in table 7. Gas content in total discharge is given
table 8. MVTW-2G-8 is the least air-contaminated of the 1984 samples, and
its analysis is considered the most reliable and representative of the
August 1984 geothermal system.

Gas concentrations in total discharge are extremely low (0.02 percent),
and a slight decline in total gases occurred between 1983 and 1984. Hydrogen

Table 6. Chemical analyses of exhaust pipe waters from Makushin Valley test well ST-1 corrected for reservoir conditions assuming 60°C end point flash temperature.[1] (Concentrations in mg/l unless otherwise specified).

Sample #	Date	Cations				Li	Sr	Cs	HCO_3	Anions					SiO_2	B	As	Fe	TDS	Steam fraction
		Na	K	Ca	Mg					SO_4	F	Cl	Br							
RM83-64	8-24-83	2120	270	160	0.2	11	2.3	1.2	nd	140	1.2	3650	14	337	64	12	nd	6780	0.252
RM83-74	9-01-83	1800	130	130	0.1	9.4	2.4	nd	nd	nd	nd	3110	nd	294	55	11	nd	5540	0.252
RM83-75	9-02-83	1850	230	130	0.2	9.6	2.5	nd	nd	nd	nd	3170	nd	296	57	11	nd	5760	0.252
RM83-76	9-02-83	1810	230	130	0.1	9.7	2.5	nd	nd	nd	nd	3140	nd	301	58	11	nd	5690	0.252
RM83-77	9-03-83	1840	230	140	0.1	9.7	2.3	nd	nd	nd	nd	3160	nd	296	58	11	nd	5740	0.252
RM84-01	8-04-84	1710	220	120	1.0	8.8	2.4	1.2	nd	86	1.0	3130	10	297	58	11	0.24	5660	0.252
RM84-02	8-07-84	1710	230	110	0.5	8.5	2.4	1.1	nd	84	1.0	3120	10	287	59	10	0.18	5640	0.252

[1] Alaska Division of Geological and Geophysical Surveys, Fairbanks, Alaska, M.A. Moorman, analyst.

Table 7. Makushin test well, air corrected gas analyses, mole percent.

Sample code	Date sampled	RO_2	Xg	CO_2	H_2S	H_2	CH_4	NH_3	N_2	Ar	N_2/Ar	C/S
MVTW-1 DS/CJ	8-27-83	0.00	0.070	87.74	1.80	0.28	0.006	0.76	9.24	0.18	50.4	48.9
MVTW-2A DS/CJ	9-01-83	0.00	0.098	89.61	2.71	0.46	0.007	0.18	6.92	0.10	67.3	33.0
MVTW-3B DS/CJ	9-02-83	0.00	0.081	92.54	2.27	0.17	0.005	0.25	4.68	0.07	66.8	40.7
MVTW-4B DS/CJ	9-02-83	0.00	0.109	91.61	3.15	0.12	0.007	0.20	4.84	0.08	63.8	29.1
MVTW-5A DS/CJ	9-03-83	0.00	0.105	92.73	2.28	0.10	0.006	0.18	4.63	0.07	63.2	40.7
MVTW-1G-C RM/CJ	8-04-84	0.27	0.089	86.26	2.52	0.04	tr	0.46	10.57	0.15	70.5	34.2
MVTW-2G-A RM/CJ	8-07-84	0.50	0.058	85.94	2.52	0.06	tr	0.67	10.69	0.12	89.6	34.1
MVTW-2G-B RM/CJ	8-07-84	0.14	0.064	93.81	2.02	0.02	tr	0.30	3.77	0.07	51.7	46.3

DS/CJ = D. Sheppard, Department of Scientific and Industrial Research, New Zealand, and C. Janik, U.S. Geological Survey, Menlo Park, analysts.
RM/CJ = R. Motyka, Alaska Division of Geological and Geophysical Surveys, Fairbanks, and C. Janik, U.S. Geological Survey, Menlo Park, analysts.
Xg = Ratio, moles gas to moles steam in percent.
RO_2 = Ratio, oxygen in sample to oxygen in air.

Table 8. Mass percent gas content of total discharge, using O_2 corrected gas analyses.

Sample no.	Steam fraction	Mass percent gas in steam	Mass percent gas total discharge
MVTW-1 DS/CJ	0.144	0.163	0.023
MVTW-2A DS/CJ	0.116	0.231	0.027
MVTW-3B DS/CJ	0.119	0.192	0.023
MVTW-4B DS/CJ	0.093	0.260	0.024
MVTW-5A DS/CJ	0.092	0.252	0.023
MVTW-1G-C RM/CJ	0.127	0.208	0.026
MVTW-2G-A RM/CJ	0.124	0.132	0.016
MVTW-2G-8 RM/CJ	0.124	0.154	0.019

content in particular seems to have decreased significantly, nearly an order of magnitude since the well was first opened. Methane concentrations appear also to have declined and were present only in trace amounts in the 1984 samples. Hydrogen sulfide, although 2 to 2.5 percent of total non-steam gases, has such a low concentration in the total discharge that it should not pose significant pollution problems.

The CO_2-H_2S-N_2 composition of ST-1 gases are plotted on a tri-lateral diagram which also shows compositions of fumarolic gases in the Makushin geothermal area (fig. 4). The ST-1 gases are similar in composition to gases from fumarole fields 1 and 2, which suggests they are derived from a common source at depth. Gases from the superheated fumarole (3sh, 150°C) show the highest relative concentrations of H_2S. Gases from other fumaroles and from ST-1 trend to increasingly greater proportions of N_2, which indi-cates that the H_2S in these discharges is being selectively removed by oxidation with air or air dissolved in water. At ST-1, H_2S may also be being removed by reactions with the drillhole casing.

The decrease in H_2 during the 1983 well-test period and the nearly order-of-magnitude decrease in the proportion of H_2 between 1983 and 1984 may also be attributable to interaction of hot water with the casing. Once a protec-tive scale is deposited on the casing, excess H_2 gas generation would decline. Alternatively, the decrease in H_2 may indicate a preferential out-gassing of the lighter gases from the reservoir fluids early in the well-test.

The ratio of N_2 to Ar is plotted against H_2 to Ar in figure 5. The N_2/Ar ratios in the atmosphere and for air dissolved in water at 25°C are also shown for comparison. Except for 688, all ST-1 samples fall between these two values, indicating air is the primary source of N_2 dissolved in the reservoir waters.
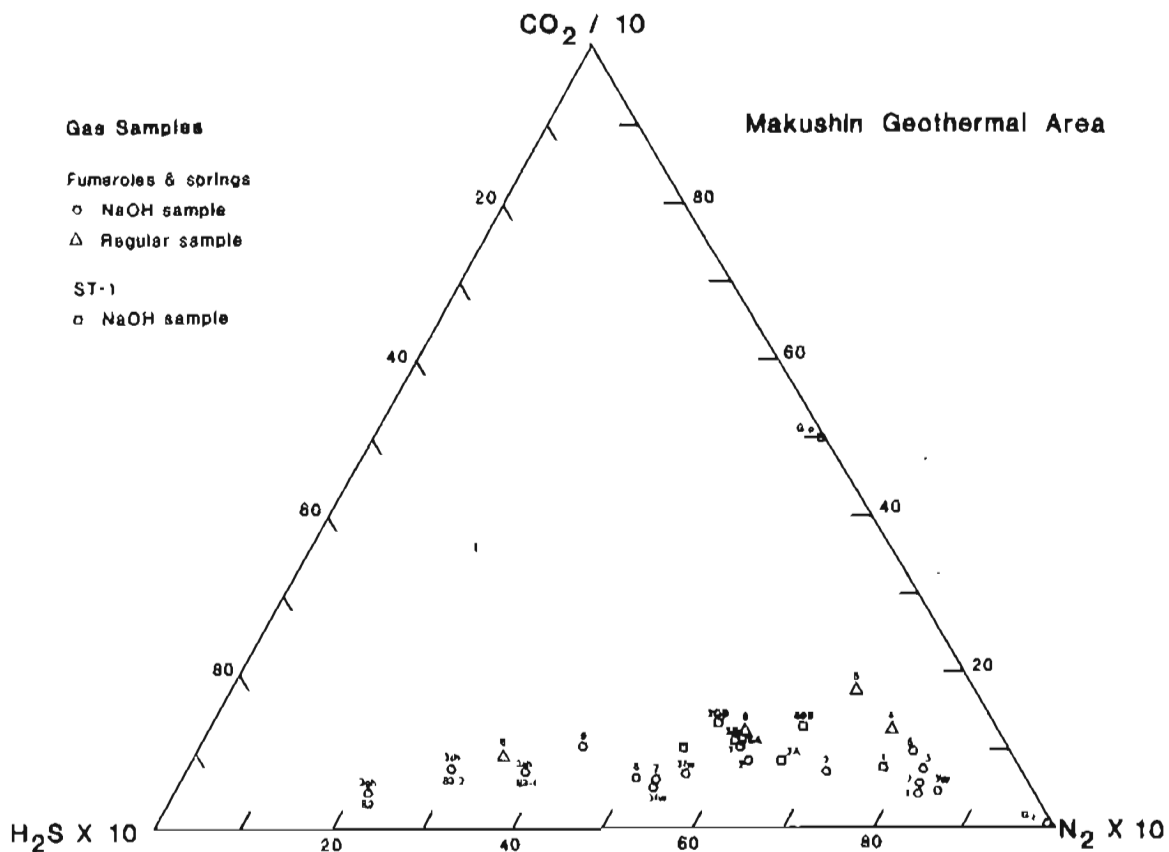
Figure 4. CO_2-H_2S-N_2 compositions of well ST-1 and fumarolic gases from Makushin geothermal area.
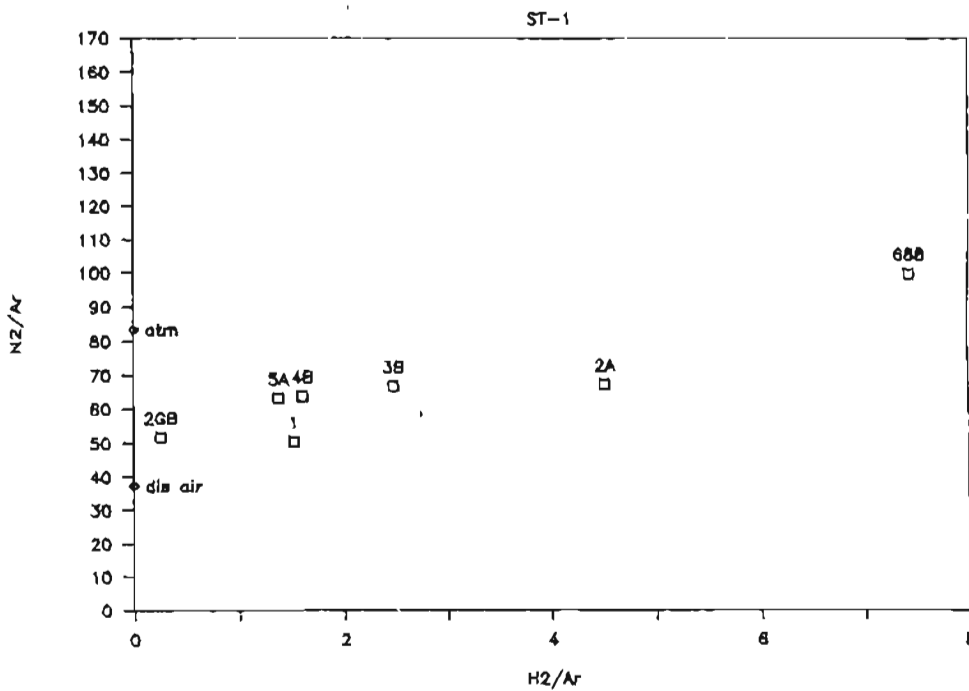
Figure 5. N_2/Ar vs. H_2/Ar plot for well ST-1 gases, Makushin geothermal area.

Reservoir Fluid Composition

Concentrations of chemical species dissolved in the aquifer waters feeding ST-1 at the 593 m fracture were calculated using ENTHALP, a program originally developed by Truesdell and Singers (1973) and recently updated by Singers and Henley (personal commun., 1984). Results of the computer calculations in molal units are given in table 9. Water analysis 2W was used with both gas analyses 2G-A and 2G-B. Because the 2G-B gas sample is considered more reliable, only the 2W, 2G-B modal composition was used in determining the average constituent concentrations and standard deviations. The average pH of ST-1 waters at the reported flowing down-hole temperature is 5.6, compared to neutral pH of 5.65 for waters at this temperature.

The partial pressures of CO_2 and H_2S in the aquifer waters are given in table 10. The average PCO_2 in 1983 was 0.58 bars compared to 0.49 bars in 1984. PH_2S also declined from 0.005 bars in 1983 to 0.004 bars in 1984.

The oxygen partial pressures, PO_2, of the ST-1 fluids can be estimated from the relation between temperature and PO_2 determined by D'Amore and Panichi (1980),

$$\log PO_2 = 8.20 - (23643/T) \tag{1}$$

where T is the fluid temperature in °K. For 193°C, the PO_2 of the ST-1 fluids is on the order of 10^{-43} atm. A check can be made on PO_2 using the equation

$$\log PO_2 = 12.5 - 26888/T - 9/7 \log (PH_2S/PCO_2)$$
$$+ 6/7 \log PCO_2 \tag{2}$$

(D'Amore and Panichi, 1980). Using values from table 10 in equation (2) gives results nearly identical to those derived using equation (1).

Fluid Saturation

Three hydrothermally deposited minerals were found layered on the gabbronorite wallrock retrieved from the open fracture at the bottom of ST-1. The innermost layer was composed primarily of quartz; the second layer was mostly calcite; while the outermost layer consisted primarily of anhydrite. The degrees of saturation of SiO_2, $CaCO_3$, and $CaSO_4$ were examined to determine whether any of these minerals are presently being deposited in the system.

The solid curve in figure 6 is the solubility of quartz in water at the vapor pressure of the solution from Fournier and Potter, 1982. All the samples obtained from ST-1 are slightly supersaturated with respect to the measured bottom-hole temperature of 193°C. The quartz-silica equilibrium

Table 9. Concentrations of chemical species in m moles/1000 gm H_2O for reservoir waters at 193°C with gas.

Sample Water	Gas	pH	Li	Na	K	Cs	Mg	Ca
71	1	5.9	1.4	76.6	5.9	0.009	0.004	2.9
74	2A	5.9	1.4	75.3	6.3	0.009	0.002	2.8
75	3B	5.7	1.4	74.7	6.0	0.009	0.002	2.9
76	4B	5.4	1.3	72.7	5.7	0.010	0.002	2.7
77	5A	5.7	1.3	77.0	5.7	0.010	0.002	3.0
1W	1G-C	5.1	1.3	70.2	5.7	0.009	0.004	2.7
2W	2G-A	5.9	1.3	71.2	5.5	0.009	0.004	2.7
2W	2G-B	5.8	1.3	71.2	5.5	0.009	0.004	2.7
Average*		5.6	1.3	74.0	5.8	0.009	0.003	2.8
Std. dev.*		0.3	0.1	2.4	0.2	0.003	0.001	0.1

Sample Water	Gas	Fe	Al	F	HF	Cl	NaCl	KCl
71	1	nd	nd	0.052	0.002	86.7	2.41	0.077
74	2A	nd	nd	0.053	0.003	86.3	2.36	0.083
75	3B	nd	nd	0.051	0.005	85.1	2.32	0.079
76	4B	nd	nd	0.041	0.006	80.8	2.17	0.072
77	5A	0.002	0.00068	0.045	0.003	84.3	2.36	0.074
1W	1G-C	0.004	nd	0.040	0.015	83.9	2.17	0.075
2W	2G-A	0.003	0.00013	0.053	0.003	84.7	2.21	0.073
2W	2G-B	0.003	0.00013	0.052	0.003	84.7	2.21	0.073
Average*		0.003	-	0.048	0.006	84.5	2.3	0.076
Std. dev.*		0.002	-	0.005	0.004	1.8	0.1	0.003

Sample Water	Gas	Br	SO_4	HSO_4	$NaSO_4$	KSO_4	$MgSO_4$	$CaSO_4$
71	1	0.15	0.22	0.002	0.44	0.021	0.003	0.13
74	2A	0.14	0.22	0.003	0.43	0.022	0.002	0.12
75	3B	0.13	0.21	0.004	0.42	0.021	0.002	0.12
76	4B	0.14	0.20	0.006	0.39	0.019	0.002	0.11
77	5A	0.15	0.20	0.003	0.41	0.019	0.002	0.12
1W	1G-C	0.13	0.24	0.017	0.45	0.023	0.003	0.13
2W	2G-A	0.13	0.25	0.002	0.48	0.023	0.003	0.14
2W	2G-B	0.12	0.25	0.003	0.48	0.023	0.003	0.14
Average*		0.14	0.22	0.005	0.43	0.021	0.002	0.12
Std. dev.*		0.01	0.02	0.005	0.03	0.002	0.001	0.01

Sample Water	Gas	HBO_2	BO_2	SiO_2	H_4SiO_4	H_3SiO_4	As
71	1	5.4	0.007	4.9	4.9	0.009	0.14
74	2A	5.3	0.005	5.0	5.0	0.007	0.13
75	3B	5.3	0.004	5.0	5.0	0.005	0.15
76	4B	5.0	0.002	4.6	4.6	0.002	0.15
77	5A	5.2	0.004	4.9	4.9	0.006	0.15
1W	1G-C	nd	nd	4.8	4.8	0.001	0.14
2W	2G-A	5.5	0.006	4.8	4.8	0.008	0.13
2W	2G-B	5.5	0.005	4.8	4.8	0.006	0.13
Average*		5.3	0.005	4.9	4.9	0.005	0.14
Std. dev.*		0.2	0.002	0.1	0.1	0.002	0.01

Sample Water	Gas	H_2CO_3	HCO_3	$CaCO_3$	$CaHCO_3$	H_2S	HS
71	1	4.3	0.38	0.0010	0.20	0.09	0.009
74	2A	5.2	0.34	0.0007	0.17	0.23	0.017
75	3B	4.6	0.22	0.0003	0.11	0.15	0.008
76	4B	5.0	0.13	0.0001	0.06	0.18	0.005
77	5A	4.7	0.25	0.0004	0.14	0.14	0.009
1W	1G-C	5.3	0.06	0.0002	0.03	0.16	0.002
2W	2G-A	3.1	0.25	0.0006	0.12	0.11	0.010
2W	2G-B	4.0	0.25	0.0005	0.12	0.11	0.008
Average*		4.7	0.23	0.0004	0.12	0.15	0.008
Std. dev.*		0.5	0.10	0.0003	0.05	0.04	0.004

*Average and standard deviation does not include 2W, 2G-A.

Table 10. Partial pressure of CO_2 and H_2S in solution, reservoir conditions.

Sample	millimole fraction in total fluid		Partial pressure bars	
	CO_2	H_2S	CO_2	H_2S
1983:				
MVTW-1	0.0882	0.0018	0.55	0.0036
MVTW-2A	0.1026	0.0031	0.64	0.0062
MVTW-3B	0.0893	0.0022	0.56	0.0043
MVTW-4B	0.0943	0.0033	0.60	0.0065
MVTW-5A	0.0909	0.0023	0.57	0.0045
Average	0.0931	0.0025	0.58	0.0050
Std. dev.	0.0052	0.0006	0.03	0.0011
1984:				
MVTW-1W	0.0979	0.0029	0.62	0.0057
MVTW2G-A	0.0601	0.0018	0.38	0.0035
MVTW2G-B	0.0749	0.0016	0.47	0.0032
Average	0.0776	0.0021	0.49	0.0041
Std. dev.	0.0156	0.0006	0.10	0.0011
All samples				
Average	0.0873	0.0024	0.55	0.0047
Std. dev.	0.0128	0.0006	0.08	0.0012

temperature for the ST-1 waters is ~207°C, which suggests that the waters have cooled before entering the borehole.

The solid curve in figure 7 is the calcite saturation curve, and the crosses are the values for ST-1 waters as determined by ENTHALP. The ST-1 waters are all undersaturated at 193°C. However, calcite was found deposited on an instrument cable that was left in the borehole for several days in mid-July, 1984. The ST-1 waters apparently became supersaturated with respect to calcite as they boiled upon ascending the borehole. The potential for calcite scaling of production well boreholes therefore exists and must be reckoned with in future development.

An estimate of the temperature of deposition of the calcite was obtained by determining the degree of fractionation of ^{18}O between the water and the calcite. The $\delta^{18}O$ of the calcite scale was analyzed by the Stable Isotope Laboratory at Southern Methodist University and determined to be +0.6 with respect to standard mean ocean water (SMOW). Using a value of -10.2 for $\delta^{18}O$ of the water (cf. table 13) and the fractionation equation of O'Neil and others (1969) gives a temperature of deposition of -177°C.

The state of anhydrite saturation in ST-1 waters is shown by crosses in figure 8. The anhydrite equilibrium solubility curve (solid) is taken from Helgeson (1969), with the activity product of anhydrite as defined by Helgeson plotted on the Y-axis. Activity coefficients and molal concentrations for Ca and SO_4 ionic species were determined using ENTHALP. As can be seen
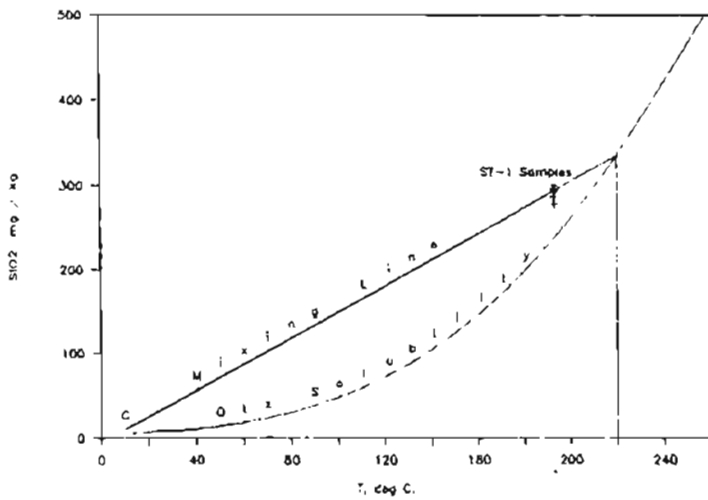
Figure 6. Quartz solubility curve and values for well ST-1, Makushin geothermal area. Mixing time for a cold-water end member, C, and the average value of ST-1 silica concentrations is also shown.

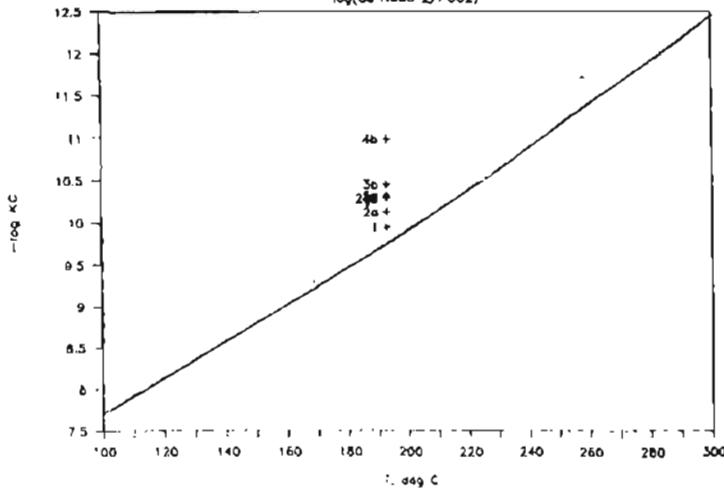
Figure 7. Calcite saturation curve and values for well ST-1, Makushin geothermal area.
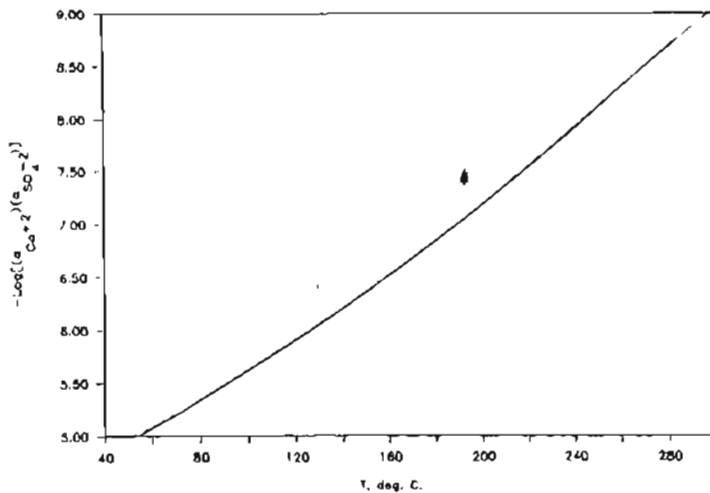
Figure 8. Anhydrite saturation curve and values for well ST-1, Makushin geothermal area.

- 23 -

Table 11. $^{18}O/^{16}O$ in anhydrite obtained from test well core.[1]

Depth, m (ft)	$^{18}O/^{16}O$ - $CaSO_4$, WRT SMOW	T °C, equil.[2]	
		[3]	[4]
148 (486)	-2.98	351	249
592.5 (1944)	-1.87	319	226
593.1 (1946)	-0.91	295	208

[1] Analyzed at U.S. Geological Survey, Menlo Park.

[2] T °C. equil. = equilibration fractionation temperature assuming $^{18}O/^{16}O$ for H_2O is -10.2, the current reservoir water value (U.S. Geological Survey analysis).

[3] Temperature computed using Lloyd (1968) fractionation equation:

$$1000 \ln = 3.88 \ (10^6)/T^2 - 2.90, \ T = °K.$$

[4] Temperature computed using fractionation equation of Chiba and others (1981):

$$1000 \ln = 3.21 \ (10^6)/T^2 - 4.72, \ T = °K.$$

from the figure, the waters would have to be somewhat warmer for anhydrite deposition to occur at ST-1.

An estimate of the temperature at which the anhydrite deposition occurred was obtained by determining the degree of fractionation of ^{18}O between the anhydrite and the reservoir waters (table 11). Using the fractionation equation of Chiba and others (1981) and assuming a $\delta^{18}O$ of (-10.2) for the reservoir waters gives a temperature of deposition of ~208°C for anhydrite found at the bottom-hole fracture. In contrast, using the same technique, anhydrite found in a vein 592.5 m deep has an estimated temperature of deposition of 226°C, whereas anhydrite found in a vein 148 m deep has an estimated temperature of deposition of 249°C.

ISOTOPE ANALYSES

Oxygen 18 and Deuterium

Results of oxygen and deuterium isotope analyses of water and steam samples that were collected using the mini-cyclone separator at the ST-1 wellhead are given in table 12. The corresponding pre-flash isotopic compositions of ST-1 waters are given in table 13 and plotted in figure 9. Because of suspected sampling and analyses problems, samples 76 and 84-1 are not included on figure 9. Also plotted on figure 9 are isotopic compositions of local meteoric waters (LMW), low Cl, high HCO_3-SO_4 thermal spring waters, Cl-rich thermal spring waters, the meteoric water line defined by Craig (1961), and the Adak precipitation line (Motyka, 1982).

The majority of meteoric and low-chloride thermal spring water samples plot to the left of both meteoric water lines; chloride thermal spring and ST-1 waters plot to the right. Meteoric stream waters whose source regions lie at mid- to lower elevations on the volcano have heavier isotopic compositions than meteoric stream waters whose source regions are at higher elevations. The range of isotopic compositions for low-chloride thermal spring

Table 12. Makushin Valley test well ST-1, oxygen and deuterium isotope analyses--steam and water. (Parts permil with respect to SMOW).

Sample OGGS no.	USGS no.	Date	Water D/H (SMU)	$^{18}O/^{16}O$ (SMU)	$^{18}O/^{16}O$ (USGS)	Steam D/H (SMU)	$^{18}O/^{16}O$ (SMU)	$^{18}O/^{16}O$ (USGS)
71	1	8/27/83	-79	-9.7	-9.2	-97	-13.9	-13.45
74	2	9/1/83	-77	-10.05	-9.5	-90	-13.2	-13.05
75	3	9/2/83	-77.5	-9.95	-9.6	-90	-13.2	-13.05
76	4	9/2/83	-77.5	-8.4	-9.6	-87.3	-13.15	-12.85
77	5	9/3/83	-77.6	-9.8	-9.6	-88.3	-13.1	-13.0
84-1		8/4/84	-66	-10.25	-	-86	-11.25	-
84-2		8/7/84	-81.5	-9.95	-	-90	-12.3	-

SMU = Southern Methodist University, Stable Isotope Laboratory; R. Harmon and J. Borthwick, analysts.
USGS = U.S. Geological Survey, Menlo Park, C. Janik, analyst.

Table 13. Makushin Valley test well ST-1, stable isotope analyses corrected to reservoir conditions. (Parts permil with respect to SMOW).

1983	71	74	75	76	77	Average	S.D.
D/H (SMU)	-81	-78.5	-79	-78.5	-78.5	-79.1	1.1
$^{18}O/^{16}O$ (SMU)	-10.3	-10.4	-10.3	(-8.8)[1]	-10.1	-10.3	0.13
$^{18}O/^{16}O$ (USGS)	-10.2	-9.9	-10.0	-9.9	-9.9	-10.0	0.13

1984	84-1[2]	84-2
D/H (SMU)	-69	-83
$^{18}O/^{16}O$ (SMU)	-10.4	-10.2

[1] Suspect value; not used in computing average.
[2] A large amount of chloride was detected in the 84-1 condensate indicating incomplete separation. Values for this sample are therefore not considered to accurately represent reservoir isotope composition.

waters directly overlaps the mid-range for meteoric waters, which indicates that thermal waters are derived from meteoric waters at mid-elevations.

On the basis of similarities in deuterium composition of meteoric and thermal waters, reservoir waters in the majority of explored hydrothermal systems are thought to be derived mostly from meteoric sources (Craig, 1963). The Makushin system is no exception, although the high chloride concentration suggests a small amount of seawater contamination. The seawater mixing would tend to shift the deuterium to slightly heavier values. Deuterium values of ST-1 waters correlate with the mid- to upper range for meteoric waters, which suggests that waters charging the reservoir feeding ST-1 originated as precipitation on the mid- to lower flanks of the volcano
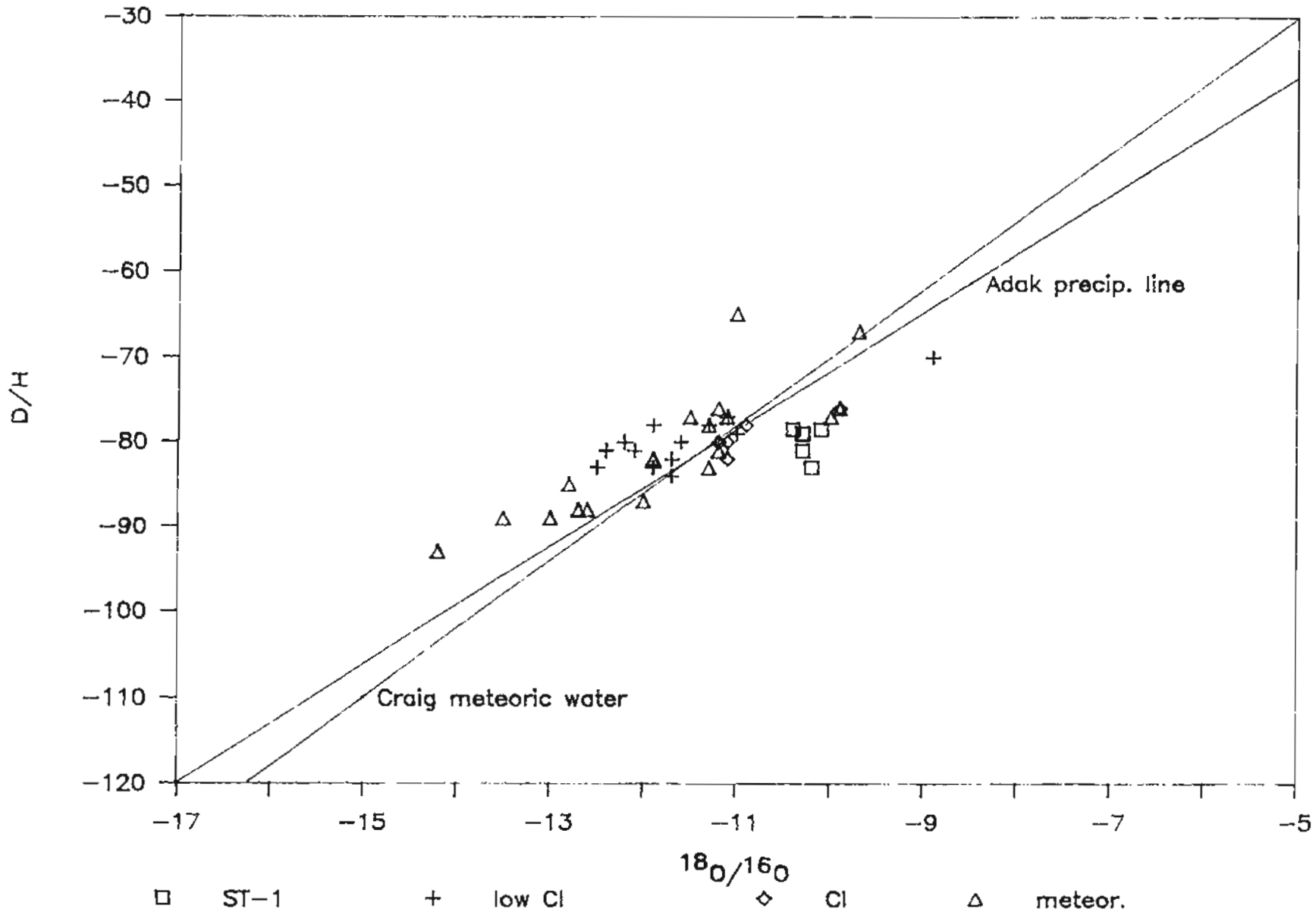
Figure 9. Stable isotope analyses of well ST-I, thermal springs, and meteoric waters from the Makushin geothermal area.

if seawater contamination is minimal. These meteoric waters probably filtrate in the reservoir system through fractures on the periphery of the hydrothermal system.

ST-1 waters show a positive shift of 1 permil in $\delta^{18}O$ with respect to the two meteoric water lines and a shift of about 1.5 permil with respect to Makushin meteoric waters. Such shifts are commonly observed in geothermal systems and are caused by high-temperature oxygen isotope exchange between the thermal waters and the reservoir rock. Similar shifts are not seen for deuterium because of the lack of hydrogen-bearing minerals in the reservoir rock. The magnitude of an oxygen isotope shift is a function of water temperature, duration of contact, and the magnitude of the difference in the water vs. rock isotopic compositions. The gabbronorite reservoir rock at Makushin was found to have a $\delta^{18}O$ composition ranging from -4.0 for highly altered rocks to +2.8 for slightly altered rocks (table 14). The difference in unaltered vs. altered composition indicates isotope exchange has occurred in the Makushin hydrothermal system, and thus the $\delta^{18}O$ shift observed for ST-1 waters is probably due to high temperature exchange. However, a part of the shift could also be due to seawater mixing.

Table 14. ST-1 whole rock oxygen isotope data.[1]

Sample #	$^{18}O/^{16}O$	Description
ST-1-201	-4.0	Gabbro. Plagioclase altered to clays.
ST-1-664	-2.7	Gabbro altered to wairakite. Steam entry.
ST-1-1066	-2.0	Albite-K spar-biotite-epidote vein.
ST-1-1638	+2.8	"Unaltered" gabbro. Pyroxenes altered to anthophyllite-cummingtonite.
ST-1-1937	-0.1	Chloritically altered gabbro.
- -	+6.4	Average of 11 Makushin area volcanic rocks.

[1] Analyzed at U.S. Geological Survey, Menlo Park, CA., I. Barnes lab.

Tritium

Results of tritium analyses for waters collected from ST-1 and from various springs and streams are given in table 15 and plotted in figure 10. Panichi and Gonfiantini (1978) have reviewed the use of tritium as an indicator of age and mixing of waters in geothermal systems. Tritium was introduced into the atmosphere in large quantities during the years of thermonuclear weapons testing following 1952. Since the test ban treaty of 1963, tritium in the atmosphere has steadily diminished, but far exceeds pre-1952 levels. Because of its relatively short half-life (12.3 yr), tritium provides a good marker for waters of recent age. To provide a comparison for Makushin waters, the tritium levels in 1980 precipitation at Anchorage

(the nearest station and most recent year for which data are available) are also plotted on figure 10. The weighted-average tritium content of precipitation in Anchorage in 1980 was 29 Tritium Units (T.U.), with a seasonal variation ranging from a winter minimum of 16 T.U. to a late-spring maximum of 51 T.U.

Table 15. Analyses of tritium in waters from Makushin geothermal area.

Sample code	Locality	Date collected	TU
MVTW-3	ST-1	9-02-83	0.46±0.08
MVTW-5	ST-1	9-03-83	0.29±0.08
RM82MV-cs	cold str., Mk. Val	7-21-82	11.3±0.3
RM82MV-ru	hot spr. M-c	7-22-82	16.4±0.4
RM82GV-E	hot spr. G-j	7-20-82	36.5±0.8
RM82GV-wv	hot spr. G-1	7-20-82	28.2±0.7
RM82GV-24	hot spr. G-m	7-20-82	10.5±0.3
RM82PV	hot spr. G-p	7-20-82	6.1±0.2

Analyst: H. Gote Ostlund, U. of Miami, Miami, Florida.
TU = Tritium units.

A water sample collected from a cold stream in Makushin Valley fed by snow melt has a tritium level of 11 T.U., which is consistent with winter precipitation. Tritium concentrations in low-Cl, HCO_3-SO_4 thermal springs ranged from 16 to 36 T.U., which indicates these waters are very young and probably originated as local precipitation. The two samples collected from Cl-rich thermal springs, although lower in tritium (6 and 10 T.U.) than any of the other spring waters sampled, are still high enough in tritium to indicate that thermal waters are probably mixing with meteoric waters near the surface before emerging as springs.

In contrast, two water samples collected from ST-1 have tritium concentrations of 0.3 and 0.5 T.U. Concentrations this low indicate the waters are at least 25 yr old, probably older (Panichi and Gonfiantini, 1978). Furthermore, the low level of tritium in the ST-1 waters argues against any mixing of present-day meteoric water at ST-1. Tritium concentrations in waters older than 60 yr would be expected to be <0.1 T.U. (Truesdell and Hulston, 1980). If we assume this value as the limit for deep thermal waters at Makushin and use 29 T.U. for a cold water end member, then the fraction of any present-day meteoric water would be at most 1.4 percent.

Carbon 13 in Carbon Dioxide

Results of analyses of $\delta^{13}C$ composition of CO_2 gas collected from ST-1 are given in table 16 and plotted in figure 11. Also plotted are $\delta^{13}C$ compositions of CO_2 gas collected from various fumaroles and hot springs. Mantle-derived CO_2 is thought to have $\delta^{13}C$ compositions ranging from -4 to -8 permil (Craig, 1953; Welhan, 1981), while CO_2 from organic-sedimentary
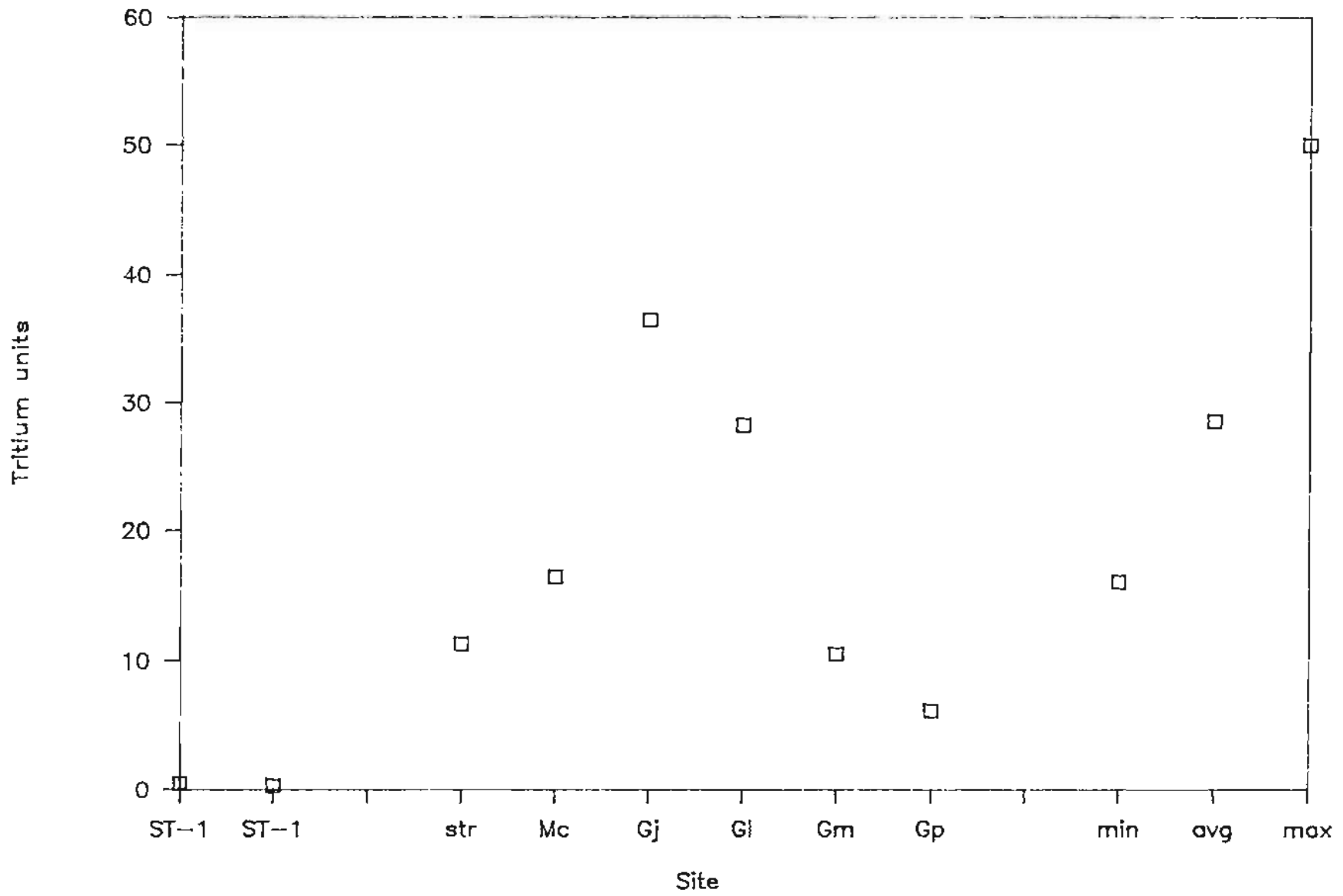
Figure 10. Tritium analyses of well ST-1, thermal springs, and ground water streams in the Makushin geothermal area. Sample sites are keyed to table 15. The three values at right give 1980 data from Anchorage for comparison.

Table 16. Makushin Valley test well ST-1, Unalaska Island, Alaska, carbon isotope analyses, CO_2 in gas and steam.[1]

Sample #	Date collected	T, °C Sep	$^{13}C_{PDB}$
MVTW-1	8/27/83	120	-13.3
MVTW-3	9/02/83	134	-13.5
MVTW-4	9/02/83	148	-13.3
MVTW-5	9/03/83	148	-13.3
MVTW-1G-C	8/04/84	130	-15.1
MVTW-2G-A	8/07/84	131	-15.0
MVTW-2G-B	8/07/84	131	-15.1

[1] C. Janik, U.S. Geological Survey, Menlo Park, California, analyst.

sources have $\delta^{13}C$ values < -11 permil. The heaviest $\delta^{13}C$ compositions at the Makushin geothermal area were found for the samples from the summit and from the superheated fumarole in field 3. The majority of sampled gases, including those from ST-1 in 1983, fall in the narrow range of -11.5 to -13.5 permil, which lies at the upper end of values for organic-sedimentary CO_2. The $\delta^{13}C-CO_2$ in 1984 ST 1 fluids was found to be -15 permil, 1.5 permil less than the 1983 values. This change could be attributable in part to fractionation between the CO_2 and the calcite being deposited on the well casing.

The $\delta^{13}C-CO_2$ compositions at Makushin suggest that the CO_2 is being generated in part from thermogenic breakdown of organic-sedimentary material underlying the volcano, with a magmatic intrusion acting as the heat source. These thermogenic gases then mix with CO_2 outgassing from the magma body itself and migrate into the hydrothermal reservoir.

Helium Isotopes

Samples of gases obtained from ST-1 were analyzed for helium isotope compositions. Enrichments in ^3He with respect to atmospheric levels have been correlated with magmatic activity on a worldwide basis, and the excess ^3He is thought to be derived from the mantle (Craig and Lupton, 1981). Samples of gases for $^3He/^4He$ testing were collected in 50-cc glass flasks (Corning 1720) fitted with high-vacuum stopcocks. The procedures followed for gas extraction, measurement of absolute helium amounts, mass spectrometer measurement of $^3He/^4He$ ratios, and application of He/Ne correction for air contamination are described in Lupton and Craig (1975), Torgersen and others (1982), and Poreda (1983).

Table 17 presents helium isotope data for ST-1 and for gases collected from fumaroles and hot springs in the Makushin geothermal area. The R/R_a value ($^3He/^4He$ ratio of sample vs. air) of 7.8 obtained for the summit fumaroles falls within the range of values of 5 to 8 found at other volcanic vents in the Aleutian Arc and convergent margin volcanic arc settings else-
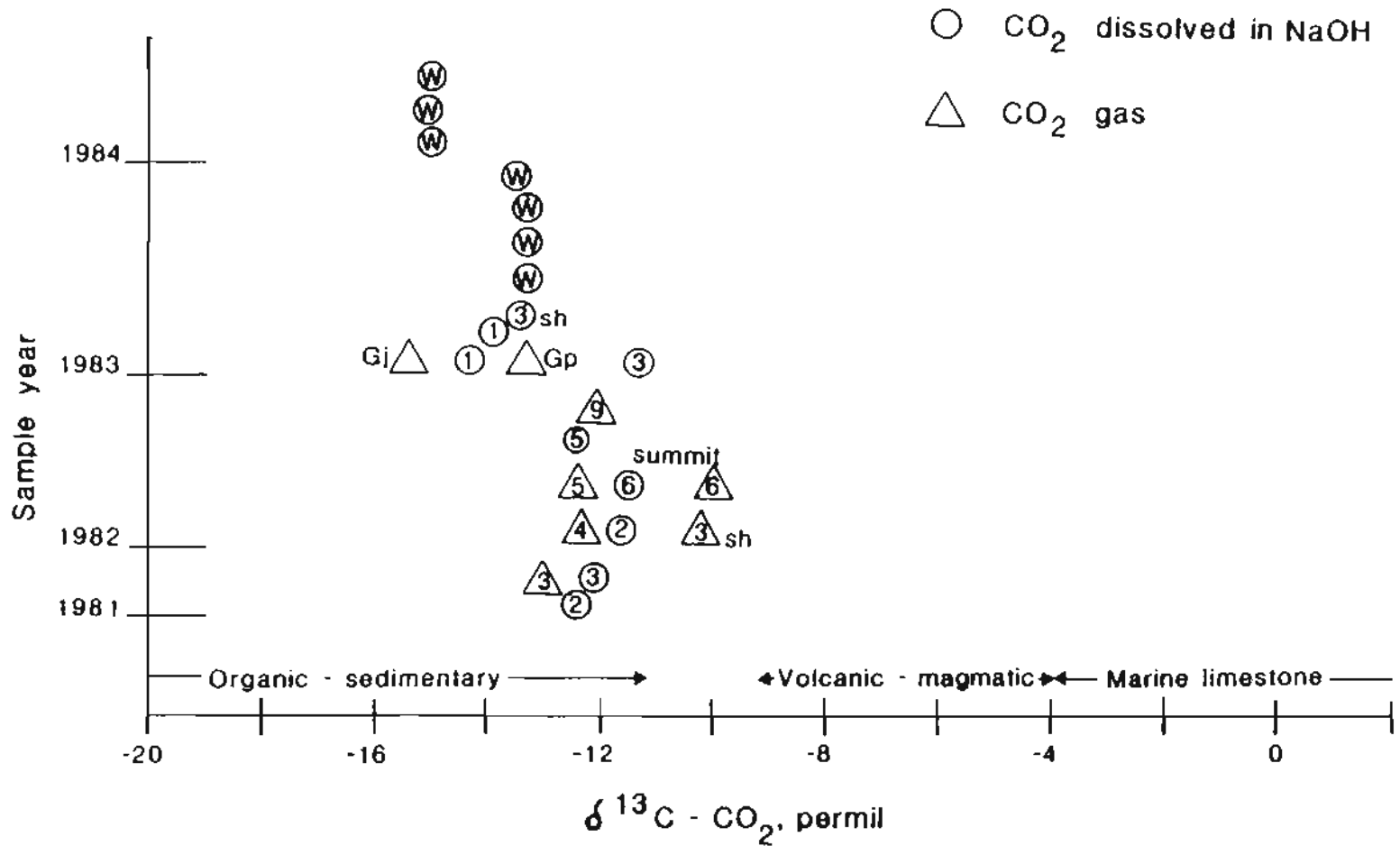
Figure 11. $\delta^{13}C$ values of CO_2 in gases from well ST-1 (W) (table 16), and fumaroles, and hot springs in the Makushin geothermal area (table A9).

Table 17. Helium isotope data, Makushin geothermal area.[1]

Location	Year collected	R/Ra[2]	(He/Ne)/air	Rc/Ra[3]
Fum. field #1	1980	6.6	110.0	6.6
Fum. field #2	1980	4.9	37.0	5.1
Fum. field #2	1981	5.0	94.0	5.1
Fum. field #3, sp	1981	3.8	24.0	4.0
Fum. field #3	1981	4.4	53.0	4.5
Fum. field #3, SH	1982	4.1	11.4	4.4
Fum. field #5	1982	5.0	50.0	5.1
Fum. field #6, SU	1982	7.8	1500.0	7.8
Fum. field #7	1983	5.9	300.0	5.9
Spring G-p	1983	(1.3)[4]	(1.5)[4]	(1.9)[4]
Test well ST-1	1983	3.6	41.0	3.7

[1] R. Poreda analyst, Scripps Institute of Oceanography, Stable Isotope Lab.

[2] $R = {}^3He/{}^4He$ ratio in sample, $Ra = {}^3He/{}^4He$ ratio in air.

[3] Rc = Sample ratio corrected for air contamination using He/Ne ratios.

[4] Helium concentration in sample was extremely low.

where in the world (fig. 12) (Craig and others, 1978a; Poreda, 1983). R/R_a values for gases from the flanks of Makushin are all lower than those from the summit, with the lowest values occurring at fumarole field 3 and for ST-1.

Variations in R/R_a have been found at other volcanically related geo-thermal systems (Craig and others, 1978b; Welhan, 1981; Torgersen and others, 1982; Torgerson and Jenkins, 1982). A high value for R/R_a in gases from geothermal systems suggests a more direct connection to magmatic sources with little or no crustal contamination--although it may also result from leaching of young volcanic rock (Truesdell and Hulston, 1980). Lower values indicate a greater crustal influence of radiogenic ^4He.

If the summit value of R/R_a is taken to represent the $^3He/^4He$ ratio of the parent cooling magma, then the R/R_a values for sites on the flanks of the volcano represent varying degrees of mixing with a crustal ^4He component. One effective method for increasing the amount of ^4He present in the gases is by hot-water interaction with and leaching of reservoir wall rock. At Makushin the host reservoir rock is a gabbronoritic pluton. Cal-culations by Torgersen and Jenkins (1982) indicate that the R/R_a ratio in an intrusive would fall to <0.1 through radiogenic decay of U and Th for emplacement ages >1.0 Ma. A mixing of 55 percent crustal He and 45 percent magmatic He would produce an R/R_a value of 3.7 with 7.8 for the magmatic component and 0.1 for the crustal component.

Makushin Geothermal Area

Helium Isotope Data

$$R_c/R_a$$

R = 3He / 4He

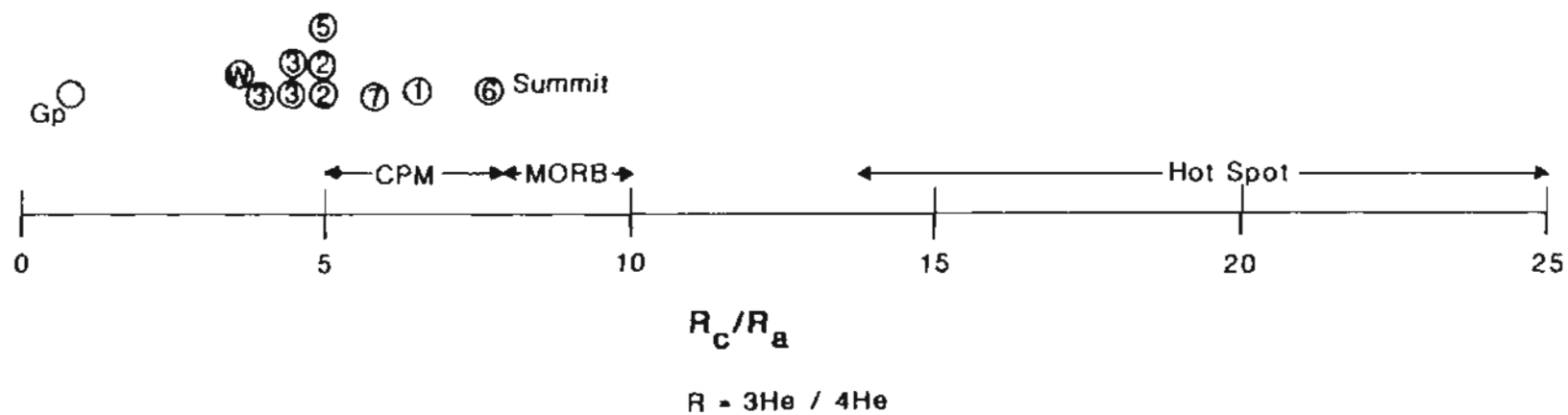Table 12. He isotope analyses from well ST-1 (W), and fumaroles, and hot springs in the Makushin geothermal area (table 17) compared with values from various tectonic settings.

GEOTHERMOMETRY

The results of applying water, isotope, and gas geothermometers to ST-1 thermal fluid geochemistry are given in tables 18, 19, and 20 and compared in figure 13.

Nearly all the geothermometers that were applied to ST-1 predict temperatures substantially higher than the reported flowing bottom-hole temperature of 193°C. Only two of the geothermometers, the chalcedony geothermometer of Fournier (1981) and the Na-Li geothermometer of Foullic and Michard (1981), give temperatures in agreement with the flowing bottom-hole temperature of 193°C reported by RGI. Free quartz is found in the gabbronorite, and, for temperatures greater than 180°C, quartz is the silica phase most likely to control dissolved silica (Fournier, 1981). Thus, for ST-1 the quartz temperatures which average about 207°C are the more appropriate estimates to use.

Of the three Na-K geothermometers that have been proposed, Arnorsson's (1983) equation for basaltic rocks is chosen as the most appropriate for ST-1 since the host reservoir rock is a gabbronorite. The average temperature of 225°C given by this geothermometer is slightly higher than Truesdell's (1976) Na-K geothermometer and 17°C lower than Fournier's (1981) geothermometer for Na-K. Because calcite appears to have precipitated during the ascent and boiling of the ST-1 thermal waters, caution must be exercised in applying the Na-K-Ca geothermometer of Fournier and Truesdell (1973). Disequilibrium removal of Ca from the ST-1 water would yield temperature estimates that are too high. However, the close agreement of the Na-K-Ca geothermometer with the results of Arnorsson's (1983) Na-K geothermometer suggests Ca removal by calcite precipitation is too small to appreciably affect the Na-K-Ca geothermometer.

The gas geothermometer of D'Amore and Panichi (1980) is based on an empirical relationship between ratios of H_2S, H_2, and CH_4 to CO_2 and the partial pressure of CO_2 in the reservoir. For analyses in which CH_4 was present in only trace amounts, a value of 0.001 mole percent was used in the computations. The H_2S geothermometer of D'Amore and Truesdell (1983) is based on equilibria between constituents affecting H_2S concentrations. The CO_2 geothermometer of Arnorsson and others (1983) is based on an empirical relationship between temperature and PCO_2 observed in geothermal waters from drillholes in Iceland. The average temperature given by the gas geothermometers, 217, 217, and 219°C, respectively, are in close agreement with each other and the Na-K geothermometers of Truesdell (1976) and Arnorsson (1983) and the Na-K-Ca results. However, calcite precipitation and interactions between the thermal fluids and the well casing could be affecting gas compositions, and caution must be exercised in interpreting these geothermometers.

Table 18. Geothermometry for Webre separator waters from Makushin Valley test well ST-1 corrected for reservoir conditions. (Temperatures in °C.)

Sample #	Date	Qz. cond (1)	Chal. cond (2)	Na/K (3)	Na/K (4)	Na/K (5)	Na-K-Ca (6)	Na/Li (7)
RM83-71	8-27-83	208	191	240	216	222	224	193
RM83-74	9-01-83	208	192	247	226	231	229	194
RM83-75	9-02-83	209	193	243	221	227	227	196
RM83-76	9-02-83	203	186	241	218	224	225	194
RM83-77	9-03-83	208	191	238	213	220	223	193
RM84-1W	8-04-84	nd	nd	245	223	229	227	194
RM84-2W	8-07-84	206	189	240	217	223	224	193
Average		207	190	242	219	225	226	194
Std. dev.		2	2	3	4	4	2	1

[1] Fournier and Potter, 1982, improved SiO_2 (quartz).
[2] Fournier, 1981, chalcedony.
[3] Fournier, 1981, Na/K.
[4] Truesdell, 1976, Na/K.
[5] Arnorsson, 1983, Na/K, basalt.
[6] Fournier and Truesdell, 1973.
[7] Fouillac and Michard, 1981.

Table 19. Sulfate-water $^{18}O/^{16}O$ isotope temperatures, Makushin Valley test well, ST-1.[1]

Sample #	Date collected	Temp sep. °C	$^{18}O/^{16}O-SO_4$, WRT SMOW	$^{18}O/^{16}O-H_2O$ WRT SMOW at sep	$^{18}O/^{16}O-H_2O$, WRT SMOW res	T1, °C[3]	T2, °C[4]
MVTW-74	9-01-83	135	-3.8	-9.5	-9.9	245	256
MVTW-75	9-02-83	134	-3.4	-9.6	-10.0	235	245
MVTW-76	9-02-83	148	-3.4	-9.6	-9.9	235	248
MVTW-77	9-03-83	148	-3.3	-9.6	-9.9	235	244
MVTW-1W	8-04-84	130	-3.9	-10.3[2]	-10.4[2]	230	246
MVTW-2W	8-07-84	131	-3.6	-10.0[2]	-10.2[2]	232	246
Average						235	248
Std. dev.						5	4

[1] Isotope analyses performed at U.S. Geological Survey, Menlo Park, except as noted.

[2] Analysis performed at Southern Methodist University, Stable Isotope Laboratory.

[3] Temperature calculated using method described in McKenzie and Truesdell (1977) for the case of single-stop steam-loss. The separator water composition was used for $^{18}O/^{16}O - H_2O$.

[4] Temperature calculated using the $^{18}O/^{16}O - H_2O$ value determined for the reservoir water and the equilibrium fractionation equation of Mizutani and Rafter (1969): $1000 \ln = 2.88 (10^6/T^2) - 4.1$, T=°K.

Table 20. Gas geothermometers applied to Makushin test well.

Sample #	Date sampled	T°C[1]	T°C[2]	T°C[3]
MVTW-1 DS/CJ	8-27-83	228	212	220
MVTW-2A DS/CJ	9-01-83	250	222	227
MVTW-3B DS/CJ	9-02-83	217	216	222
MVTW-4B DS/CJ	9-02-83	213	223	223
MVTW-5A DS/CJ	9-03-83	204	216	222
MVTW-1G-C RM/CJ	8-04-84	218	220	225
MVTW-2G-A RM/CJ	8-07-84	216	211	199
MVTW-2G-B RM/CJ	8-07-84	190	212	213
Average		217	217	219
Std. dev.		17	5	9

[1] Gas geothermometer of D'Amore and Panachi, 1980.
[2] H_2S geothermometer of D'Amore and Truesdell, 1980.
[3] CO_2 geothermometer of Arnorsson and others, 1983.

The water-sulfate oxygen isotope geothermometer of McKenzie and Truesdell (1977) predicts significantly higher temperatures than all but Fournier's (1981) Na-K geothermometer (table 19). Using the isotopic composition of ST-1 waters (cf. table 13) the average temperature given by this geothermometer for the reservoir is 248°C.

The highest reservoir temperatures predicted by the geothermometers indicate that the ST-1 fluid chemistry is in equilibrium with hotter parts of the reservoir and that the reservoir fluids have cooled before entering the ST-1 borehole. Differences in the quartz, cation, and sulfate-water oxygen isotope geothermometers have been observed at many other high-temperature hot-water systems and have been commonly attributed to the combination of cooling of the thermal fluids upon ascent and the differences in the re-equilibration times of the various geothermometers (Fournier, 1981). For example, quartz equilibrates fairly rapidly, on the order of days to weeks at T ~200°C, whereas the cations in saline solution equilibrate on the order of weeks to months for T ~200°C.

In contrast, the sulfate-water oxygen isotope geothermometer takes much longer to equilibrate at lower temperatures. Experimental studies by Chiba and Sakai (1985) on the fractionation of ^{18}O between H_2O and SO_4 showed the equilibration time to be weakly dependent on pH and strongly dependent on temperature. For a pH of 6 (similar to ST-1 waters) and a temperature of 250°C, the equilibration half time, $T_{1/2}$ is on the order of 10 to 20 yr. Thus, the sulfate-water oxygen isotope geothermometer is a good indicator of deep reservoir temperatures.

Temperature-pressure conditions at the bottom of ST-1 preclude boiling as a cooling mechanism and leave conduction and dilution as alternatives. The correlation of lower calculated temperatures with shorter equilibration
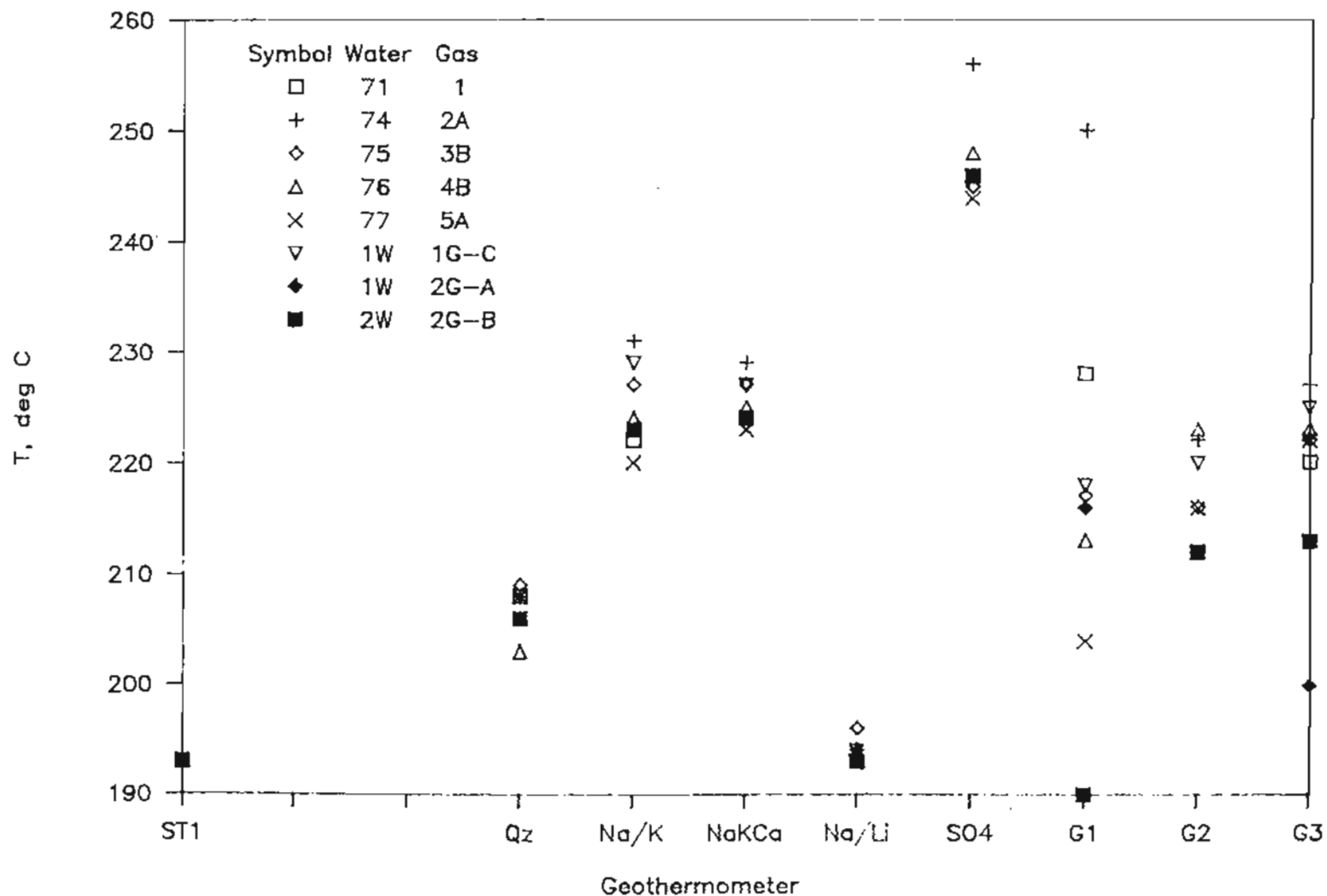
Figure 13. Comparison of geothermometry of well ST-1, Makushin geothermal area (tables 18, 19, and 20). Qz = quartz conductive of Fournier and Potter (1983); Na-K = basalt cation of Arnorsson (1983); Na-K-Ca = cation of Fournier and Truesdell (1973); Na-Li = cation of Fouillac and Michard (1981); SO_4 = $\delta^{18}O$, H_2O-SO_4 of McKenzie and Truesdell (1977); G1 = gas geothermometer of D'Amore and Panichi (1980); G2 = H_2S geothermometer of D'Amore and Truesdell (1980); G3 = CO_2 geothermometer of Arnorsson and others (1983).

times for the geothermometers applied to ST-1 fluids suggests that the thermal waters have cooled slowly by conduction upon ascent, before entering the ST-1 borehole. However, dilution may have also played a role in cooling the reservoir water and could explain the differences between the quartz and cation geothermometer temperatures. Cation geothermometers, which are based on ratios of constituents, are not as susceptible to the effects of dilution as the silica geothermometers which are directly related to silica concentrations. The effect of dilution on the Na-K-Ca geothermometer is generally negligible if the high-temperature geothermal water is much more saline than the diluting water and the diluting fraction is less than 20 to 30 percent (Fournier, 1981).

Following methods described in Truesdell and Fournier (1977), the mixing line shown on the silica vs. temperature diagram (fig. 6) uses a cold-water end member similar to surface meteoric waters (SiO_2 = 10 ppm; T = 10°C) and the average for the analyzed ST-1 silica concentrations corrected to bottom-hole conditions (291 ppm). This mixing line intersects the quartz solubility curve at a temperature of 220°C, in close agreement with both the cation geothermometers and the gas geothermometers. The estimated cold water fraction for this mixing model is 12 percent. Thus, waters entering ST-1 could have cooled by a combination of conduction from 248°C to 220-225°C and by dilution from 220-225°C to 193°C. As seen from the results of the tritium analyses, mixing with present-day cold meteoric waters appears minimal. If the mixed water is assumed to have a tritium concentration of 0.4 T.U., the average of the two ST-1 analyses, then the tritium concentration of the diluting water must be on the order of, at most, 4 T.U. If surface meteoric waters having a tritium concentration of 20-30 T.U. are the ultimate source of the diluting waters then 25-35 yr would be required for these surface waters to reach the zone of mixing. Such infiltration times are not unreasonable for most confined aquifers (Panichi and Gonfiantini, 1978).

HYDROTHERMAL ALTERATION

Methods

The description of lithology and minerals is based largely on hand-samples. As a control, selected samples were chosen for additional study by X-ray diffraction and optical petrography. Locations of the samples taken from the cores are shown on the core logs (figs. 14, 15, 16, 17, 18). Alteration minerals that could not be immediately identified by physical properties, because of either their fine-grained nature (clays) or their rarity (zeolites), were identified using X-ray diffraction. Once positively identified, these minerals could be located elsewhere in the core by their physical properties. Thin sections of representative samples, both from the core and from similar rocks at the surface, were used to assist in the description of the lithology. The lithologic units used in this paper are those of Nye and others (1984).

Figure 14. Lithologic log and temperature profile of geothermal gradient hole D-1, Makushin geothermal area.
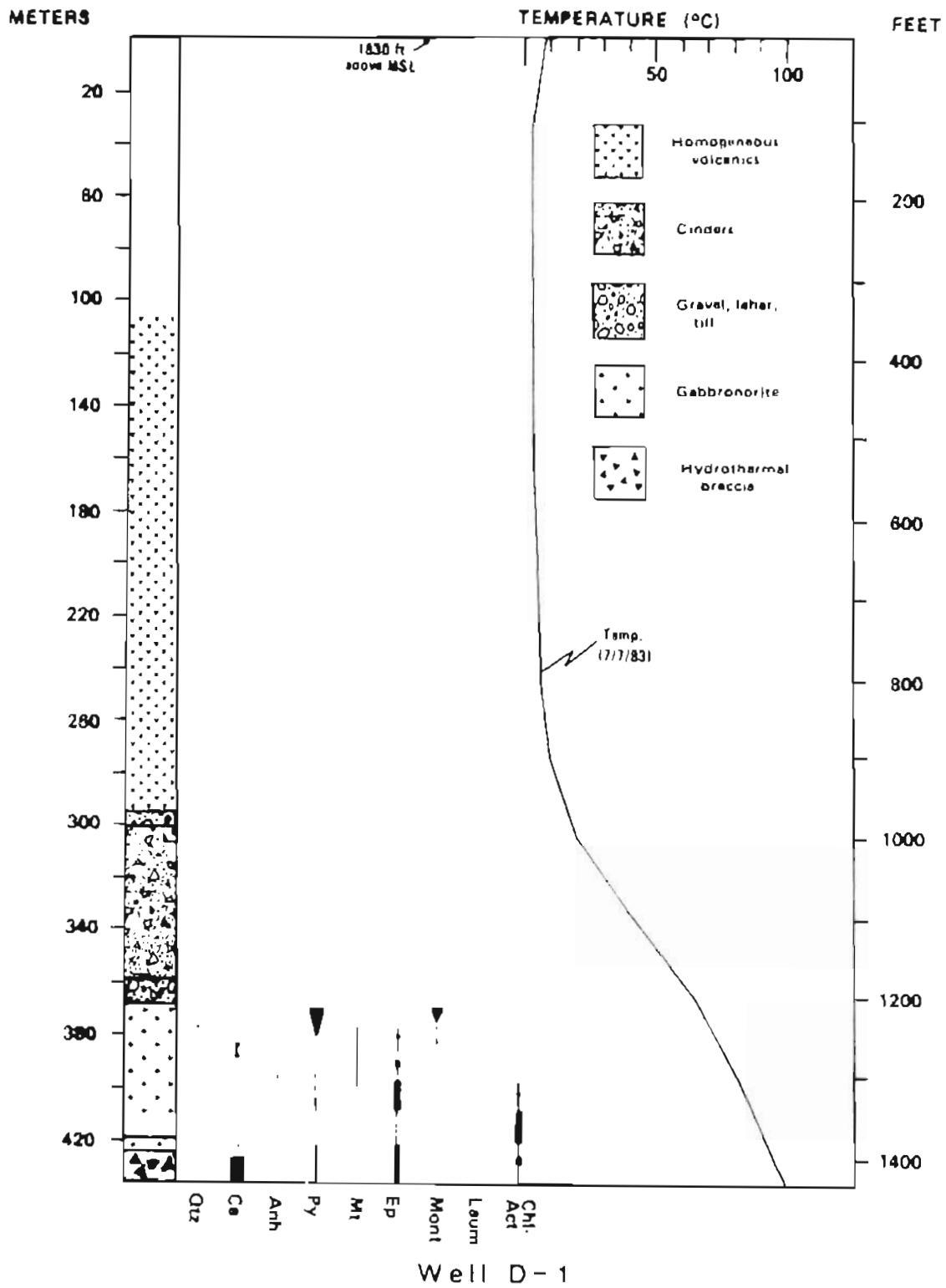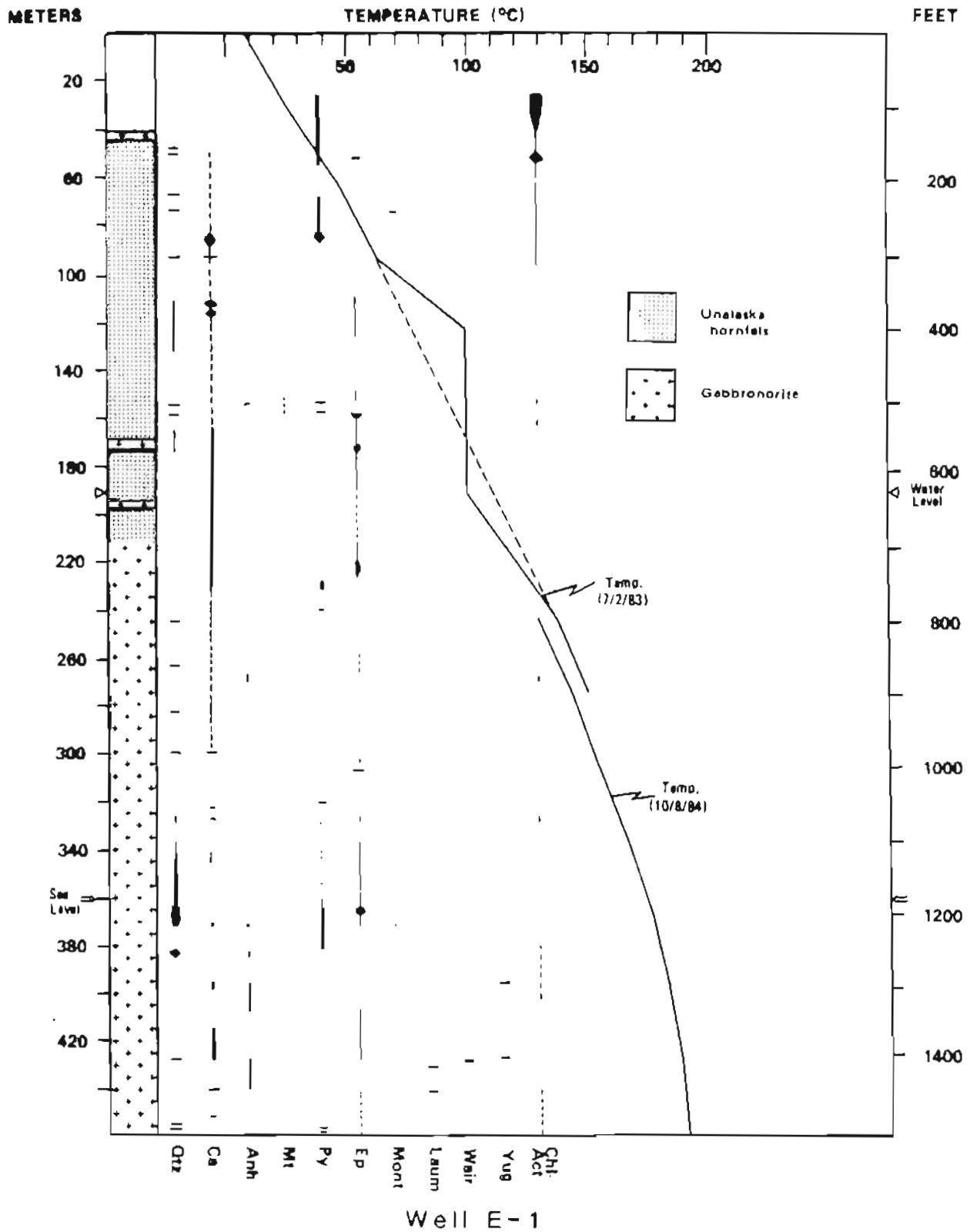
Figure 15. Lithologic log and temperature profile of geothermal gradient hole E-1, Makushin geothermal area.
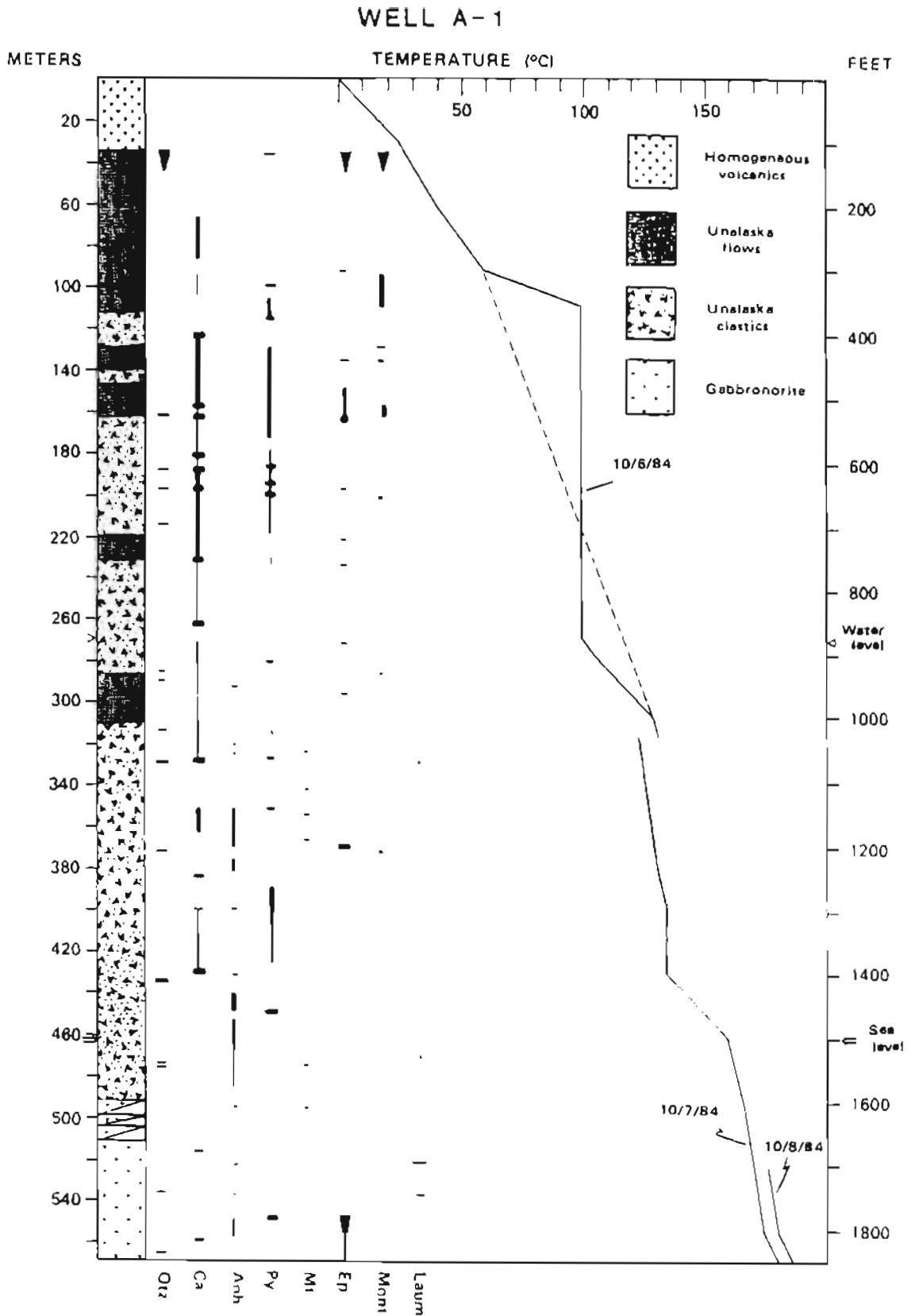
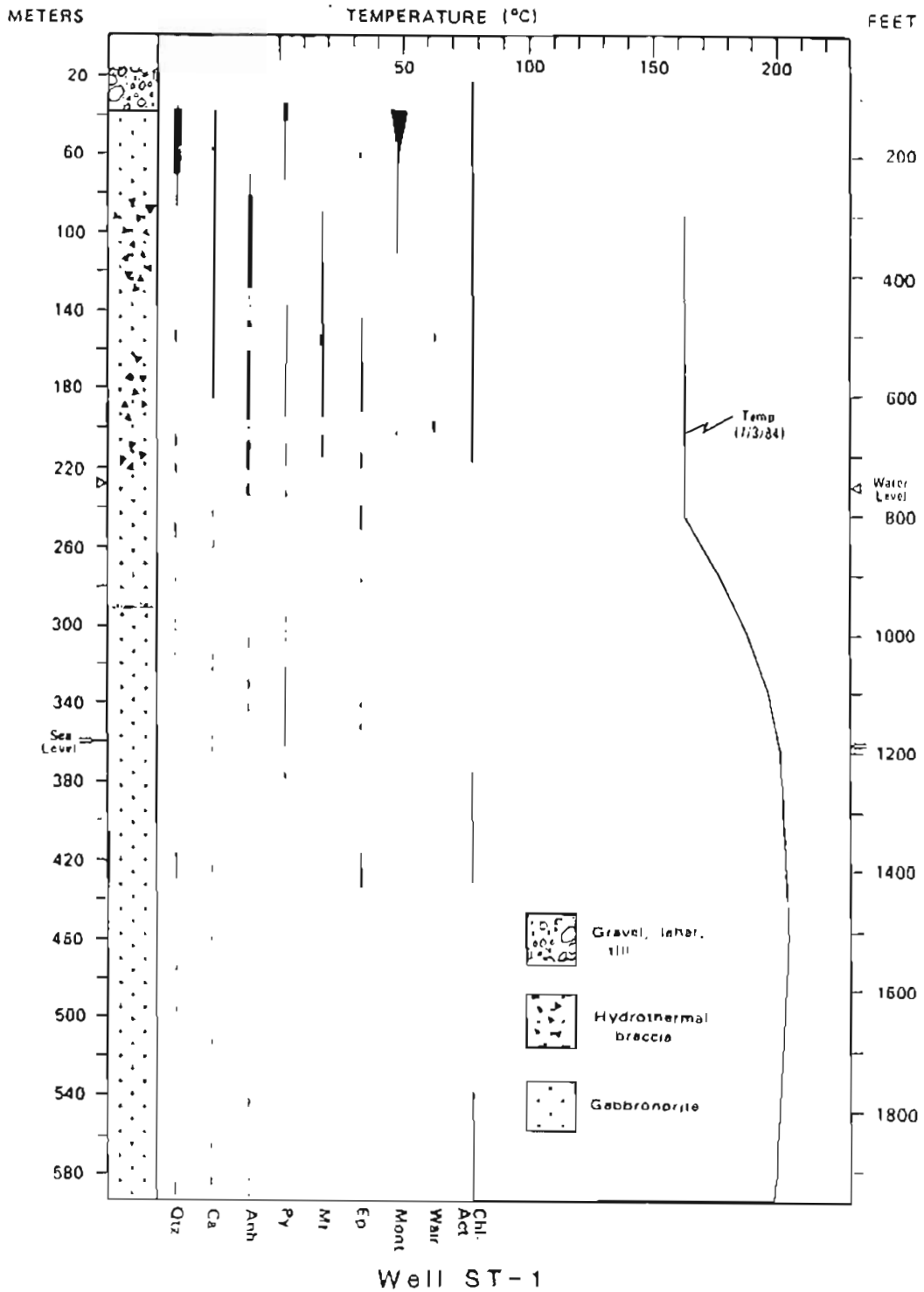Figure 18. Lithologic log and temperature profile of geothermal gradient hole A-1, Makushin geothermal area.

Figure 17. Lithologic log and temperature profile of geothermal well ST-1, Makushin geothermal area.

Surface Alteration

Alteration minerals related to the active hydrothermal system in the Makushin area occur both at the surface and at depth. The alteration minerals at the surface reflect the vapor-dominated nature of the upper portion of the Makushin hydrothermal system. Since surface alteration may not reflect the conditions of the deep production zones, this study focused mainly on subsurface alteration. Distribution and mineral assemblages of the surface alteration are discussed in Parmentier and others (1983). A brief discussion of the surface alteration follows.

At the surface, hydrothermal alteration is restricted to areas around fumarole fields--both active and fossil. Alteration minerals also occur to a lesser degree near active and fossil hot springs. Both active and fossil fumarole fields exhibit the same alteration assemblage. Kaolinite is the dominate mineral in the fumarole fields with lesser amounts of pyrite, iron oxides, and amorphous silica. Sulfur and pickeringite have been identified from the fumarole encrustations. Pyrophyllite is also locally present. Outside the area of the main vents montmorillonite becomes the major clay mineral. This assemblage is interpreted to be a result of acid alteration caused by the shallow vapor-dominated zone (Parmentier and others, 1983; Reeder, 1982).

The active hot springs in the area are low-chloride bicarbonate, sulfate springs. Active formation of authigenic minerals around these springs appears restricted to travertine. However, in Glacier Valley there are several altered zones, interpreted to be fossil hot spring deposits, in recent morainal deposits which contain significant amounts of halite. Motyka and others (1983) suggested that this is evidence of chloride-rich hot springs in the area in the recent past

Alteration Minerals in the Core

Quartz is common in all the alteration groups. Its habit varies from gray cryptocrystalline veins to clear, doubly terminated, 1-2 cm long crystals in an anhydrite matrix. The most common occurrence is as veins ranging in width from 0.5 mm to 2.0 cm. The quartz in the veins is often an opaque milky-white. The grains of quartz in the veins are anhedral to euhedral and range in size from cryptocrystalline to 1 cm in length. The finer grained material typically contains numerous fluid and clay inclusions while the larger euhedral crystals contain only a few scattered fluid inclusions. The quartz veins occasionally show fracturing and resealing by second generation quartz, but more frequently the quartz veins are cut by calcite and anhydrite veins.

Calcite occurs in veins, as fine-grained mixtures with clay alteration, and as euhedral crystals in open-space quartz and calcite veins. Most of the calcite veins are thin (1-2 mm) and contain fine-grained (<0.5 mm)

anhedral calcite. The calcite crystals in open-space veins are principally
scalenohedral, but in the upper parts of well A-1 bladed calcite crystals
also occur. At the bottom of well D-1, calcite is present in the brecciated
hornfels as a sparry breccia filling with pyrite. The sparry calcite is
translucent and is relatively free of inclusions. These calcite grains are
anhedral and are ~2 mm diam.

Anhydrite is present in two distinct habits. The more common is as a
fine-grained vein filling. These anhydrite veins also contain calcite,
quartz, pyrite, and occasional zeolites. Some veins are vuggy and lined
with terminated anhydrite crystals. The fine-grained anhydrite veins are 1-
20 mm wide and are composed of subhedral anhydrite blades 0.5-1.0 mm wide
and 1-3 mm long.   The alteration around these anhydrite veins is about
equal to the thickness of the veins. Plagioclase in the alteration envelope
is typically altered to montmorillonite. The mafic minerals are altered to
either chlorite or pyrite.

The second habit of anhydrite is as sparry, coarsely crystalline (to 3 mm
wide and 15 mm long) vein and breccia fillings. The sparry anhydrite occurs
with quartz, calcite, and magnetite. Vugs containing euhedral crystals of
anhydrite, quartz and calcite are common in the breccia zone of ST-1.   The
veins and breccia clasts commonly exhibit an alteration envelope of chlorite
rather than montmorillonite. The fine-grained anhydrite veins are younger
than the sparry anhydrite veins.

Epidote occurs both in veins and as disseminated anhedral grains in the
gabbro. When present in a vein it is never the dominant mineral. Epidote is
absent from the fine-grained anhydrite veins and is uncommon in the other
vein types. The epidote-bearing quartz and calcite veins are among the old-
est veins in the core and many show multiple stage fracturing and deposi-
tion. Epidote occurs as euhedral crystals in irregularly shaped miarolitic,
albite-epidote-quartz veins. It can make up to 10 percent of the mode in
the albite-quartz-epidote veins. In its disseminated form epidote occurs as
anhedral grains (0.5-1.0 mm diam.) scattered throughout altered zones,
especially those near contacts between hornfels and gabbro.

Albite and K-feldspar are among the oldest alteration minerals. The
albite occurs as white subhedral to euhedral crystals (0.5-1 mm) in short
(1 cm) pegmatitic veins found scattered throughout the gabbro. K-feldspar
occurs with the albite in these veins. The K-feldspar grains are typically
larger (3-4 mm) than those of the albite and are a pinkish gray. They are
always anhedral.

Chlorite and actinolite were logged together because of their intimate
association in some assemblages and the general difficulty in distinguishing
them in the hand samples. They are pale green and appear fibrous in hand
sample. They occur in veins and as disseminated replacement of pyroxenes.
The veins are generally short (0.5-1.5 cm), thin (<2 mm), and monomineralic.

They lack alteration envelopes. The disseminated alteration is more common than the veins. Pyroxenes in much of the pluton have been completely altered to chlorite-actinolite. The alteration of pyroxenes is the only alteration present in some parts of the core.

The alteration of pyroxenes, particularly orthopyroxenes, to anthophyllite-cummingtonite is probably the most widespread alteration in the core. It is difficult to see in hand specimens, but in thin section it is readily apparent that most of the orthopyroxene has been altered to anthophyllite-cummingtonite, and much clinopyroxene shows some degree of alteration. Like the chlorite-actinolite alteration, it appears to be unrelated to hydrothermal vein alteration. The anthophyllite-cummingtonite is thought to be the oldest alteration in the area.

Sphene is locally present in the alteration envelopes around anhydrite veins and less commonly in the veins themselves. It is most abundant in the altered rock of the hydrothermal breccia found in ST-1. It commonly occurs as irregularly shaped aggregates of grains, although some subhedral crystals have been found in the veins.

Illite is found at a single occurrence, a clay zone in I-1 at a depth of 358 m. The clay is greenish gray and contains a mixture of montmorillonite, illite, chlorite and calcite.

Montmorillonite is the most abundant clay mineral in the Makushin Geothermal Area. It is the dominant mineral in the clay zones which occur throughout the upper portions of the cores. Generally the clay zones do not occur much deeper than 40 m below surface, but in well I-1, montmorillonite clay zones occur to a depth of 450 m below surface. The clay zones are 2-to 20-cm-wide fractures filled with a friable, fine-grained mixture of clay, chlorite and calcite. The clay mixture is gray-green to gray to blue-green.

Montmorillonite also replaces plagioclase in the alteration envelopes around the anhydrite veins. The montmorillonite forms soft, white pseudomorphs after plagioclase laths.

Kaolinite is rare in the core samples from Makushin, even though it is abundant in the fumarole fields in the area. It has been identified in some of the clay samples from the upper portions of wells ST-1 and E-1.

Laumontite is the most common zeolite from the core. It occurs as white, euhedral crystals in open-space calcite veins. The crystals are typically 2-3 mm in length and may locally form clusters.

Mordenite occurs as white acicular crystals in an open-space calcite-quartz vein in well I-1. The crystals are 6-7 mm in length.

Yugawaralite is restricted to two occurrences in well E-1. The yugawaralite occurs as tiny, 0.5-mm euhedral crystals in an altered gabbro honeycombed with small vugs.

Wairakite has been identified in two samples from ST-1 and one from E-1. The sample from E-1 occurs at 426 m. The wairakite in this sample occurs as white, euhedral crystals on calcite crystals which, in turn, are on a quartz vein. The wairakite from ST-1, at 158 m and 202 m, forms massive, white alteration zones in the gabbro. In thin-section, euhedral crystals of wairakite can be seen. The alteration zones are about 15-20 cm wide. The 202-m occurrence is associated with a steam producing fracture.

Stilbite is restricted to a single occurrence at 65 m in well ST-1. The stilbite forms numerous small (0.5 mm) euhedral crystals on the faces of quartz crystals in a vuggy quartz-clay vein.

Hematite is present as stains, small crystals lining fractures, and rarely, as replacement of magnetite. The hematite crystals are <0.5 mm euhedral and metallic red. The occurrences seem restricted to the upper-cooler portions of the system.

Pyrite is ubiquitous throughout the core. The most common habit is as an anhedral replacement of the primary magnetite and pyroxenes. Pyrite also replaces some of the authigenic magnetite.

Pyrite may occur in veins as an accessory mineral. In the veins it occurs as small euhedral cubes (0.5-1.0 mm). Euhedral pyrite is also a common phase in the vein alteration envelopes.

Authigenic magnetite is present in all wells except E-1, occurring as large sooty anhedral grains associated with sparry anhydrite. The magnetite grains commonly appear somewhat rounded. In polished section they are homogeneous and quite distinct from the ilmenite-bearing primary magnetite. Rarely, large grains of magnetite will occur in the gabbro, seemingly removed from other alteration.

Marcasite has been found in several of the open-space quartz veins. The marcasite is tarnished and has cockscomb habit.

Paragenesis and Alteration Assemblages

The paragenetic sequence for the authigenic minerals was determined from the depositional sequence of vein minerals, cross-cutting relationships between veins, and replacement textures. Figure 19 is a paragenetic chart for all the authigenic minerals found in the drill core. Co-deposition of minerals as shown on this chart does not imply equilibrium among the phase being deposited. Local equilibrium is the rule in near-surface hydrothermal systems. Conditions can vary greatly over short distances. Minerals which
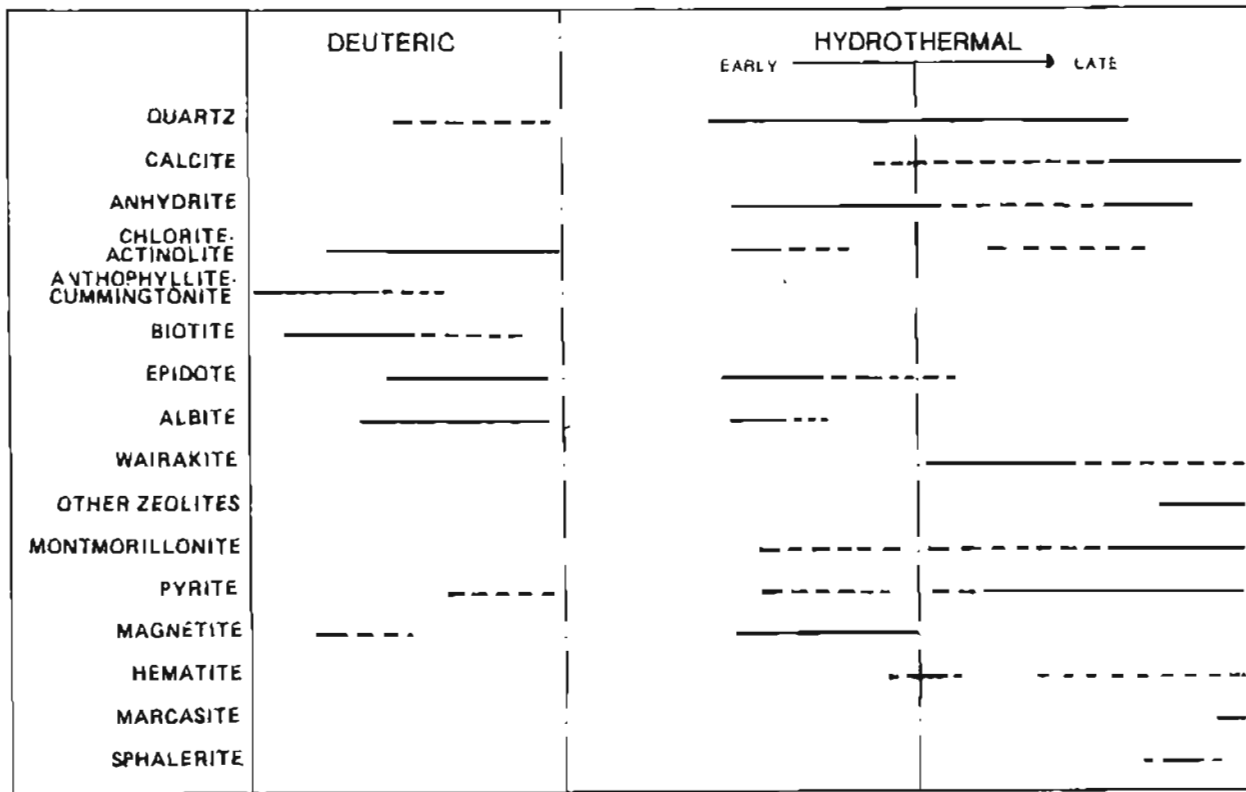
Paragenetic Chart of Makushin Alteration Minerals

Figure 19. Paragenetic chart of Makushin alteration minerals.

cannot coexist can thus form at the same time in different parts of the system. The paragenetic chart, therefore, tells very little about equilibrium in the system.

The utility of the paragenetic chart is that it allows one to see major changes in the Makushin hydrothermal area over time. For example, minerals such as biotite, hornblende and albite were deposited early on while the zeolites were deposited more recently. From the paragenetic chart and information about mineral stabilities, two major alteration events can be identified. The early alteration event is the result of deuteric alteration of the pluton and is unrelated to the active hydrothermal system. The late alteration is the work of the Makushin hydrothermal system.

The deuteric alteration comprises two assemblages: an albite ± biotite ± hornblende ± actinolite ± epidote ± quartz assemblage found in comagmatic breccias and aplite dikes, which occur randomly throughout the pluton, and an anthophyllite ± cummingtonite ± actinolite ± magnetite ± pyrite

- 49 -

assemblage which replaces mafic phases, in particular the orthopyroxenes, in the gabbronorite and hornfels. The deuteric alteration occurs throughout the pluton so that it is difficult to find unaltered orthopyroxenes.

Perfit and Lawrence (1979) found that the rocks of the Captain's Bay pluton showed depleted $^{18}O/^{16}O$ values with respect to normal igneous rocks. They interpreted this to be a result of the interaction of circulating meteoric water with the cooling pluton. Samples of the Makushin gabbro were analyzed for oxygen isotopes. The results are shown in table 14. Like those of the Captain's Bay pluton, they show depleted $^{18}O/^{16}O$ values compared to normal igneous rocks. It is therefore likely that the Makushin pluton also interacted with circulating meteoric water as it cooled. The greenschist metamorphism of the Unalaska Formation is also believed to be related to hydrothermal systems set up by the cooling plutons (Perfit and Lawrence, 1979).

The alteration related to the Makushin geothermal system is divided into two periods of deposition; an early and late period. The early period authigenic minerals seem to be a single assemblage of anhydrite ± magnetite ± calcite ± pyrite ± chlorite ± epidote ± sphene. This will be referred to as the 'magnetite' assemblage. The authigenic minerals of the late period form two distinct assemblages; a montmorillonite ± chlorite ± calcite ± pyrite assemblage, the 'argillic' assemblage, and anhydrite ± calcite ± quartz ± zeolite ± epidote ± pyrite ± sphalerite ± sphene assemblage, the 'zeolite' assemblage.

The magnetite assemblage occurs principally in the hydrothermal breccias which are abundant in the upper 220 m of ST-1. The breccias occur less frequently in the other wells. The breccias consist of clasts of gabbro surrounded by a matrix of sparry anhydrite, anhedral magnetite, euhedral quartz crystals, and rarely, calcite crystals. The clasts are angular, 0.5-4 cm in diam, and almost always have a chloritic alteration rind. In well D-1, the breccias are slightly different: hornfels clasts in a matrix of sparry calcite and anhedral pyrite. The clasts are approximately the same size and shape and have chloritic alteration rinds.

The sparry anhydrite, as opposed to the finer grained anhydrite of the zeolite assemblage, and the magnetite serve to distinguish this assemblage. The anhydrite and magnetite appear to have formed together. This is most unusual for a geothermal system. While anhydrite is common in explored geothermal areas, authigenic magnetite has been reported from only two other geothermal areas: Tongonan, Philippines, and Tatun, Taiwan (Browne, 1978; Lan and others, 1980). The Tongonan system has temperatures of above 300°C, much higher than those so far encountered in the Makushin system.

The Makushin hydrothermal system clearly cannot have formed the magnetite assemblage under the present conditions. The breccias found in ST-1 are above the water table, and the magnetite assemblage must have formed in a

liquid-dominated system. It also does not appear possible to deposit anhydrite and magnetite together at the present temperatures. Despite this, the magnetite assemblage does appear to be related to the Makushin system. No evidence of any earlier hydrothermal systems can be found in the Makushin area. Extensive exploration of the pluton at the surface indicated only the deuteric alteration and the alteration around the fumaroles and hot springs. An unpublished geochemical study of the Makushin well drill chips by R. Bamford for Republic Geothermal, Inc. indicated no other hydrothermal activity than the present system. Finally, salinity data from the fluid inclusions (discussed later in this report) indicate the fluids that formed the magnetite assemblage are similar to the present fluids. Taken together, this is good evidence that the magnetite assemblage was formed by the Makushin system at an earlier stage.

The zeolite and argillic assemblages are much more easily related to the present system. The argillic assemblage is fairly typical of the vapor-dominated and cooler liquid-dominated portions of other geothermal systems (Ellis, 1979). It is basically confined to areas above the known water table to liquid-dominated zones with temperature below ~ 100°C.

The zeolite assemblage is representative of the liquid-dominated portions of the active system. The assemblage occurs in every core and is the most common of the hydrothermal assemblages. There is a rough temperature zoning for the zeolites. Mordenite was only found in I-1 and is assumed to be stable below 100°C. Laumontite is by far the most common zeolite in the Makushin system. It has been found at temperatures as low as 70°C. However, this may be a relict of the early stage. More reasonable is the occurrence in A-1, which starts at about 125°C. The upper temperature limit is probably around 190°C. Wairakite, like the laumontite, is found at temperatures that are too low to be reasonable for formation. In other systems wairakite first appears around 175°C and disappears at about 250°C. Yugawaralite is rare in the Makushin core but probably has stabilities similar to wairakite.

The only other zoning seen in the Makushin system is the zoning between bladed and scalenohedral calcite. In well I-1 bladed calcite occurs from 100 m to about 340 m, below which point the calcite is scalenohedral.

As mentioned, there are occurrences of the zeolite assemblage which, like the magnetite assemblage, are outside the stability limits for the assemblage. In ST-1, wairakite occurs at 137 m and at 190 m. Both zones are above the present water table and are at temperatures well below those reasonable for wairakite formation. The 190-m occurrence is gabbro altered to wairakite surrounding a steam-producing fracture. In order for wairakite to form, the fluids must be supersaturated with respect to quartz. This is impossible in a vapor-dominated system. Wairakite has been found in vapor-dominated systems, but these occurrences are rare and always at temperatures close to 200°C. The wairakite in ST-1 must have formed during an earlier

period when the water table was higher than at present, and the temperatures near the surface must also have been higher.

Evidence from the authigenic minerals, therefore, indicates that a change in the Makushin hydrothermal system has taken place. This change certainly involved a drop in the water table and a lowering of the temperature in the upper parts of the system.

FLUID INCLUSIONS

Methods

The fluid inclusion study was undertaken to determine the temperature and salinity of the fluids which formed the early hydrothermal minerals. Three samples from E-1, three samples from ST-1, and one sample from I-1 were selected for the homogenization and salinity investigation. The samples were selected on the basis of four criteria: (1) the samples had to contain quartz; (2) the quartz grains had to be larger than 2 mm in diam; (3) the veins the quartz came from had to be of hydrothermal origin; and (4) the sample depths had to be varied to allow a paleogeothermal gradient to be determined. Descriptions of the samples are given in table 21.

Table 21. Description of fluid inclusion samples.

Sample number	Description
ST-277	Clear, euhedral quartz crystals (0.5 cm diam.) from a vuggy anhydrite, quartz, magnetite breccia infilling. Primary and pseudo-secondary inclusions present. Some primary inclusions form phantoms within the quartz crystals.
ST-295	Clear, euhedral quartz crystal (1.0 cm diam.) from an anhydrite, quartz, calcite, magnetite breccia infilling. Inclusions are rare. Primary and secondary inclusions.
E-1-791	Quartz from a calcite, quartz, epidote vein. Quartz grains are euhedral and surrounded by calcite. Some epidote grains in the calcite. Surrounding gabbro only slightly altered. Plagioclase to montmorillonite. Mafics to chlorite and pyrite.
E-1-1155	Quartz crystals from sealed quarts vein. Vein is 2 cm wide. Individual quartz crystals are subhedral. Crystals are 1 cm long and 0.3-0.5 cm wide. Surrounding rock is extensively altered.
E-1-1396	Quartz vein. Wairakite is present in vug along one side of vein. The wairakite is younger than the quartz vein.
I-1-164	Fine grained quartz vein (2.5 cm wide). Much of the sample can not be used because of numerous clay inclusions and most of the inclusions are too small. Acceptable inclusions are present in the small (1.0-0.5 mm) subhedral crystals which project into the occasional small vugs. The host rock is highly altered to the argillic assemblage and only pyrite traces of the mafic minerals remain.

Although anhydrite and calcite also contain fluid inclusions and are abundant in the core, they were not used in the fluid inclusion study. They were judged unsuitable for the study for two major reasons: First, grains of anhydrite and calcite large enough to have usable inclusions were not as abundant as large grains of quartz. Second, anhydrite and calcite are thought to be more susceptible to possible re-equilibration during retrograde events than is quartz.

The fluid inclusion samples were prepared according to procedures outlined in Roedder (1984). Special care was taken to avoid heating the samples above 80°C during preparation. The melting and homogenization measurements were done on a Linkam 600 heating-cooling stage. To determine fluid salinities, the sample was cooled to -40°C, then heated at a rate of 10°C/min until the sample temperature reached -5°C. The sample was allowed to equilibrate at this temperature for one minute. Heating was then continued at 1.0°C/min until the last ice melted. After the last ice melted, heating was continued at the same rate to +12°C in order to check for clathrates.

To measure homogenization temperatures, the sample was heated at 20°C/min until the sample temperature reached 180°C. The sample was allowed to remain at 180°C for one minute. The rate of heating was then reduced to 5°C/min and heating continued until homogenization was achieved. Multiple homogenization runs were made on selected inclusions to determine the repeatability of the results. Homogenization temperatures measured at heating rates of 1°C/min were within ±1°C of homogenization temperatures measured at heating rates of 5°C/min.

The inclusions used in the study ranged from 0.01 mm to 0.5 mm in diam. Most of the inclusions were primary, but some psuedo-secondary and secondary inclusions were also used. The vapor fillings were between 5 and 10 percent. The vapor bubbles were slightly darker than one would expect for pure H_2O vapor. Typical inclusions are shown in figure 20.

About half the inclusions contained thin, transparent, daughter minerals (fig 21). The daughter mineral did not show any visible dissolution even at 400°C. This may indicate that the minerals are accidental inclusions and not true daughters.

Fluid Salinity

Figure 22 shows the temperature of last ice melting for 80 inclusions from five samples (ST-1:277, ST-1:295, E-1:791, E-1:1155, E-1:1396). The variation shown by the melting temperatures is within the error limits for the cooling stage. Thus it is reasonable to assume that the composition of the fluid inclusions is constant.
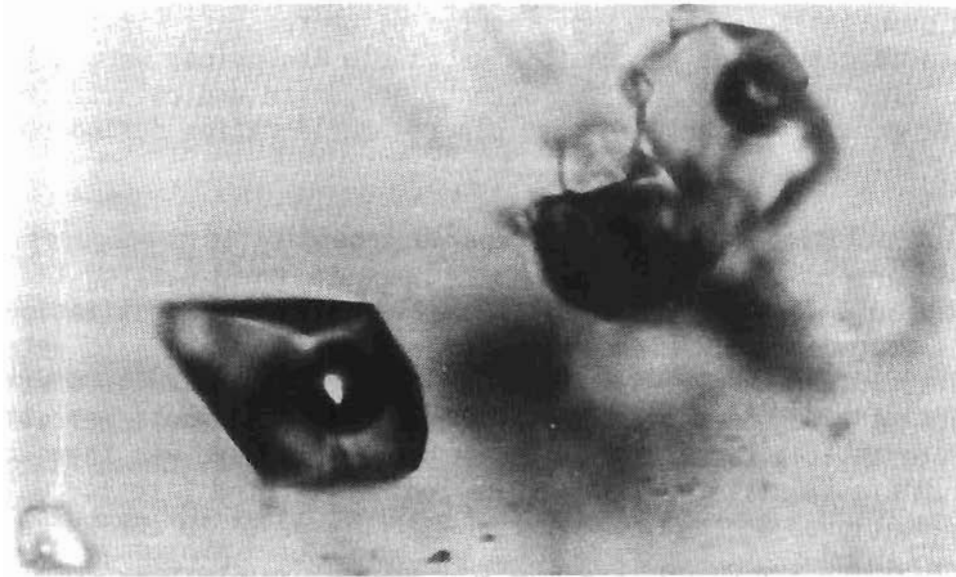
Figure 20. Fluid inclusions in quartz from the Makushin geothermal area.
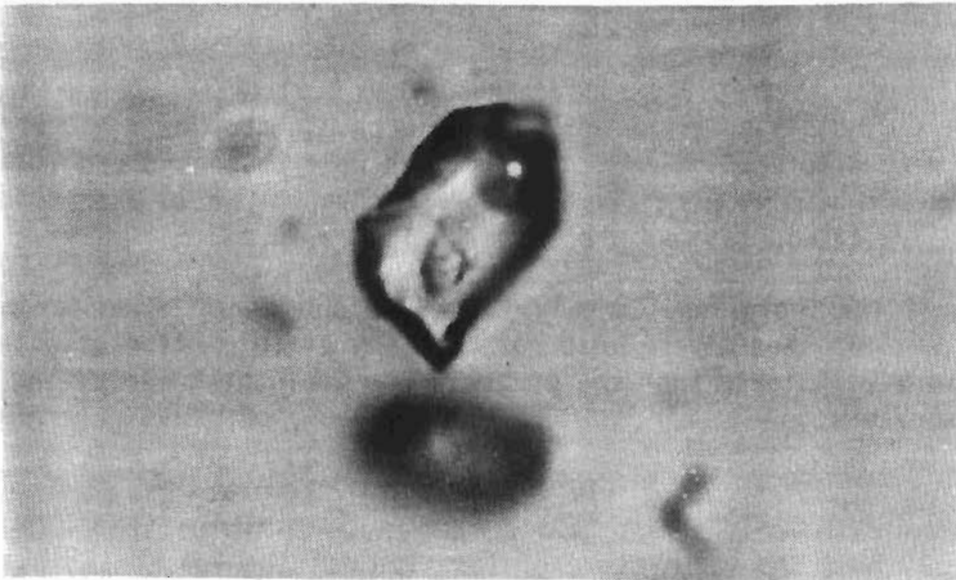
Figure 21. Fluid inclusions showing daughter minerals.

Using the equation given by Potter and others (1978) to determine the inclusion salinity in NaCl molar equivalents from the temperature of last ice melting, one obtains for the mean temperature a salinity of 0.106 M NaCl or 6,194 ppm. The measured salinity of the ST-1 waters is 0.098 M NaCl or 5,868 ppm. Even ignoring the difficulty in measuring the salinity of low salinity inclusions, the agreement between present system salinities and the fluid inclusion salinities is remarkable.

After the last ice melted, the samples were checked for clathrates. Although the dark vapor bubble indicated the presence of some CO_2, no clathrates were observed. The active hydrothermal system has CO_2 partial pressures of 0.5 bars, which are much too low to allow clathrate formation.

Thus, from the compositional information that can be obtained by freezing the inclusions, the paleofluid and the present fluids appear the same. This seems to rule out any major changes in composition during the life of the Makushin hydrothermal system. Although it would be desirable to obtain quantitative chemical analysis of the fluid inclusion, this seems unlikely at present, because of the dilute nature of the fluid inclusions.

Homogenization Temperatures

Figures 23a, b, and c show the fluid inclusion homogenization temperatures (given by mean) at appropriate sample depth in each well. Also shown are the measured thermal gradients(MTG) and the hydrostatic reference boiling curve (RBC).

The degree of vapor filling in the inclusions at 40°C was essentially constant, being between 5 and 10 percent by volume. All of the inclusions homogenized to a high density fluid (that is, the vapor bubble shrank). These observations are generally taken to indicate that the fluid inclusions were formed in a liquid-dominated environment and that the liquid was not boiling. However, experience in other geothermal fields indicates that similar inclusions can form from fluids which are boiling (Roedder, 1984). Therefore, one cannot say that boiling has not occurred, but only that there is no evidence for boiling.

The lack of evidence for boiling prevents the determination of the pressure correction to be applied to the homogenization temperatures to get the true temperature of trapping. However, in many explored geothermal system the pressure is close to hydrostatic. Since the Makushin samples came from fairly shallow depths, the pressure correction should be small. Nevertheless, the homogenization temperatures should be regarded as minimum temperature of trapping.

The most striking feature of the homogenization temperatures is that they are all above the measured well-temperatures for the sample depth. In some samples the highest homogenization temperatures are >100°C above the maximum

TEMPERATURE OF LAST ICE MELTING

Fig. 22
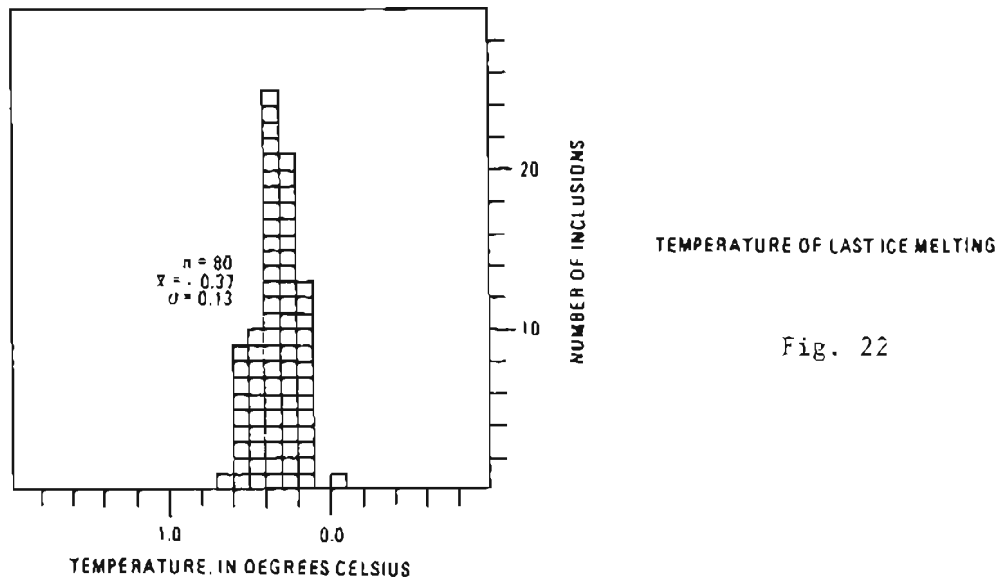
Figure 22. Histogram of fluid inclusions, temperature of last ice melting.
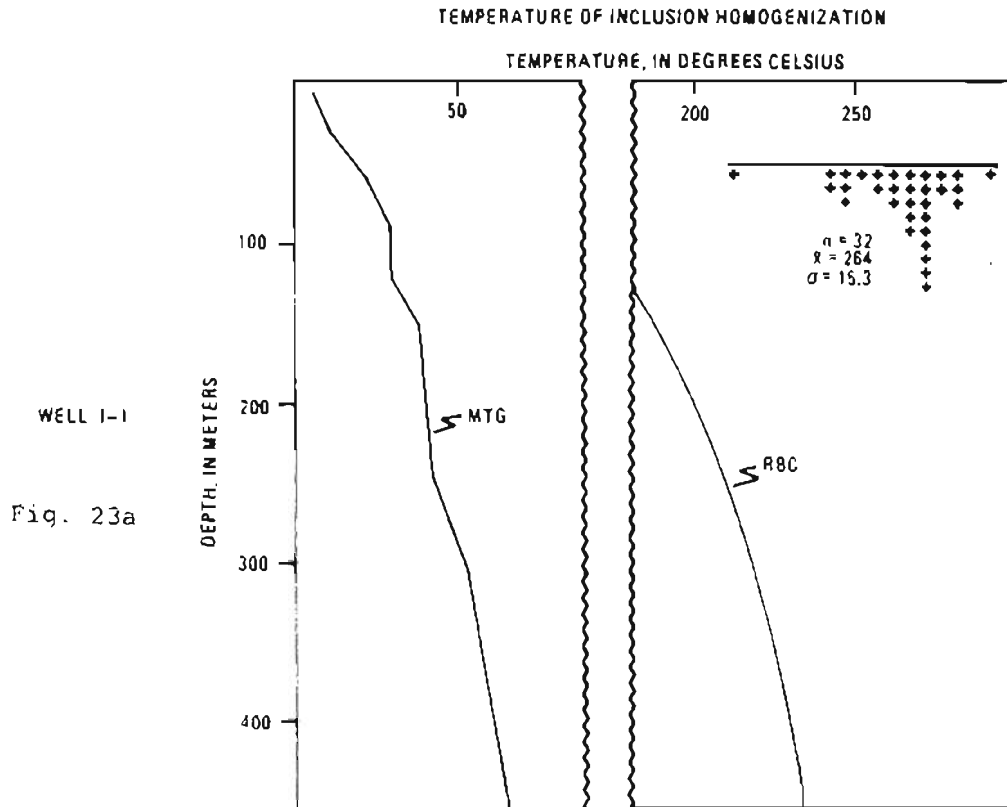
Figure 23a,b,c. Temperatures of fluid inclusion homogenization at sample depth in Wells I-1, ST-1, and E-1.

TEMPERATURE, IN DEGREES CELSIUS

WELL ST-1

Fig. 23b

WELL E-1

Fig. 23c

- 57 -
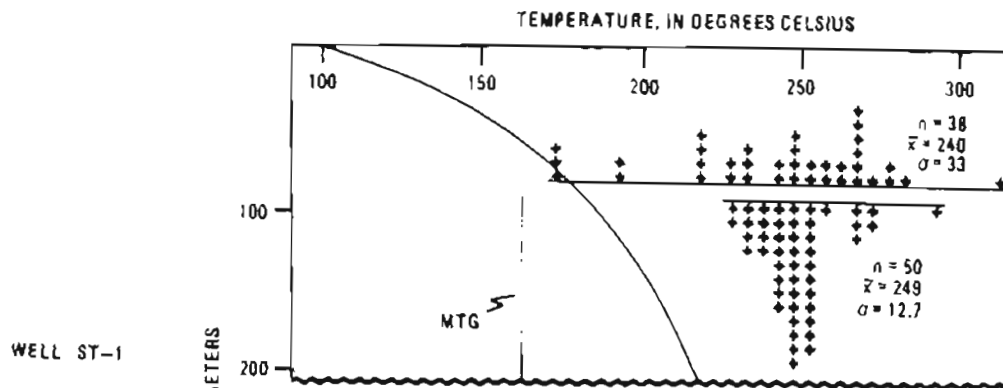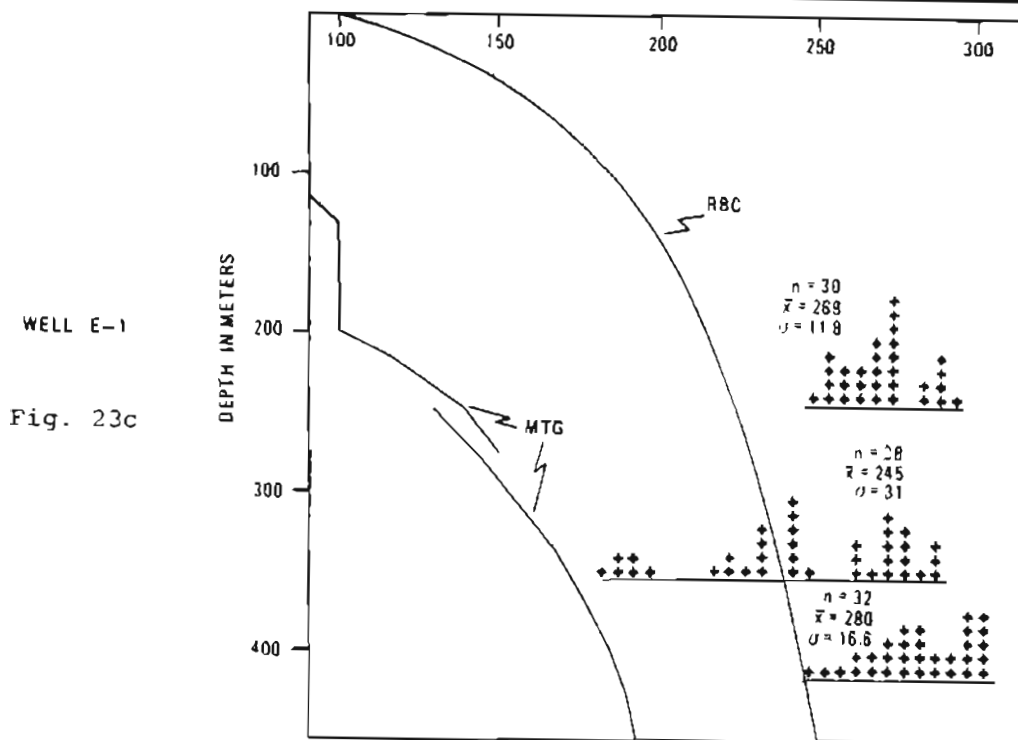
bottom-hole temperature so far measured in the Makushin system. Despite this, the inclusions do probably represent the conditions of the early Makushin Geothermal System. As discussed earlier in this report, the evidence strongly suggests that all the hydrothermal alteration in the wells is related to one hydrothermal system.

Fluid inclusion homogenization temperatures are often significantly greater than the present measured temperatures for a well (Bargar and Beeson, 1984; Bargar and others, 1984; Keith and others, 1984; Huang, 1977; Taguchi and others, 1980; Taguchi, 1983). The lower homogenization temperatures are, however, in most fields within ±5°C of the preproduction measured temperature curve. The higher homogenization temperatures are, therefore, usually interpreted as evidence that the geothermal system has cooled. Thus the fluid inclusion homogenization temperatures suggest that the Makushin geothermal field has cooled as much as 100°C in places.

The difficulty with this interpretation lies in the fact that most of the homogenization temperatures are above the hydrostatic boiling curve. As can be seen in figures 23a, b, and c, the mean temperature of homogenization of all the samples is at or exceeds the hydrostatic boiling curve--indicating boiling should have taken place. The fluid inclusion data do not rule out boiling at the time of the inclusion trapping, but if boiling were taking place, the homogenization temperatures could not exceed that of the boiling curve. The boiling curve must have, therefore, been shifted toward higher temperatures for a given present depth in the early geothermal system.

A shift of the boiling curve can be affected by an increase in salinity or an increase in pressure. For the Makushin geothermal system the increase in salinity can be ruled out, on the basis of the fluid inclusion freezing data. This means the shift in the boiling curve must have been due to increased pressure in the past. Additional pressure can be supplied if the system is self-sealed, so that lithostatic, rather than hydrostatic, pressures apply. The lithostatic pressures are nonetheless too small to prevent boiling in all but the deepest samples. Self-sealed geothermal systems can over-pressure; however, the over-pressure cannot exceed the lithostatic pressure by more than approximately 30 per cent (Muffler and others, 1971). In the case of the Makushin system, the over-pressure required to prevent boiling in the upper samples exceeds the lithostatic pressure by a factor of 3.

We must therefore invoke another mechanism to increase the hydrostatic and/or the lithostatic pressure. This can be done only by increasing the overburden on the system. In many fossil systems the overburden is assumed to be rock. If we assume that the Makushin system was solely under hydrostatic pressure, then the amount of rock that has been eroded must exceed 300 m. A lithostatic load would require 100 m of rock.

This is probably an unreasonable amount of material to erode during the expected lifetime of this geothermal system. Rates of erosion by two large glaciers in Iceland were calculated to be 6.4 and 55 cm/100 yr, respectively (Okko, 1955). Assuming these values to be an upper and lower limit to the erosion rate in the Makushin area, we can estimate the amount of time required to erode the 100-300 m of rock overburden; the result would be 20,000-500,000 yr. While these numbers are reasonable given the length of time the geothermal system could exist, the surface alteration suggests that this is not what occurred.

If the additional pressure were supplied by rock now eroded away, one would expect to find evidence of the liquid-dominated system at the surface. The evidence would be in the form of veins and liquid-dominated alteration. As discussed earlier the surface alteration is confined to vapor-dominated alteration. Thus, it does not seem likely that rock was the source of the additional pressure.

Instead, as we will discuss in a subsequent section, we propose that the additional pressure was supplied by glacial loading.

Alteration Equilibrium in the Makushin System

Having established the likely temperatures and pressures of the paleo-geothermal system, it is now possible to apply thermodynamic data to the alteration mineral assemblages and check for consistency.

The authigenic minerals of a hydrothermal system are the end result of the interaction among several physical-chemical factors. Browne (1978) grouped these factors under six major headings: (1) temperature, (2) pressure, (3) rock type, (4) fluid composition, (5) permeability, and (6) duration of activity. These factors vary from field to field, and in most cases vary greatly even within an individual field. Most of these factors can be more or less directly measured to determine the present conditions. Chemical thermodynamics allows us to predict the results of some of the factors. The model created by chemical thermodynamic data can then be compared to what is actually seen.

Figure 24 is the chemical potential diagram for the system $CaO-Al_2O_3-SiO_2-H_2O$. The phases shown are all found in the Makushin system. Reliable thermodynamic data are unavailable for some phases, and this precludes their being shown on a standard activity diagram. One can, however, obtain information about the system from the shape of their fields and their location on chemical potential diagrams. There are some restrictions which can be applied to the chemical potential diagram shown.

Wairakite is known to form only at or above quartz saturation. This means, that for a given temperature, all the phases to the right of wairakite form at silica activities above quartz saturation. Margarite is
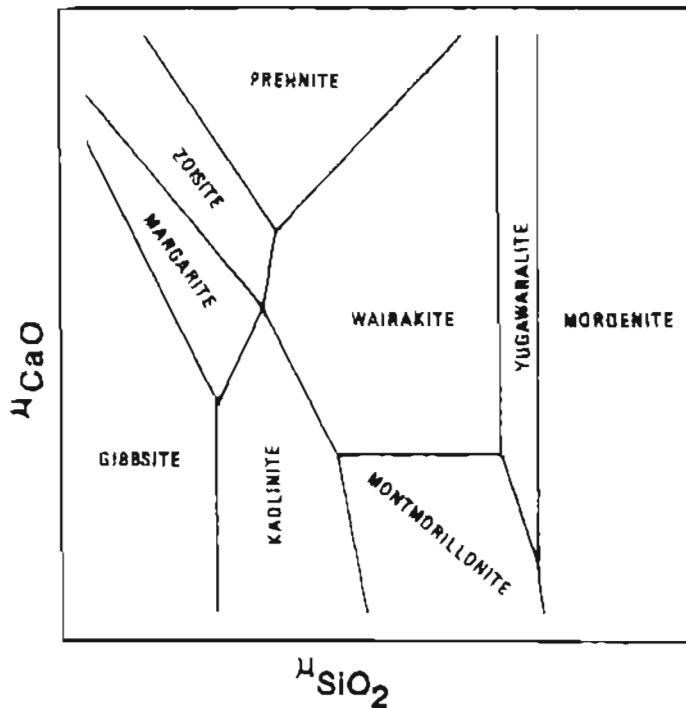
Figure 24. Chemical potential diagram for the system CaO-Al_2O_3-SiO_2-H_2O.

also known to form only at silica activities below quartz saturation. Thus, one would not expect to find zeolites and margarite together, and indeed, this is the case; zeolites are present in the Makushin system, and margarite and gibbsite are absent. Prehnite is also absent in the system. This could indicate that Ca activity is limited by some mechanism or that H+ is too low.

The zoning of zeolites on the diagram reflects the zoning of zeolites with temperature shown in the system. Similar zoning patterns are seen in other systems. The mechanism for this zoning appears to be related to the change in the silica activity buffer with temperature. At temperatures above 180°C, water is usually saturated with respect to quartz; at lower temperatures, however, the stable silica phase becomes chalcedony or opal (Arnorsson, 1975). This allows the higher silica zeolites to form at the lower temperatures and thus creates the zoning pattern (Browne, 1978; Henley and Ellis, 1983).

Figure 25 is the activity diagram for the CaO-Al_2O_3-SiO_2-H_2O system at 200°C. As one can see, the Makushin water plots in the kaolinite stability field. However, kaolinite is not an abundant mineral in the cores. This might be caused by: (1) the actual temperature of the water being 195°C and the diagram therefore being drawn at an inappropriate temperature; (2) kaolinite being present but in such small amount it was overlooked; or (3) the water not plotting correctly. The last cause appears to be the
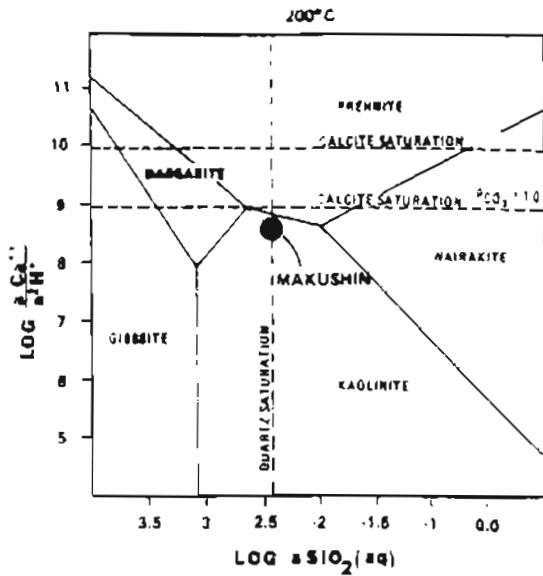
Figure 25. Makushin reservoir waters plotted on the activity diagram for the system $CaO-K_2O-Al_2O_3-SiO_2-H_2O$ at 200°C.
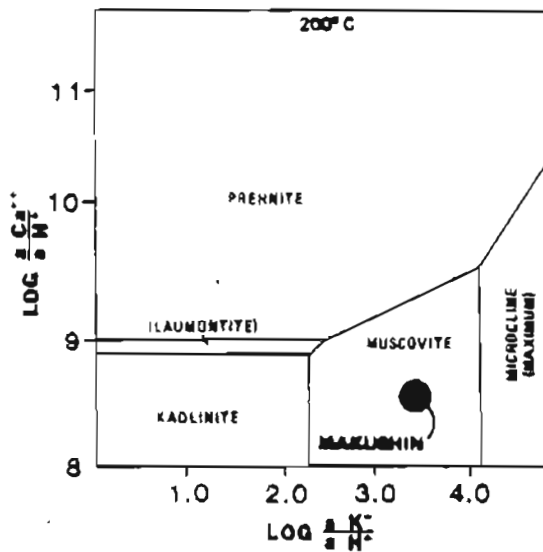
Figure 26. Makushin reservoir waters plotted on the activity diagram for the system $CaO-K_2O-Al_2O_3-SiO_2-H_2O$ at 200°C.
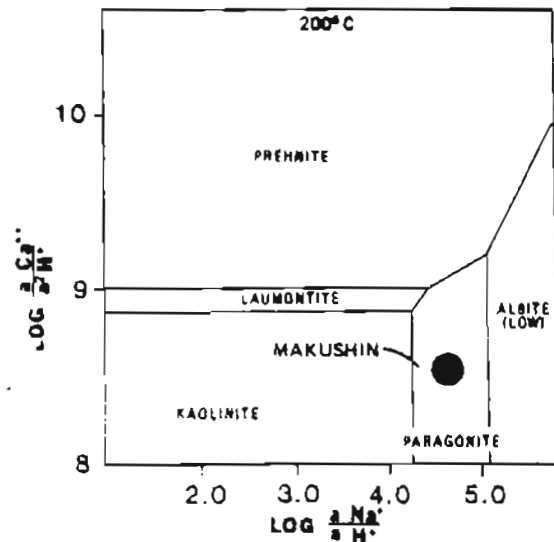
Figure 27. Makushin reservoir waters plotted on the activity diagram for the system $CaO-Na_2O-Al_2O_3-SiO_2-H_2O$ at 200°C.

case. The difference between the actual temperature of the fluid and that on the diagram is not enough to change the relative position of the point in the fields. If kaolinite is present in small quantities that have been overlooked, then it would indicate a non-silicate mineral represents the bulk of the calcium bearing alteration. This is possible, but it would be unusual for most geothermal systems. The water is saturated with respect to quartz at about 207°C. The change from 207°C to 195°C would allow silica activity to rise, but would not be sufficient to allow the deposition of wairakite--it would be sufficient to allow for the deposition of laumontite. Laumontite is close to its upper thermal boundary at 200°C, but in the Makushin system it does appear to be stable.

Laumontite might well be the stable zeolite in the Makushin system under present conditions. The wairakite may have formed shortly after formation of the magnetite assemblage while the system was cooling. If this were accomplished in a rapid fashion (that is, boiling), then the silica activity would have been allowed to rise considerably above the quartz saturation limit. This would in turn have allowed the formation of wairakite. Thus the wairakite may be more indicative of the past conditions than present.

Figures 26 and 27 are activity diagrams for the systems K_2O-Al_2O_3-CaO-H_2O and Na_2O-Al_2O_3-Ca-H_2O, respectively. The Makushin waters in these diagrams fall in the white mica fields. Although white mica is not shown in the alteration charts, it is present in the cores. The plagioclase around some of the recent veins always has some white mica alteration--the amounts are small but significant. White mica has also been reported as the most recent mineral from vein material recovered from the bottom fracture of ST-1. In this case it does seem likely that the activity diagrams do reflect the equilibrium in the present system.

A final phase diagram has been drawn to help explain the unusual magnetite assemblage from the ST-1 breccias. All the available evidence indicates the magnetite breccias formed during or shortly after the end of the high temperature stage of the Makushin hydrothermal system. Figure 28 is a fO_2-pH diagram for the system Fe-O-S at 250°C. Also shown are the calcite and anhydrite insoluble lines. From the homogenization temperatures, 250°C is a reasonable guess at the temperature of the high temperature stage.

The original fluid must have had a pH and fO_2 such that calcite and anhydrite were soluble. Furthermore, the fO_2 cannot have been lower than the pyrite-pyrrhotite line, since pyrrhotite is not present in the Makushin system. For geothermal systems at 250-300°C, Ellis and Mahon (1977) have proposed fO_2 values of between 10^{-40} and $10^{-37.5}$. If we assume these fO_2 values for the original system, then anhydrite, calcite and magnetite could not have formed (if the system had a pH similar to present-day conditions).

Figure 28. Fugacity of oxygen vs. pH diagram for the system Fe-S-H2O at 250°C (after Crerar and Barnes, 1970).

Deposition could be accomplished by changing the fO_2 values, but changes in oxidation are difficult and slow at these conditions. Instead, it is much easier to change the pH. One simply allows the fluids to boil. The pH change in the present Makushin waters from boiling is over 2.0 pH units, because of loss of CO_2 and H_2S to the vapor phase. Since fluid inclusion data indicate that the composition of the paleofluids were similar to the present fluids, it is reasonable to assume similar changes in pH if the early Makushin system boiled rapidly. Such a change could result in the deposition of anhydrite, magnetite, calcite and quartz.

GLACIER UNLOADING: CAUSE OF RECENT CHANGE IN THE GEOTHERMAL SYSTEM

We have accumulated evidence indicating that a rapid decline in the water table and a cooling of the upper part of the Makushin hydrothermal system occurred in the geologically recent past. The current depth to the pressurized hydrothermal system, as determined from drill holes, lies at 230-240 m below the surface in upper Makushin Valley. A vapor-dominated zone presently extends from this depth to the surface. By inference, a shallow vapor-dominated zone of similar magnitude is thought to exist at the head of

Glacier Valley in the vicinity of fumarole field 3. Yet halite was found coating hydrothermally cemented rocks in neoglacial moraines and outwash deposits in the upper part of Glacier Valley (Motyka and others, 1983).

These salt deposits are thought to be relicts of fossil chloride-rich thermal springs and indicate a hot-water system reached the surface in recent times in a region that is now dominated by fumarole activity and HCO_3-SO_4 thermal springs.

The hydrothermal-alteration mineral-assemblages found in the upper parts of holes E-1 and ST-1 (which include quartz, calcite, anhydrite, wairakite, and montmorillonite) could only have been formed under hot-water neutral to slightly alkaline conditions, and not the acid-steam conditions that presently exist in this zone. Furthermore, trace-element enrichment and depletion studies of core from the Makushin geothermal area indicate neutral pH hot-water rather than acid-steam conditions in the upper parts of the drill holes (Isselhardt and others, 1983). The apparent absence of steam-dominated mineral assemblages and trace-element geochemistry in these zones indicates the hydrothermal system water level dropped fairly recently.

The evidence from our fluid inclusion studies indicates that the temperature of the hot-water hydrothermal system, at the time the fluid inclusions were entrapped in vein-deposited quartz in the upper parts of the system, were substantially hotter than present-day temperatures. Examination of figure 23 shows that paleotemperatures at depths as shallow as 100 m below the present surface were as high as 250°C. The studies also indicate that the waters from which the quartz was precipitated had a salinity nearly the same as the present-day system. If the paleofluid is assumed to have had a $\delta^{18}O$ composition similar to present reservoir waters, we can then apply the equilibrium fractionation equation of Chiba and others (1981) to anhydrite found in a vein at a depth of 149 m (cf. table 11). The result gives a temperature of formation of ~250°C, which is similar to temperatures of formation of fluid inclusions in the associated quartz.

The pressure required to sustain such high temperatures at saturation boiling point conditions is about 40 bars--equivalent to a hydrostatic head of over 400 m. To produce such high pressures, the system either must have been self-sealed or some other mechanism of pressure loading must have been in effect. We reject the hypothesis of lithostatic self-sealed pressurization, because of the high pressures involved and because of the highly fractured nature of the host gabbronorite, as evidenced by the numerous fumaroles and hot springs that exist throughout the area.

We prefer instead to invoke ice-loading of the hydrothermal system during a neoglacial advance to explain the anomalously high temperatures recorded by the fluid inclusions. Ice thicknesses of 400-500 m are common in present valley-type glaciers in Alaska, and it is reasonable to assume such ice

thicknesses existed in Makushin and Glacier Valleys in neoglacial times. The increased hydrostatic pressure exerted by the ice would be sufficient to produce the elevated temperatures recorded by the fluid inclusions. Such interactions between ice loading and hydrothermal systems exist today in Iceland, particularly in the Vatnajokull Grimsvotn caldera area (Bjornsson, 1974), and are also thought to have occurred during glacier advances and retreats in the Yellowstone National Park geothermal areas (Muffler and others, 1971; R. Fournier, USGS, personal commun.)

The thermal fields at Makushin lie at the heads of valleys on the flanks of a volcano which still maintains a sizeable ice-cap and a system of valley glaciers. At least two neoglacial advances that reached tidewater have been documented elsewhere in the Aleutians (Black, 1981; 1983), and it is reasonable to assume that correlative glacial advances occurred at Makushin. There are, in fact, abundant neoglacial moraines, outwash deposits, and glacial scouring marks in Glacier, Makushin, and Driftwood Bay Valleys. The most recent advance and retreat in the Aleutians is estimated by Black (1983) to have occurred about 3,000-4,000 yr ago.

At the Vatnajokull in Iceland, meltwater generated by subglacial geothermal heating becomes entrapped in large, hydrostatically sealed subglacial chambers. The seals on these subglacial meltwater reservoirs are periodically broken, resulting in a catastrophic release of entrapped water, known as a jokulhlaup (Bjornsson, 1975). Similar pressure-release phenomena probably occurred at the Makushin geothermal area during neoglacial times and could have caused the breccias found in the ST-1 and D-1 drill cores. As discussed previously, vigorous boiling would increase the pH and could explain the curious co-precipitated mineral assemblage of quartz-calcite-anhydrite-magnetite that is found in the breccias in the upper parts of ST-1 and E-1.

Subsequent deglaciation would decrease the hydrostatic pressure and cause boiling to increase in the upper part of the hydrothermal system. A net loss of water, from boiling and from the decrease in recharging glacier meltwater, would in turn result in a decline of the system's water table.

If our hypothesis is correct, the drop in temperature in the upper part of the hydrothermal system may largely reflect an episode of intense boiling and water loss rather than cooling in the deeper part of the system. The sulfate-water oxygen isotope geothermometer does predict a deep reservoir temperature of ~ 250°C which is similar to fluid inclusion temperatures found in the upper part of the system.

DISCUSSION OF PREMIER GEOPHYSICS ELECTRICAL RESISTIVITY STUDY

At the recommendation of DGGS scientists, an electrical resistivity survey of upper Makushin Valley was incorporated into the geothermal exploration program for the summer of 1984. The rationale for the survey was
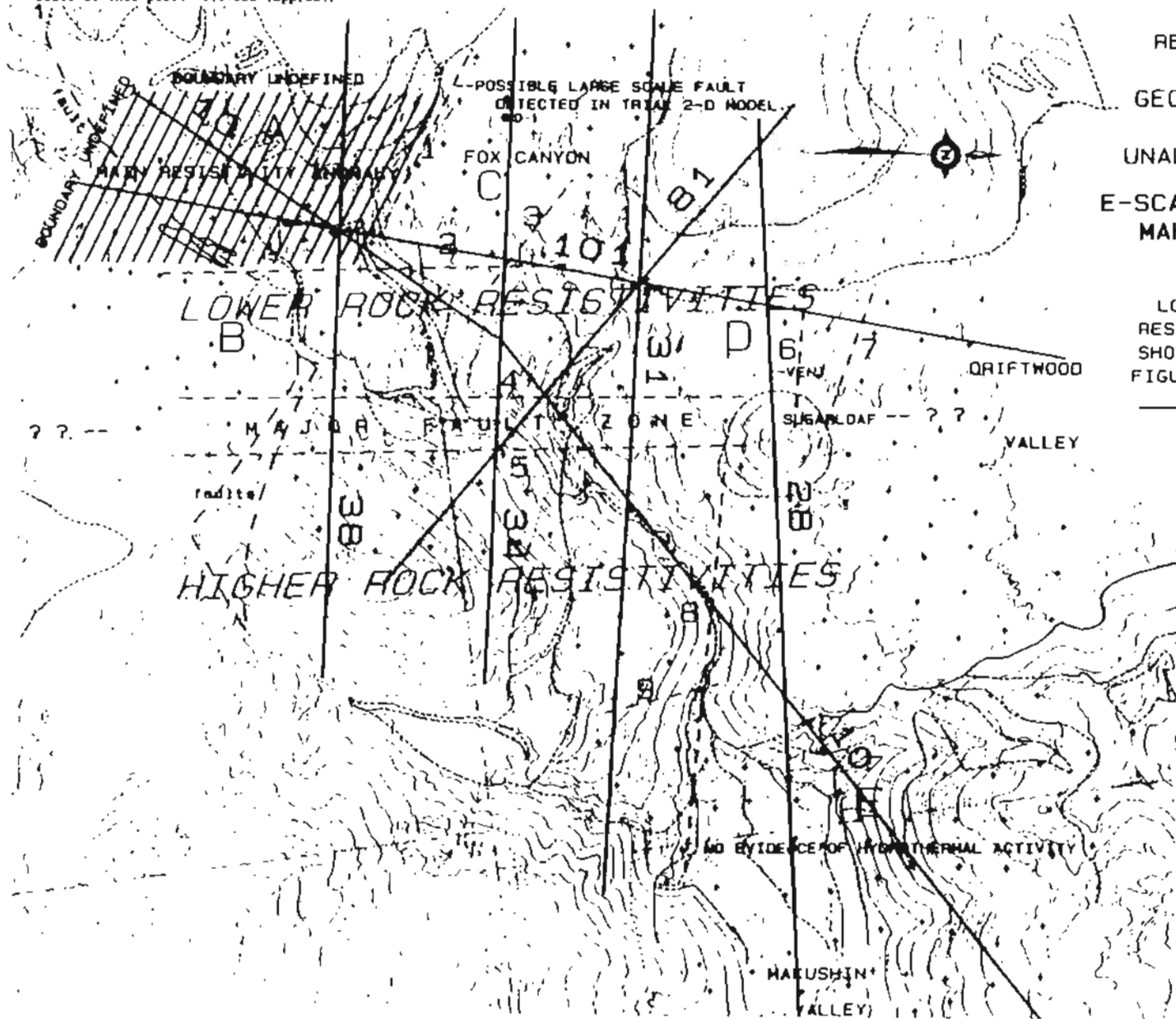
Figure 29. Boundaries and generalized results of E-scan electrical resistivity survey of the Makushin geothermal area performed by Premier Geophysics, Inc. of Vancouver, Canada (taken from app. E of RGI final report to APA, 1985).

that data on reservoir fluid composition and drill hole temperature profiles
were now available to guide the survey and that the survey could potentially
delimit the lateral boundaries of the subsurface hydrothermal resource.
Economic feasibility of developing the resource would be greatly enhanced if
the resource could be shown to exist further down Makushin Valley or at the
head of Driftwood Valley. The electrical resistivity survey would also help
test the proposed hypothesis that the geothermal system is offset east-
southeast of Makushin Volcano as suggested by the regional alignment of fu-
marole fields and thermal springs.

The electrical resistivity survey was conducted by Premier Geophysics of
Vancouver, Canada. The outcome of the electrical resistivity survey is dis-
cussed in detail by G. Shore of Premier Geophysics in Appendix E of RGI's
final report of 1985. The surveyed area, reproduced in figure 29, covered
all of upper Makushin Valley and the plateau at the head of Driftwood Val-
ley. The survey penetrated to depths of 2,000 m. A brief summary of
Shore's more pertinent findings are reviewed here:

(1) The survey defined the north and east boundaries of a main
    resistivity anomaly which was taken to be indicative of the main
    hydrothermal reservoir. These boundaries, shown on figure 29, are
    located in Fox Canyon on the north and east of ST-1. The conductive
    zone extends west and south for at least 2 km and is then beyond the
    range of the survey.
(2) A sloping lower boundary separates the conductive reservoir rocks
    from an underlying higher resistivity regime as depicted in figure
    30.
(3) No resource is thought to underlie the part of Fox Canyon covered by
    the survey.
(4) No other parts of the survey coverage area, including Sugarloaf,
    yielded results comparable to those of the known reservoir area.
(5) A major near-vertical discontinuity in resistivity occurs in a zone
    extending south from Sugarloaf. The discontinuity is inferred by
    Shore to be a fault zone. An alternate explanation for the dis-
    continuity is a change in bedrock mineralization.

We now attempt to resolve the conclusions of the resistivity survey with
data from geologic mapping and geochemistry. No known geological boundary
correlates with the change in resistivity demarcating the eastern edge of
the main resistivity anomaly. The northern boundary is on strike with the
block fault found to the southeast and is perhaps an extension of this
fault. An alternate explanation for the discontinuity is that the canyon is
the approximate boundary between the gabbroic intrusive and the hornfelsed
Unalaska Formation border zone. Pyritization was found to occur mostly
along the hornfelsic border zone, and thus the resistivity change could
reflect sulfide mineralization.

We believe the sloping contact between low and high resistivity zones found by the survey in the vicinity of E-1 and ST-1 is the large open fracture at bottom of ST-1. The surface location of the dipping horizon is constrained to ±50 m of the position shown in figure 30. However, the uncertainty in the slope of the boundary increases with depth, and the boundary could be very well be placed at the bottom of ST-1.

It is possible that the fracture and the dipping horizon are related to the fault mapped through the canyon adjacent to fumarole field 2 (fig. 2). The fault dips steeply to the north-northwest, and its projection passes through the vicinity of fumarole field 1. The fault, which is also the contact between Unalaska Formation rocks to the south and hornfelsic rocks to the north, could be acting as a conduit for thermal fluids that are feeding the fumaroles and hot springs.

No surface expression could be found of any major fault through the Sugarloaf region as suggested by the resistivity data. We prefer Shore's alternate explanation for the resistivity contrast: that of a steeply dipping contact between rock types. The nature of the subsurface contact between the two different Unalaska Formation rock types is concealed by the thick sequence of Holocene lavas that fill upper Driftwood Valley. The eastern valley wall consists mainly of Unalaska Formation lava flows while the west side is mostly pyroclastic flows. The pyroclastic flows were found to be much more altered and pyritized than the lava flows. Thus, the change in resistivity could be due to a change in mineralization.

Although drill hole A-1 encountered temperatures as high as 180°C at a depth of -580 m, the electrical resistivity survey found no indication of a hydrothermal resource in this area. The ST-1 site and the region upvalley from it therefore appear to offer the best potential for future resource development.

The resistivity survey results have strong implications regarding the source of the geothermal fluids. The resistivity models indicate that the hydrothermal system extends in a wedge shape towards the south and west of ST-1 and E-1. The boundaries on the main resistivity anomaly essentially rule out any major hydrothermal system offset from the volcano. Instead, the resistivity data support a model in which thermal fluids ascend from a reservoir overlying a centrally located heat source beneath the volcano. The fluids migrate upward, then spread laterally as they approach the surface, with fractures and faults acting as conduits which feed fumaroles and ST-1.

MODEL OF MAKUSHIN GEOTHERMAL SYSTEM

Our investigations lead us to believe that the Makushin geothermal system is geologically very young. Nye and others (1985), using geochemical
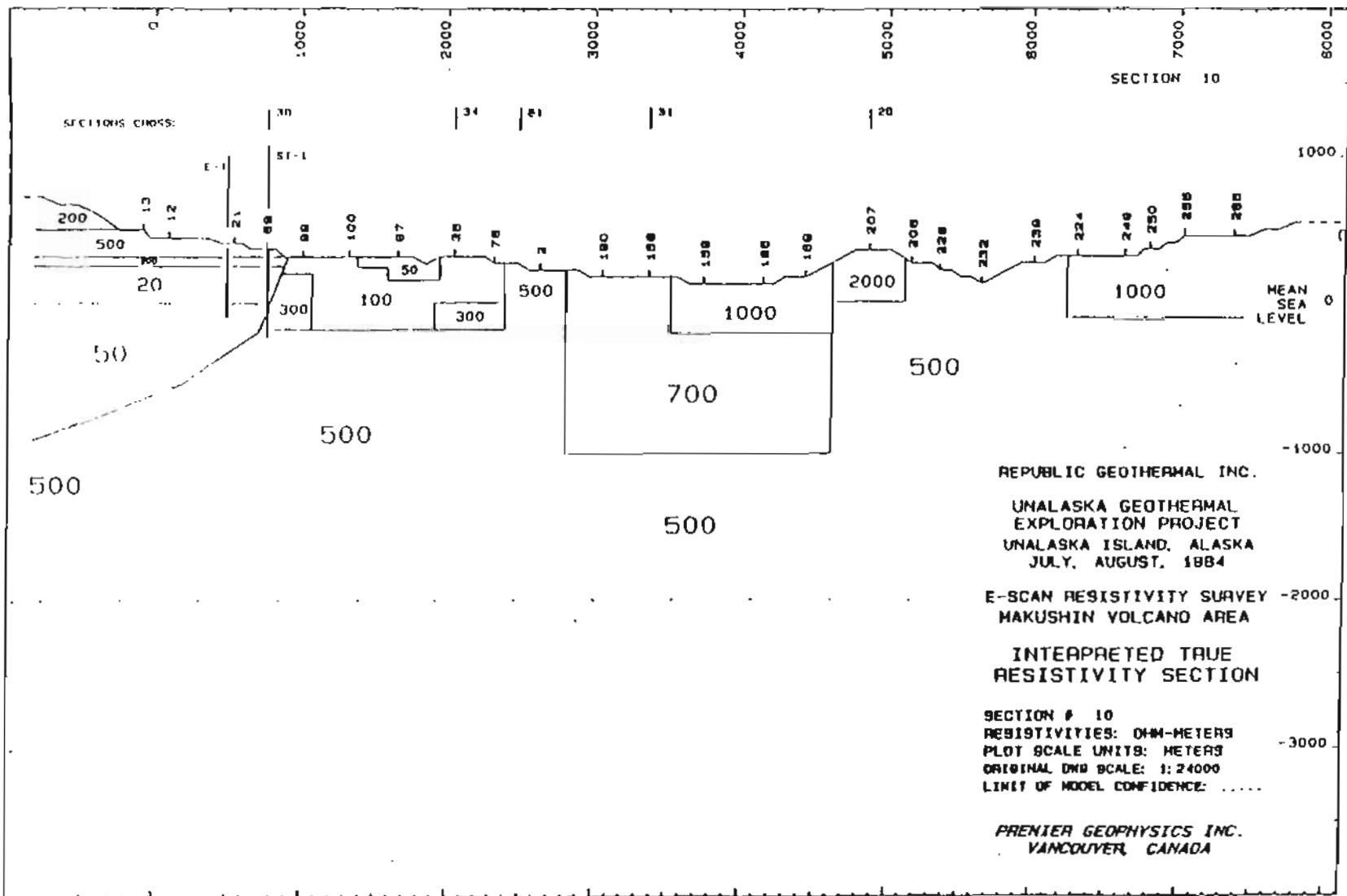
Figure 30. Model of resistivity section through E-1 and ST-1 by Premier Geophysics, Inc. of Vancouver, Canada (taken from app. E of RGI final report to APA, 1985).

evidence derived from Makushin volcanic rocks, argue that prior to the late-Pleistocene, any shallow magmatic heat source at Makushin would have to have been relatively small--1/2 km^3 or less in volume. A magma chamber this size appears much too small to sustain geothermal activity over an area as large as that presently found at Makushin for any reasonable length of time. Instead, Nye and others (1985) suggest that the heat source driving the Makushin geothermal system formed relatively recently and is related to a voluminous post-Pleistocene outpouring of chemically homogeneous lavas and pyroclastic flows that issued from the east flank of Makushin Volcano. The large volume and rapid outpouring of these flows, and the fact that these volcanics are considerably more siliceous than Pleistocene Makushin volcanic rocks, suggests that the post-Pleistocene flows had become fractionated in a newly formed and much larger shallow magma system than had previously existed.

Based on post-Pleistocene glacial history, the age of the lava flows filling Driftwood Valley is estimated to be 3,000-11,000 yr, with a most probable age of 7,000-11,000 yr. Thus, the shallow magmatic system would have been in place by the late-Pleistocene to early Holocene.

Evidence from investigations of hydrothermal alteration mineral assemblages and fluid inclusions indicates that there has been only one hydrothermal system active at Makushin, but that this system has undergone changes and has been affected by interactions with post-Pleistocene glaciers. The hot-water system at Makushin at one time extended to the surface and was substantially hotter than at present, at least within the explored upper portions. During a neoglacial advance, the hydrostatic pressure exerted by glacier ice increased the boiling point and caused temperatures to reach as high as 250°C at depths as shallow as 100 m at the head of Makushin Valley. Periodic release of meltwaters trapped in geothermally generated subglacial vaults caused rapid decreases in pressures in the hydrothermal system. The ensuing vaporization caused explosive brecciation of the gabbronoritic host rock near the ground surface. Increased pH and saturation of chemical constituents in the flashed waters caused co-precipitation of anhydrite, magnetite, calcite, and quartz. Subsequent deglaciation resulted in a gradual decline in pressure and a decrease of meltwaters that may have been charging the hydrothermal system. The combination of boiling and loss of charging waters led to a general lowering of the hydrothermal system water table.

Although geothermometry predicts deep reservoir temperatures as high as 250°C, similar to the fluid inclusion temperatures found in near-surface quartz veins, an overall cooling of the hydrothermal system may also have occurred. Bottom-hole temperatures measured in both test well ST-1 and in TGH E-1 (~200°C) are well below the pressure boiling point for their respective depths below the water table. Fluid inclusion studies of cores from both locations gave temperatures of formation of 250°C or higher throughout the cores. If cooling of the deeper system has not taken place

since the formation of the fluid inclusions, then hydrostatic boiling point temperatures would be expected throughout most of the depth of the drill holes, unless the upper part of the system has become more fractured and therefore more open. In the latter case, pressures within the system may not be great enough to sustain the higher temperatures in its upper parts. Despite the apparent overall cooling of at least the upper part of the Makushin geothermal system, we hasten to point out that more than ample energy exists for geothermal resource development over the foreseeable future.

The present-day Makushin geothermal system possesses many characteristics found at other geothermal systems associated with island-arc volcanoes elsewhere in the world. A model of such systems as proposed by Henley and Ellis (1983) is shown in figure 31. As discussed above, the heat source for the Makushin system is thought to be a relatively recently emplaced body of magma that is associated with the eruption of large volumes of magma during the early Holocene. The magmatic heat source is assumed to be approximately centrally located beneath the volcano, although the east flank eruptions suggest that a portion of it may be slightly offset to the east. The deep hydrothermal system is assumed to reside over the heat source so that the heated waters ascend upwards and then spread laterally as they approach the surface.

As the hot waters ascend, the reduction in hydrostatic pressure causes boiling to occur. Steam and gases evolving from the boiling water table feed the numerous fumaroles located at mid-elevations, and heat perched aquifers which result in a profusion of bicarbonate-sulfate springs below the fumarole fields. A low water table and high relief of the volcano result in a scarcity of chloride hot springs except at low elevations some distance from the central upflow.

At Makushin, the hydrothermal system is charged primarily by meteoric waters which fall at mid- to lower elevations and infiltrate along fractures located on the periphery of the volcano. Much of the recharge may come from the west flank of the volcano which lies in the track of incoming storm systems. The large thickness of highly permeable volcanic flows found on the west flank allow percolation of the meteoric waters into the deeper portions of the volcano's interior. Such a system of recharge could effectively block establishment of fumarolic activity on the west flank.

The host rock in the explored portions of the hydrothermal reservoir is a gabbronoritic pluton. Apparently this pluton possesses an optimum degree of fracture permeablity which permits waters to reside long enough to become heated.

The Makushin hydrothermal system is moderately saline in comparison to other hydrothermal systems in the world but nevertheless contains more chloride than can be reasonably accounted for by leaching from the gabbronorite.
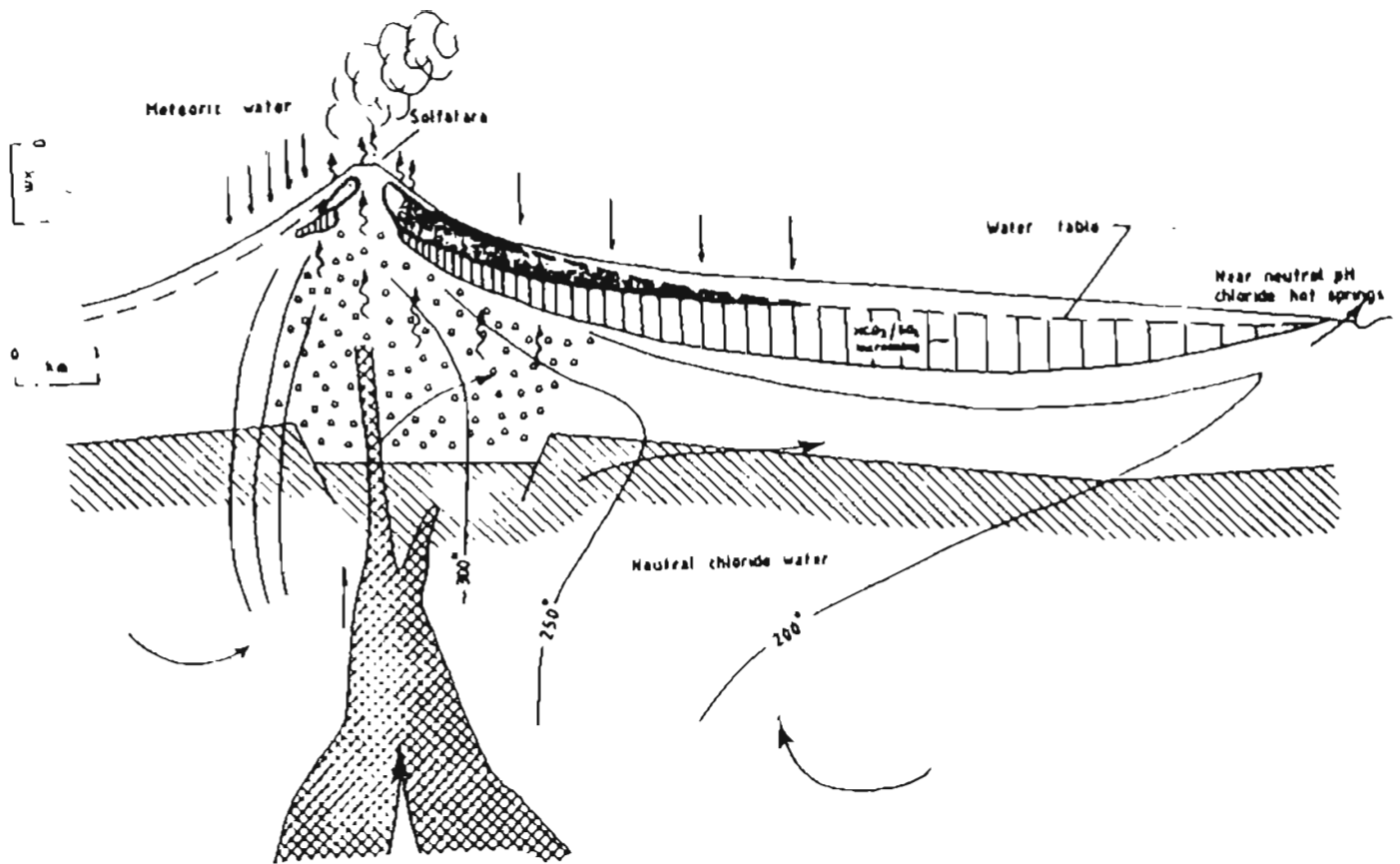
Figure 31. Generalized model of a geothermal system typical of active
island-arc andesite volcanoes (reproduced from Henley and Ellis, 1983).

Apparently, either reservoir waters circulate through marine-laid deposits
within the Unalaska Formation or the reservoir is being contaminated by sea-
water infiltration. A third possibility is that the chloride originates
from the siliceous magmatic heat source. The high concentration of Ca in
the thermal waters is attributed to breakdown of calcium-rich plagioclase in
the gabbronoritic wall-rock.

The Makushin reservoir water has a relatively low concentration of gases
and a CO_2 partial pressure of approximately 0.5 bars. Helium isotope ratios
reflect the magmatic influence on the hydrothermal system and indicate some
of the gases are of magmatic origin. Gas composition of the reservoir
fluids is similar to that found for fumarole fields 1 and 2, which suggests
a possible interconnection between these vents and ST-1. Carbon 13 isotope
ratios in the reservoir CO_2 gas indicate an organic sedimentary origin for
some of the CO_2 gas. Fluctuations and decrease of H_2 found in test well gas
samples may be due to reactions of the hot waters and H_2S gas with drillhole
casing.

Thermal fluids entering the borehole at ST-1 were found to be slightly out of equilibrium with the measured bottom-hole temperature. Application of various geothermometers to the ST-1 fluids gave temperature estimates of 207-226°C, with 250°C estimated for the deep reservoir. These temperatures suggest the thermal fluids cooled slowly by conduction and then by dilution with cold recharge waters before entering the borehole. The ST-1 fluid was found to be oversaturated with respect to quartz and slightly undersaturated with respect to calcite and anhydrite.

Figure 32 is a schematic cross-section through the Makushin geothermal field which incorporates available geological, geochemical, and geophysical information. The cross-section is taken as close as possible to the thermal gradient holes, test well ST-1, and fumarole fields 1, 2, and 3 (AA' in fig. 2). Results of the electrical resistivity survey indicate the main geothermal reservoir lies south and west of E-1 and ST-1 and does not extend under the Fox Canyon plateau or the Sugarloaf area. The southwestern boundary of the main reservoir is constrained by drillhole data to lie upslope of I-1.

We believe the hydrothermal fluids which feed ST-1 are derived from a deep parent reservoir, approximately centrally located beneath the volcano. Fluid flow towards ST-1 is controlled primarily by fracture- and fault-related conduits and, in particular, by a large fracture that dips towards the volcano at ~60°. As the fluid rises along this conduit, it cools by conduction to adjacent wallrock. Some of the fluid ascends secondary fractures and, when the boiling point pressure is eventually reached, the resulting steam and gases continue to ascend to feed fumarole fields 1 and 2. Fortuitous intersection of the primary fracture by ST-1 led to the successful confirmation of the Makushin geothermal field. Future production wells should be sited at or upvalley from ST-1.

Figure 32. Cross section of Makushin geothermal system. Location of section AA' is shown on figure 2. Isotherms based on locations of fumaroles and hot springs and on temperature data from thermal gradient holes and well ST-1. Geology from Nye and others, 1984.

REFERENCES CITED

Arnorsson, Stefan, 1975, Application of the silica geothermometer in low-temperature hydrothermal areas in Iceland: American Journal of Science, v. 275, p. 763-784.
_____ 1983, Chemical equilibria in Icelandic geothermal systems - implications for chemical geothermometry investigations: Geothermics, v. 12, no. 2/3, p. 119-128.

Arnorsson, Stefan, Gunnlaugsson, Einar, and Svavarsson, Hordur, 1983, The chemistry of geothermal waters in Iceland. III. Chemical geothermometry in geothermal investigations: Geochimica et Cosmochimica Acta, v. 47, no. 3, p. 567-578.

Bargar, K.E. and Beeson, M.H., 1984, Hydrothermal alteration in research drill hole Y-6, Upper Firehole River, Yellowstone National Park, Wyoming, U. S. Geological Survey Professional Paper 1054-B, 24 p.

Bargar, K.E., Fournier, R.O., and Theodore, T.G., 1984, Particles resembling bacteria in fluid inclusions from Yellowstone National Park, Wyoming (abstr.), Geol. Soc. Am. Abstr. Programs, v. 16, no 1.

Bjornsson, H., 1974, Exploration of jokulhlaups from Grimsvotn, Vatnajokull, Iceland: Jokull, v. 24, p. 1-26.
_____ 1975: Subglacial water reservoirs, jokulhlaups, and volcanic eruptions: Jokull, v. 25, p. 1-11.

Black, R.F., 1981, Late Quaternary climatic changes in the Aleutian Islands, Alaska, in Mahaney, W. C. ed., Quaternary Paleoclimate: Norwhich, U.K., Geoabstracts Ltd., p. 47-62.
_____ 1983, Glacial chronology of the Aleutian Islands, in Thorson, R.M., and Hamilton, T.D., eds., Glaciation in Alaska: Alaskan Quaternary Center, University of Alaska Museum, Occasional Paper No. 2, p. 5-10.

Browne, P.R.L., 1978, Hydrothermal alteration in active geothermal fields: Ann. Rev. Earth Planet. Sci., v.6, p. 229-250.

Chiba, Hitoshi, Kusakabe, Minoru, Hirano, Shin-ichi, Matsuo, Sadao, and Somiya, Shigeyuki, 1981, Oxygen isotope fractionation between anhydrite and water from 100 - 500 deg. C: Earth and Planetary Science Letters, v. 53., p. 55-62.

Chiba, Hitoshi, and Sakai, Hitoshi, 1985, Oxygen isotope exchange rate between dissolved sulfate and water at hydrothermal temperatures: Geochemica et Cosmochimica Acta, v. 49, p. 993-1000.

Craig, H., 1953, The geochemistry of the stable carbon isotopes, Geochemica et Cosmochima Acta, v. 3, p. 53-92.
_____ 1961, Isotopic variations in meteoric waters, Science, v. 133, p. 1702.
_____ 1963, The isotopic geochemistry of water and carbon in geothermal areas, in Tongiorgi, E. (ed.), Nuclear geology in geothermal areas, Spoleto, 1963: Pisa, Italy, Consiglio Nationale Delle Ricerche, Laboratorio di Geologia Nucleare, p. 17-53.

Craig, H., and Lupton, J.E., 1981, Helium-3 and mantle volatiles in the ocean and oceanic crust: in The Oceanic Lithosphere, v. 7, The Sea, John Wiley and Sons, 1981, pp. 391-428.

Craig, H., Lupton, J.E., and Horibe, Y., 1978a, A mantle helium component in Circum-Pacific volcanic gases: Hakone, the Marianas, and Mount Lassen, *in* Terrestrial Rare Gases (E.C. Alexander and M. Ozima, eds.), Cent. Acad. Publ. Japan.

Craig, H., Lupton, J.E., Welhan, J.A., and Poreda, R., 1978b, Helium isotope ratios in Yellowstone and Lassen Park volcanic gases: Geophysical Research Letters, v. 5, no. 11, p. 897-900.

D'Amore, F., and Panichi, C., 1980, Evaluation of deep temperatures of hydrothermal systems by a new gas geothermometer: Geochimica et Cosmochimica Acta, v. 44, p. 549-556.

D'Amore, F., and Truesdell, A.H., 1983, Gas geothermometry for drill hole fluids from vapor dominated and hot water geothermal fields: Proceedings 6th Stanford Geothermal Resevoir Engineering Workshop, 351-360.

Ellis, A.J., 1979, Explored geothermal systems, in Barnes, H.L., ed., Geochemistry of hydrothermal ore deposits: New York, Wiley and Sons, p. 632-683.

Ellis, A.J. and Mahon, W.A.J., 1977, Chemistry and geothermal systems: Academic Press, London, 392 p.

Fouillac, C., and Michard, G., 1981, Sodium/lithium ratio in water applied to geothermometry of geothermal reservoirs: Geothermics, v. 10, no. 1, p. 55-70.

Fournier, R.O., 1981, Application of water chemistry to geothermal exploration and reservoir engineering, *in* Ryback, L., and Muffler, L.P.J., eds., Geothermal systems: Principles and case histories: New York, Wiley and Sons, p. 109-144.

Fournier, R.O., and Potter, R.W. II., 1982, A revised and expanded silica (quartz) geothermometer: Geothermal Resources Council Bulletin, v. 11, no. 10, p. 3-12.

Fournier, R.O., and Truesdell, A.H., 1973, An empirical Na-K-Ca geothermometer for natural waters: Geochimica et Cosmochimica Acta, v. 37, p. 1255-1275.

Helgesson, H.C., 1969, Thermodynamics of hydrothermal systems at elevated temperatures and pressures: American Journal of Science, v. 267, p. 729-804.

Henley, R.W. and Ellis, A.J., 1983, Geothermal systems ancient and modern: A geochemical review: Earth Science Reviews, v. 19, no. 1, p. 1-50.

Huang, C.I., 1977, Fluid inclusion study of well cuttings from Magmamax #2 drillhole, Salton Sea geothermal area, California [abstract], Economic Geology, v. 72, p. 730.

Isselhardt, C.F., Matlick, J.S., Parmentier, P.P., and Bamford, R.W., 1983, Temperature gradient hole results from Makushin geothermal area, Unalaska Island, Alaska: Geothermal Resources Council, Transactions, v. 7, p. 95-98.

Keenan, J.H., Keyes, F.G., Hill, P.G., and Moore, J.G., 1969, Steam tables (Int. ed. metric units): Interscience, New York, 162 p.

Keith, T.E.C., Mariner, R.H., Barger, K.E., Evans, W.C., and Presser, T.S., 1984, Hydrothermal alteration in Oregon's Newberry Volcano No. 2: Fluid chemistry and secondary-mineral distribution: Geothermal Resources Council Bulletin, v. 13, p. 9-17.

Lan, C.Y., Liou, J.G., and Seki, Y., 1980, Investigation of drillhole core samples from the Tatun geothermal area, Taiwan: Water-Rock Interaction Symposium, 3rd, Edmonton, Canada, Porceedings, p. 183-185.

Lupton, J.E., and Craig, H., 1975, Excess ^{3}He in oceanic basalts: Evidence for terrestrial primordial helium: Earth and Planetary Science Letters, v. 26, p. 133-139.

McKenzie, W.F., and Truesdell, A.H., 1977, Geothermal reservoir temperatures estimated from the oxygen compositions of dissolved sulfate in water from hot springs and shallow drillholes: Geothermics, v. 5, p. 51-61.

Mizutani, Y. and Rafter, T.A., 1969, Oxygen isotopic composition of sulphates, 3. Oxygen isotopic fraction in the bisulfate ion-water system: New Zealand Journal of Science, v. 12, p. 54-59.

Motyka, R.J., 1982, High-temperature hydrothermal resources in the Aleutian arc: Alaska Geological Society Symposium on Western Alaska Geology and Resource Potential, Anchorage, Proceedings, p. 87-99.

Motyka, R.J., Moorman, M.A., and Liss, S.A., 1981, Assessment of thermal spring sites, Aleutian Arc, Atka Island to Becharof Lake---Preliminary results and evaluation: Alaska Division of Geological and Geophysical Surveys, Open-file Report 144, 173 p.

Motyka, R.J., Moorman, M.A., and Poreda, Robert, 1983, Progress report - thermal fluid investigations of the Makushin geothermal area: Alaska Division of Geological and Geophysical Surveys Report of Investigations 83-15, 48 p.

Muffler, L.J.P., White, D.E., and Truesdell, A.H., 1971, Hydrothermal explosion craters, Yellowstone National Park: Geological Society of America Bulletin, v. 82, p. 723-740.

Nye, C.J., Queen, L.D., and Motyka, R.J., 1984, Geologic map of the Makushin geothermal area, Unalaska Island, Alaska: Alaska Division of Geological and Geophysical Surveys Report of Investigations 84-3, 2 sheets, scale 1:24,000.

Nye, C.J., Swanson, S.E., and Reeder, J.W., 1985, Petrology and geochemistry of Quaternary volcanic rocks from Makushin Volcano, Central Aleutian Arc, [in prep.].

Okko, V., 1955, Glacial drift in Iceland, its origin and morphology: Comm. Geol. de Finlande Bull., no. 170, 133 p.

O'Neil, J.R., Clayton, R.N., and Mayeda, T., 1969, Oxygen isotope fractionation in divalent metal carbonates: Journal of Chemical Physics, v. 51, p. 902-909.

Panichi, C., and Gonfiantini, R., 1978, Environmental isotopes in geothermal studies: Geothermics, v. 6, p. 143-161.

Parmentier, P.P., Reeder, J.W., and Henning, M.W., 1983, Geology and hydrothermal resources of Makushin geothermal area, Unalaska Island, Alaska: Geothermal Resource Council Transactions, v. 7, p. 181-185.

Perfit, M.R. and Lawrence, J.R., 1979, Oxygen isotope evidence for meteoric water interaction with Captain's Bay pluton, Aleutian Islands: Earth and Planetary Science Letters, v. 45, p. 16-22.

Poreda, R.J., 1983, Helium, neon, water and carbon in volcanic rocks and gases: University of California, San Diego, Ph.D. thesis, 215 p.

Potter, II, R.W., Clynne, M.A., and Brown, D.L., 1978, Freezing point depression of aqueous sodium chloride solutions: Economic Geology, v. 73, p. 284-285.

Presser, T.S., and Barnes, Ivan, 1974, Special techniques for determining chemical properties of geothermal waters, U.S. Geological Survey Water-Resources Investigation Report 22-74, 11 p.

Queen, L.D., 1984, Lithologic log and hydrothermal alteration of core from the Makushin Geothermal area, Unalaska, Alaska: Alaska Division of Geological and Geophysical Surveys Report of Investigations 84-23, 1 sheet.

Reeder, J.W., 1982, Hydrothermal resources of the northern part of Unalaska Island, Alaska: Alaska Divisison of Geological and Geophysical Surveys Open-file Report 163, 17 p.

Republic Geothermal Inc., 1983, The Unalaska Geothermal Exploration Project, Phase 1B, Final Report, prepared for the Alaska Power Authority.

_____ 1984, The Unalaska Geothermal Exploration Project, Phase II Final Report, prepared for the Alaska Power Authority.

_____ 1985, The Unalaska Geothermal Exploration Project, Phase III Final Report, prepared for the Alaska Power Authority.

Roedder, E., 1984, Fluid Inclusions: Reviews in Mineralogy, v. 12, Mineralogical Society of America, 664.

Sheppard, D.S., and Giggenbach, W.F., 1985, Methods for the analysis of geothermal and volcanic waters and gases, Department of Scientific and Industrial Research, New Zealand, Report No. C.D. 2364, 78 p.

Shore, R.A., 1985, Resistivity survey and interpretation, in Republic Geothermal Inc., The Unalaska Geothermal Exploration Project, Phase III Final Report, prepared for Alaska Power Authority, Appendix E.

Taguchi, S., 1983, Study on geothermal geology of the Kirishima volcanic region: Ph.D. dissertation, Kyusha University, 131 p.

Taguchi, S., Okaguchi, M., and Yamasaki, T., 1980, Reduction in the lengths of fussion tracks by geothermal heating and its application to thermal history: Rept. Res. Inst. Industrial Sci., Kyushu University, No. 72, p. 21-26 (in Japanese; English abstract).

Torgersen, T., and Jenkins, W.J., 1982, Helium isotopes in geothermal systers: Iceland, The Geysers, Raft River, and Steamboat Springs, Geochimica et Cosmochima Acta, v. 46, p. 739-48.

Torgersen, T., Lupton, J.E., Sheppard, D.S., and Giggenbach, W.F., 1982, Helium isotope variations in the thermal areas of New Zealand, Journal of Volcanology and Geothermal Research, v. 12, p. 283-298.

Truesdell, A.H., 1976, Geochemical techniques in exploration: United Nations Symposium on the Development and Use of Geothermal Resources, 2nd, San Francisco, 1975, Proceedings, v. 1, p. liii-lxxix.

Truesdell, A.H., and Fournier, R.O., 1977, Procedure for estimating the temperature of a hot-water component in a mixed water by using a plot of dissolved silica versus enthalpy: Journal of Research, U.S. Geological Survey, v. 5, no. 1, p. 49-52.

Truesdell, A.H., and Hulston, J.R., 1980, Isotopic evidence on environments of geothermal systems: in Handbook of Environmental Isotope Geochemistry: Elsevier, p. 1979-219.

Truesdell, A.H., and Singers, Wendy, 1973, Computer calculation of downhole chemistry in geothermal areas: New Zealand Department of Science and Industry. Research Chemistry Division Report CD2136, 145 p.

Welhan, J.A., 1981, Carbon and hydrogen gases in hydrothermal systems: the search for a mantle source: University of California, San Diego, Ph.D. diss., 182 p.

APPENDIX A

Table A1. Chemical analyses of sulfate-carbonate spring waters in the Makushin geothermal area.[1]
(Values in mg/l unless otherwise specified.)

Site name	Date	T^2	pH^2	Na	K	Ca	Mg	Li	Sr	HCO_3^2	SO_4	F	Cl	SiO_2	B	Fe	TDS	SC
GV-Gd1	8-11-80	97	6.4	52	4.8	12	4.0	0.01	0.1	37	129	0.1	10.0	94	0.5	0.10	325	360
GV-Gd2	8-11-80	82	6.5	87	5.7	32	1	0.02	0.3	288	95	0.3	5.0	125	0.5	0.01	504	580
GV-Gd3	7-05-81	78	4.3	62	5.2	25	8.0	0.01	0.2	3	218	0.1	6.1	120	0.5	nd	447	nd
GV-Ge	7-05-81	68	nd	61	3.3	260	9.6	0.04	1.1	nd	491	0.3	2.3	138	0.5	0.02	nd	1400
GV-Gf	8-11-80	70	6.1	78	4.5	nd	nd	nd	nd	nd	42	nd	10.0	125	nd	nd	nd	nd
GV-Gf	7-05-81	79	6.4	81	4.8	210	7.8	0.03	1.1	256	476	0.2	7.5	142	0.5	0.21	1050	1200
GV-Gh	7-11-82	61	6.0	64	3.8	240	11	0.03	1.2	358	472	1.0	5.8	145	0.5	0.40	1120	1320
GV-Gj	7-10-82	41	6.1	53	3.4	280	11	0.03	1.4	332	581	1.0	6.6	120	0.5	0.70	1220	1430
GV-Gl	7-13-82	62	6.0	63	4.5	260	10	0.03	1.2	325	542	1.0	6.6	135	0.5	0.50	1190	1370
MV-Ma	7-17-82	84	6.0	54	9.0	65	13	0.02	0.3	nd	344	1.0	nd	155	0.5	2.5	nd	nd
MV-Mb	8-13-80	87	5.5	28	5.9	67	12	0.01	0.3	191	155	0.1	5.0	140	nd	0.09	508	600
MV-Mc	7-04-81	58	5.3	24	3.2	23	5.5	0.01	0.1	nd	25	0.1	7.8	88	0.5	0.07	nd	250
MV-Mc	7-18-82	55	6.8	32	4.3	34	6.1	0.01	0.1	201	15	1.0	7.9	105	0.5	0.10	305	351
MV-Md	8-13-80	67	5.3	14	3.4	23	8.0	0.01	0.1	116	21	0.1	5.0	88	nd	0.03	220	255
Nv-Na	8-20-83	23	6.1	88	4.2	390	36	0.14	3.1	678	710	0.7	5.6	110	0.5	nd	1680	nd

GV = Glacier Valley, MV = Makushin Valley, NV = Nateekin Valley

[1] Alaska Division of Geological and Geophysical Surveys, Fairbanks, Alaska, M.A. Moorman, analyst.
[2] Determined in the field.

Table A2. Chemical analyses of chloride spring waters in the Makushin geothermal area.[1]
(Values in mg/l unless otherwise specified.)

| Site name | Date | T[2] | pH[2] | Cations | | | | | | Anions | | | | | | | | |
				Na	K	Ca	Mg	Li	Sr	HCO_3[2]	SO_4	F	Cl	SiO_2	B	Fe	TDS	SC
DV – stream	8-21-83	14	6.9	36	3	8.8	2	0.15	0	35	6	nd	56	43.6	0.7	nd	175	nd
GV – Gm	7-20-82	39	5.9	180	19	200.0	15	0.48	1.1	463	360	1.0	160	113	4.2	1.7	1290	1380
GV – Gn	7-20-82	27	5.8	180	19	180.0	23	0.40	1.0	563	320	1.0	140	119	4.0	1.9	1260	1760
GV – Gp	7-20-82	40	6.3	300	31	160.0	39	0.86	1.4	590	180	1.0	380	104	9.9	2.1	1500	nd

DV = Driftwood Valley, GV = Glacier Valley

[1] Alaska Division of Geological and Geophysical Surveys, Fairbanks, Alaska, M.A. Moorman, analyst.
[2] Determined in the field.

Table A3. Chemical analyses of cold waters in the Makushin geothermal area.[1]
(Values in mg/l unless otherwise specified.)

| Site name | Date | T[2] | pH[2] | Cations | | | | | | Anions | | | | | | | | | | |
				Na	K	Ca	Mg	Li	Sr	HCO_3[2]	SO_4	F	Cl	Br	SiO_2	B	As	Fe	TDS	SC
DV – stream	8-21-83	14	6.9	36	3.4	8.8	2.0	0.15	0.1	35	6	nd	56	nd	43.6	0.7	0.10	nd	175	nd
GV – Gd spring	7-05-81	5	nd	4.7	0.8	8.9	1.9	0.01	0.1	nd	29	0.1	5.6	nd	20.0	0.5	nd	nd	nd	100
GV – Gd stream	8-11-80	7	6.0	78	4.5	nd	0.1	0.01	nd	nd	418	nd	10	nd	125.0	nd	nd	nd	nd	nd
GV – Gk spring	7-15-82	16	6.8	4.1	0.3	20	1.1	0.01	0.1	38	27	1.0	5.9	nd	9.4	0.5	nd	0.10	88	141
GV – Gl stream	7-18-82	5	6.5	8.5	1.4	52	6.6	0.01	0.1	13	150	1.0	12	nd	28.0	0.5	nd	0.40	264	375
GV – Gn spring	7-09-83	6	6.4	5.6	0.2	6.4	1.0	0.01	0.2	26	4	nd	5.5	nd	6.0	0.10	0.002	nd	42	nd
GV – clear river mouth	7-19-83	7	6.4	7.5	0.5	53	1.8	0.01	0.1	37	14	nd	8.8	nd	14.2	0.02	0.001	nd	117	nd
GV – kettle pond	8-19-84	nd	nd	1.9	0.1	0.5	0.3	0.01	0.1	nd	1	nd	2.0	0.1	3.0	0.04	0.001	nd	nd	nd
GV – muddy river mouth	7-19-83	5	6.5	6.3	0.7	12	2.2	0.01	0.1	11	36	nd	7.0	nd	12.0	0.16	0.001	nd	82	nd
MV – spring	7-19-82	6	6.8	2.6	0.2	1.8	0.6	0.01	0.1	11	3	1.0	3.7	nd	13.0	0.5	nd	0.1	32	34

DV = Driftwood Valley, GV = Glacier Valley, MV = Makushin Valley

[1] Alaska Division of Geological and Geophysical Surveys, Fairbanks, M.A. Moorman, analyst.
[2] Determined in the field.

Table A4. Stable isotope analyses of sulfate-carbonate spring waters in the Makushin geothermal area.[1]

Site name	Date	T°C	D/Hb	$^{18}O/^{16}O$[2]
GV - Ga	7-05-81	nd	-83	-11.9
GV - Gb	7-05-81	nd	-80	-12.2
GV - Gc	7-05-81	nd	-83	-12.5
GV - Gd1	8-11-80	97	-70	-8.9
GV - Gd2	8-11-80	82	-80	-11.6
GV - Gd3	7-05-81	78	-83	-11.9
GV - Ge	7-05-81	68	-80	-12.2
GV - Gf	7-05-81	79	-83	-12.5
GV - Gh	7-11-82	61	-82	-11.7
GV - Gj	7-10-82	41	-79	-11.0
GV - Gl	7-13-82	62	-83	-11.9
MV - Ma	7-17-82	84	-77	-11.1
MV - Mb	7-04-81	nd	-81	-12.4
MV - Mb	8-13-80	87	-78	-11.9
MV - Mc	7-04-81	58	-81	-12.4
MV - Mc	7-18-82	55	-84	-11.7
MV - Md	8-13-80	67	-81	-12.1
NV - Na	8-20-83	23	-78	-11.3

GV - Glacier Valley
MV - Makushin Valley
NV - Nateekin Valley

[1]Analyzed at Stable Isotope Laboratory, Southern Methodist University, Dallas, Texas.
[2]Values are in permil with respect to SMOW.

Table A5. Stable isotope analyses of chloride spring waters in the Makushin geothermal area.[1]

Site name	Date	T°C	D/Hb	$^{18}O/^{16}O$[2]
DV - stream	8-21-83	14	-76	-9.9
GV - Gm	7-20-82	39	-80	-11.1
GV - Gn	7-20-82	27	-82	-11.1
GV - Gp	7-20-82	40	-78	-10.9
GV - Gp	7-16-83	44	-80	-11.2

DV - Driftwood Valley
GV - Glacier Valley

[1]Analyzed at State Isotope Laboratory, Southern Methodist University, Dallas, Texas.
[2]Values are in permil with respect to SMOW.

Table A6. Stable isotope analyses of cold waters in the Makushin geothermal area.[1]

Site name	Date	T°C	D/Hb	$^{18}O/^{16}O$[2]
OV - stream	8-21-83	14	-76	-9.9
FF 1 - stream	7-18-83	nd	-81	-11.2
FF 3 - stream	7-11-83	nd	-89	-13.5
FF 6 - snow	7-18-82	nd	-121	-15.9
FF 7 - snow melt	8-20-83	nd	-88	-12.7
FF 9 - snow melt	7-11-83	nd	-65	-11.0
GV - Gd spring	7-05-81	5	-93	-14.2
GV - Gd spring	8-11-80	nd	-77	-11.1
GV - Gd stream	8-11-80	7	-87	-12.0
GV - Gk spring	7-15-82	16	-77	-10.0
GV - Gl stream	7-18-82	5	-88	-12.6
GV - Gn spring	7-09-83	nd	-78	-11.3
GV - West Fork River	7-05-81	5	-93	-14.2
GV - clear river mouth	7-19-83	7	-77	-11.5
GV - muddy river mouth	7-19-83	5	-85	-12.8
GV - snow melt	8-11-80	nd	-76	-11.2
MV - Camp spring	7-19-82	nd	-67	-9.7
MV - Mb stream	8-13-80	nd	-89	-13.0
MV - Mc stream	7-04-81	nd	-82	-11.9
MV - Md stream	8-11-80	nd	-83	-11.3
MV - spring	7-19-82	6	-82	-11.9
NV - stream	8-20-83	nd	-88	-12.7

OV - Driftwood Valley
FF - Fumarole field
GV - Glacier Valley
MV - Makushin Valley
NV - Nateekin Valley

---

[1] Analyzed at Stable Isotope Laboratory, Southern Methodist University. Dallas, Texas.
[2] Values are in permil with respect to SMOW.

Table A7. Geothermometry of chloride spring waters in Makushin geothermal area.
(Temperatures in °C.)

Site name	Date	Qz cond. (1)	Chal. cond. (2)	Na/K (3)	Na/K (4)	Na/K (5)	Na-K-Ca (6)	Na-K-Ca (7)	Ni/Li (8)
DV - stream	8-21-83	96	65	210	178	187	157	71	171
GV - Gm	7-20-82	144	118	225	197	205	166	129	139
GV - Gn	7-20-82	147	122	225	197	204	167	99	126
GV - Gp	7-20-82	139	113	221	192	200	175	64	143

DV = Driftwood Valley. GV = Glacier Valley

---

[1] Fournier and Potter, 1982, improved SiO_2 (quartz).
[2] Fournier, 1981 (chalcedony).
[3] Fournier, 1981, Na/K.
[4] Truesdell, 1976, Na/K.
[5] Arnorsson, 1983, Na/K, Basalt.
[6] Fournier & Truesdell, 1973.
[7] Fournier & Potter, Mg-corrected (Fournier, 1981).
[8] Fouillic & Michard, 1981.

Table A8. Analyses of gases collected from fumaroles and hot springs, Makushin geothermal area, in mole percent.
Analyses corrected for air contamination using ratio of O_2 in sample to O_2 in air (RO_2).

Sample code	Location	Date sample	RO_2	Xg	CO_2	H_2S	H_2	CH_4	NH_3	N_2	Ar	N_2/Ar	C/S	Gas geothermometer[3] T_1	T_2
Sodium-hydroxide charged flasks:[1]															
RM 83-46	FF#1	7-17-83	0.01	0.17	82.19	2.28	0.21	0.039	0.38	14.73	0.17	86.4	36.1	227	206
RM 83-GV1-A	FF#3 Superheated	7-08-83	0.00	0.16	88.04	6.38	0.95	0.010	0.13	4.43	0.06	80.2	13.8	298	272
RM 83-11b	FF#3 West	7-10-83	0.06	0.50	83.72	1.69	0.22	0.001	0.04	14.16	0.17	84.1	49.4	256	234
RM 83-31	FF#3 Far west	7-13-83	0.05	0.36	88.10	4.58	0.25	0.001	0.01	6.94	0.14	51.3	19.3	273	249
RM 83-57	FF#7	8-20-83	0.01	2.63	82.15	1.81	1.10	2.482	0.18	12.21	0.08	161.9	46.7	230	210
RM 83-19	FF#9	7-11-83	0.00	0.78	91.55	3.94	0.85	0.004	0.01	3.63	0.02	146.3	23.2	294	268
DS 83 BN7 DS	FF#3 superheated (98°C)	8-29-83	0.00	0.18	88.93	6.85	0.88	0.006	0.08	3.22	0.03	113.1	13.0	302	275
DS 83 BN13 DS	FF#3 Far west	8-29-83	0.00	0.25	84.93	6.25	0.66	0.003	0.06	8.06	0.01	--	13.6	299	273
RM 82-GV1	FF#3 Superheated	7-09-82	0.02	0.15	82.29	12.25	1.84	0.070	nd	3.56	0.07	54.7	6.7	313	285
RM 82-Ma sum	FF#6 Summit	7-18-82	0.00	1.67	87.47	5.53	0.21	0.047	nd	6.63	0.11	60.2	15.8	235	214
RM 82-MV FF#2	FF#2	7-17-82	0.00	--	90.40	2.92	0.35	0.012	nd	6.24	0.07	87.8	30.9	252	229
RM 82 Ma west fl.	FF#5	7-13-82	0.01	1.39	91.16	0.95	0.51	0.004	0.03	7.29	0.05	137.0	96.4	257	234
RP 81-AL3	FF#2	7-14-81	0.00	0.00	87.17	5.26	0.75	0.002	nd	6.76	0.06	120.2	16.6	308	280
RP 81-A1S	FF#3	7-05-81	0.00	0.00	87.42	1.23	1.80	0.002	nd	9.43	0.11	86.4	70.9	309	281
RM 80-MV2	FF#1	8-13-80	0.00	0.41	91.68	2.63	0.24	0.029	nd	5.36	0.07	78.4	34.9	231	210
RM 80-MV1	FF#2	8-13-80	0.00	0.59	87.90	2.65	0.54	0.002	nd	8.81	0.09	95.4	33.2	283	258
Uncharged, evacuated flasks:[2]															
RM 83 G-p	Spring G-p	7-16-83	--	--	98.22	0.02	0.005	0.052	nd	0.96	0.02	48.0	--	--	--
RM 83 G-j	Spring G-j	7-21-83	0.04	--	25.43	0.02	0.02	0.010	nd	74.13	1.02	72.4	--	--	--
RM 82 GV UW	FF#4	7-14-82	0.01	--	92.73	0.82	1.21	0.01	nd	5.50	0.05	104.8	113.5	295	269
RM 82 Ma WF	FF#5	7-13-82	0.00	--	94.89	0.68	0.59	0.01	nd	3.78	0.05	77.6	139.3	268	244
RM 82 Ma Sum	FF#6	7-18-82	0.00	--	90.60	5.68	0.12	0.02	nd	3.43	0.01	--	16.0	226	206
RM 82 GV W	FF#9	7-14-82	0.00	--	93.36	2.01	0.72	0.01	nd	4.33	0.04	108.3	46.4	293	267

[1]Samples RM 83 and RM 82 analyzed by R.J. Motyka, Alaska Division of Geological and Geophysical Surveys; samples DS 83 analyzed by D.S. Sheppard, Department of Scientific and Industrial Research, New Zealand; samples RP 81 and RM 80 analyzed by J. Whelan, Scripps Institute of Oceanography, La Jolla, and R.J. Motyka, Alaska Division of Geological and Geophysical Surveys, Fairbanks.

[2]Analyzed by W. Evans, U.S. Geological Survey, Menlo Park, and R.J. Motyka, Alaska Division of Geological and Geophysical Surveys, Fairbanks.

[3]D'Amore and Panichi, 1980. T_1 uses $P\,CO_2$ = 1 bar; T_2 uses $P\,CO_2$ = 0.5 bar.

nd = not determined.

Table A9. Makushin geothermal area, analyses of $^{13}C/^{12}C$ in CO_2 emanating from fumaroles and hot springs.

Location	Year collected	^{13}C, PDB	Type	Analyst
Fum. field #1	1983	-14.3	$SrCO_3/NaOH$	USGS
	1983	-13.9	$SrCO_3/NaOH$	USGS
Fum. field #2	1981	-12.2	$SrCO_3/NaOH$	GC
		-12.5	$SrCO_3/NaOH$	SMU
	1982	-11.6	$SrCO_3/NaOH$	USGS
Fum. field #3,sp	1981	-11.8	$SrCO_3/NaOH$	GC
		-12.4	$SrCO_3/NaOH$	SMU
lower	1981	-13.0	CO_2-gas	GC
super heated	1982	-10.2	CO_2-gas	SIO
	1983	-13.4	$SrCO_3/NaOH$	USGS
west	1983	-11.3	$SrCO_3/NaOH$	USGS
Fum. field #4	1982	-12.3	CO_2-gas	USGS
Fum. field #5	1982	-12.4	$SrCO_3/NaOH$	USGS
		-12.4	CO_2-gas	USGS
Fum. field #6	1982	-10.0	CO2-gas	USGS
		-11.5	$SrCO_3/NaOH$	SMU
Fum. field #9	1982	-12.1	CO_2-gas	USGS
Spring G-j	1983	-15.4	CO_2-gas	USGS
Spring G-p	1983	-13.3	CO_2-gas	USGS

USGS = U.S. Geological Survey, Menlo Park, California.
SMU   = Southern Methodist University, Stable Isotope Laboratory, Dallas, Texas.
GC   = Global Geochemistry, Inc., Canoga Park, California.
SIO   = Scripps Institute of Oceanography, Stable Isotope Laboratory, La Jolla, California.

Table A10. Makushin geothermal area, miscellaneous stable isotope analyses.

$^{13}C/^{12}C$ - HCO_3, thermal waters (USGS).

Location	Year collected	^{13}C, PDB
Spring G-h	1982	-11.1
Test well ST-1	1984	-23.0

$^{13}C/^{12}C$ and $^{18}O/^{16}O$ in $CaCO_3$, calcite sinter deposited on downhole
instrument cable in test well ST-1, mid-July, 1984. (SMU analysts).

	$^{13}C/^{12}C$, PDB	$^{18}O/^{16}O$, PDB: CO_2
RM84-MVTW $CaCO_3$	-12.5	-29.3

$^{13}C/^{12}C$ in methane, fumarole gases.

Location	Year collected	^{13}C, PDB	Analyst
Fum. field #2	1982	-42.3	USGS
Fum. field #6	1982	-30.6	SIO

D/H in hydrogen and methane, fumarole gases.

Location	Year collected	D/H - H_2 SMOW	D/H - CH_4, SMOW	Analyst
Fum. field #3, sp	1981	-601	---	GC
Fum. field #3, superheated	1982	-582	---	USGS
Fum field #6, summit	1982	-719	-132.6	USGS

USGS = U.S. Geological Survey, Menlo Park, California.
SMU = Southern Methodist University, Stable Isotope Laboratory, Dallas, Texas.
GC = Global Geochemistry, Inc., Canoga Park, California.
SIO = Scripps Institute of Oceanography, Stable Isotope Laboratory, La Jolla, California.